2024-01-01

Investigating the roles of plants, fungi, and biocrusts in nutrient movement within dryland ecosystems

Catherine E. Cort
University of Texas at El Paso

INVESTIGATING THE ROLES OF PLANTS, FUNGI, AND BIOCRUSTS IN NUTRIENT MOVEMENT WITHIN DRYLAND ECOSYSTEMS

CATHERINE E. CORT

Doctoral Program in Ecology and Evolutionary Biology

APPROVED:

Anthony Darrouzet-Nardi, Ph.D., Chair

Jennie McLaren, Ph.D.

Michael Moody, Ph.D.

Jonathan Mohl, Ph.D.

Stephen L. Crites, Jr., Ph.D.
Dean of the Graduate School

Dedication

This dissertation is dedicated to my grandmothers, Jeanne and Mary Rose, whose courage and accomplishments have brought me so far.

INVESTIGATING THE ROLES OF PLANTS, FUNGI, AND BIOCRUSTS IN NUTRIENT MOVEMENT WITHIN DRYLAND ECOSYSTEMS

by

CATHERINE E. CORT, B.S.

DISSERTATION

Presented to the Faculty of the Graduate School of

The University of Texas at El Paso

in Partial Fulfillment

of the Requirements

for the Degree of

DOCTOR OF PHILOSOPHY

Department of Biological Sciences

THE UNIVERSITY OF TEXAS AT EL PASO

December 2023

Acknowledgements

This research was funded through National Science Foundation grants 1557162, 1557135, 1919904, and grants awarded by the Sevilleta LTER and the UTEP Les and Harriot Dodson Fund.

Thank you to the many project collaborators who made every step of this work possible, including Eva Stricker, Jenn Rudgers, Grace Crain-Wright, Kristina Young, Mariah Patton, Vanessa Moreira Fernandes, Ari Jumpponen, Michael Mann, Benjamin Brunner, Jayne Belnap, and to Isa Siles Asaff, Javier Rodriguez, John Powers, and Mayra Melendez for their invaluable field and lab assistance. I'm so grateful to have met and worked with many influential and inspiring soil scientists over the past 7 years, including Katy Schaeffer, Jennifer Holguin, Jane Martinez, Kalpana Kukreja, Daniela Aguirre, Parikrama Sapkota, Kelly Ramirez, Marguerite Mauritz, Nicole Pietrasiak, Sasha Reed, and April Ulery.

Many thanks to my dissertation committee members for their continued patience and guidance throughout this process, and to my fellow graduate students for much bonding and solidarity. Thank you to my teaching mentors, especially Anthony Darrouzet-Nardi, Jennie McLaren, Kelly Ramirez, as well as my many undergraduate students for tolerating (and sometimes sharing) my interest and enthusiasm for the fungal/microbial world. Special thanks to my first mycology mentors at SUNY-ESF including Drs. Lauren Goldmann, Alex Weir, Tom Horton, Robin Kimmerer, and Dr. Chun-Juan Wang.

Eternal gratitude for my sister, parents, and friends for their support – my PhD journey would not have been possible without the gracious care of my community both near and far.

Abstract

In dryland ecosystems, plant productivity and microbial decomposition are often separated in space and time due to the asynchronous availability of soil moisture and organic matter inputs. It has been proposed that fungi play a key functional role in connecting these cycles by facilitating movement of water, carbon (C), and nitrogen (N) through a network of shared hyphae between plant roots and biological soil crust (biocrust) communities at the soil surface. This connection, also known as the "fungal loop," effectively re-couples processes of nutrient release and uptake between primary producers and minimizes ecosystem N losses due to leaching, erosion, and gaseous pathways. However, direct support for the existence of these nutrient exchanges and for the importance of fungal networks in dryland biogeochemical cycles remains scarce. In this dissertation, I addressed several direct and indirect lines of evidence underlying the fungal loop hypothesis, described in the following chapters: Ch. 2 presents a greenhouse study comparing foliar recovery and uptake of inorganic and organic N forms applied to roots of three dryland plant species and summarizes our current ecological understanding of dryland plant N uptake rates and methods of quantification; Ch. 3 identifies the abundance, composition and similarity of fungal communities in both biocrust soils and roots of black grama (*Bouteloua eriopoda*) and compares the responses of biocrust and root-associated fungi to different global change factors; and Ch. 4 attempts to isolate the role of fungi in nutrient translocation of N between biocrust soils and plants by impeding fungal connections to plant roots and evaluating the conditions affecting N uptake from biocrust soils to plant leaves. My findings from Ch. 2 demonstrate that dryland plants with different growth requirements can take up both inorganic and organic soil N within 12-48 hours, and there is little evidence for N niche specialization among nutrient-limited plants in this habitat. Results from Ch. 3 illustrate the relative dissimilarity of biocrust and root-

associated fungal communities, the potential sensitivity of root fungal diversity to N fertilization, and the reordering of biocrust fungal communities under increased precipitation variability and combined inputs of water and N inputs. Findings from Ch. 4 did not support the central importance of fungal connections to rapid N transfer through surface soils, as we found that plant ^{15}N uptake was not inhibited by neither fungal exclusion mesh treatments nor surface soil barriers, and significant movement was only observed after 3-10 days. We conclude that (i) nutrient uptake can occur rapidly (< 24 h) in co-occurring dryland plant species following application of water and N to the roots, (ii) there are taxonomically diverse and abundant saprotrophic fungi in biocrust soils, and functionally distinct, symbiotrophic taxa in plant roots that may have differential responses to fluctuations in N and water inputs in this system, and (iii) N transfers from surface biocrusts to plant leaves are fairly rare at the ~0.5 m^2 scales we tested, and relatively slower rates of nutrient movement into plants could be driven by soil diffusion and plant root uptake processes, rather than active fungal facilitation. Overall, I did not find strong direct or indirect evidence supporting the occurrence of fungal-mediated nutrient exchanges in this semiarid grassland; however, I did gain a clearer picture of the diversity, composition, abundance and potential trophic roles of dryland fungi and the potential mechanisms underlying N translocation through soils and biotic pools. Cultivating a better understanding of the relationships between short-term nutrient uptake, soil and plant microbes, and soil nutrient movement in dryland has important implications for understanding patterns and mechanisms of nutrient cycling and retention in these globally important ecosystems.

Table of Contents

List of Tables

List of Figures

Chapter 1: Introduction

THE ROLES OF FUNGI IN DRYLAND ECOSYSTEMS

Fungi in Drylands

Fungi inhabit every continent on Earth due to their abilities to adapt to a variety of conditions and colonize even the most inhospitable substrates. In dryland ecosystems, fungi occupy multiple niches within soils and plant tissues due to their diverse lifestyles and trophic modes (Jumpponen et al., 2017; Ladwig et al., 2021). Soil fungal communities are species rich with hundreds to thousands of taxa found in < 1 g of surface soil (Taylor & Sinsabaugh, 2015), and diverse assemblages of fungi and other microbes can be found in the upper < 10 cm of dryland soils where organic matter inputs, labile carbon (C) and nitrogen (N) pools, and microbial activity are highest (Hansen et al., 2023; Mueller et al., 2015; Pombubpa et al., 2020). In dryland soils with high pH and generally low soil moisture, saprotrophic fungi express oxidative enzymes (i.e., phenol oxidases and peroxidases) both intracellularly to synthesize cell protective compounds (described below), and extracellularly to degrade lignin, cellulose, and other soil organic matter components to acquire essential nutrients (Sinsabaugh, 2010). Additionally, mycorrhizal fungi that obligately associate with plant roots can secrete different organic acids, proteins and enzymes to access soil organic N and phosphorus (P) and transfer them to host plants (Hodge et al., 2000). Studies of dryland fungi also indicate that fungal metabolism can dominate N transformation reactions, particularly denitrification and the production of N_2O from soils (Crenshaw et al., 2008; McLain & Martens, 2006), and fungi may play key roles in N cycling processes in some arid environments (Marusenko et al., 2013). In drylands, just as in other ecosystems, soil microbial communities are arguably the most important drivers of biogeochemical cycling, and fungi undoubtedly serve important functions in

these cycles of soil C and N decomposition, turnover, and transfer (Collins et al., 2008; Rudgers et al., 2018).

Adaptations

Fungi have several key adaptations for withstanding environmental stressors such as low water availability and periodic drying/rewetting in dryland soils (Schimel 2018). They display a high degree of phenotypic plasticity and have diverse morphology which allows them to respond quickly to changing availability of soil moisture and nutrient substrates, especially in habitats with patchy resource distribution (Dighton, 2018). Some xerophytic fungi can function at lower soil water potentials than either plants or bacteria (Table 1), which makes them uniquely responsive to even small moisture inputs (Allen, 2007; Ndinga-Muniania et al., 2021). Fungi also have a suite of physiochemical adaptations for cell protection and osmoregulation that may be particularly relevant in drylands, including protective molecules like melanin, mycosporines, and carotenoids; osmoregulatory solutes like glycerol, erythritol, and mannitol; and surface-active proteins (hydrophobins), all of which maintain cell integrity and preserve internal solute concentrations while tolerating periods of extreme abiotic stress from temperature, pH, and/or osmotic conditions (Gostinčar et al. 2012; Schimel et al. 2007; Sterflinger et al. 2012). Melanin production in cell walls has been hypothesized to be a key functional trait contributing to water and UV stress tolerance in various fungal lineages (Fernandez & Koide, 2013), and may prevent cell damage from multiple types of radiation that would destroy the cellular structure of other organisms (Dadachova & Casadevall, 2008). At the soil surface, particularly in hot deserts with high levels of UV radiation, these protective molecules may contribute to the survival of various fungal taxa and allow them to persist under extreme environmental stress.

Fungi also have diverse morphological adaptations and growth forms, and filamentous taxa with multicellular, branched hyphal networks can facilitate acquisition and cycling of water and dissolved nutrients in dryland soils (Porras-Alfaro et al., 2011). For example, once a water molecule is taken up by a hydrophilic hyphal tip, it is protected from external soil conditions within hydrophobic, multilayered cell walls that prevent desiccation (Allen 2007; Allen 2009), and hyphal networks can draw water along the outside of hydrophobic cell surfaces via surface tension (Allen, 2007). Mycorrhizal hyphae have also been found to translocate hydraulically lifted water from tree roots into surrounding soils (Querejeta et al. 2003). Relatively small hyphal diameters (>1.5 μm; Teste et al., 2006) allow for access to water and minerals from within rock matrices and soil pore spaces which plant roots cannot penetrate, and hyphae may also bridge gaps across soil pores in dry soils, which could facilitate water and nutrient movement even under extended drought conditions in drylands (Allen 2011).

Finally, diverse fungal lineages have adapted a multitude of reproductive strategies (Warren et al., 2019). For example, pathogenic fungi can survive on multiple hosts during different phases of their life cycle and survive in a dormant state in the soil via the production of resistant spores which germinate when environmental conditions are favorable (Hajek et al., 2018). Systemic endophytes found in tissues of ~20-30% of all grass species can be vertically transmitted via infected inflorescences to seeds and horizontally transmitted via asexual (e.g, epiphyllous conidia) or sexual propagules (e.g., ascospores; Rodriguez et al. 2009). Some dryland fungi form thick-walled, melanized cell aggregations and others may grow in microcolonies where individual cells serve as vegetative propagules, thus eliminating the energetic expense of spore production (Sterflinger et al., 2012; Taylor & Sinsabaugh, 2015).

Table 1.1 Soil moisture potential limits on activity of different organisms, ordered from least to most tolerant of dry soil conditions.

Organism	**Growth limits**	**Reference**
Nitrifying bacteria	-0.6 MPa	Stark & Firestone 1995
Vascular plants	-1.5 MPa	Ratliff et al. 1983 Savage et al. 1996
Gram negative bacteria	-2 MPa	Freckman 1986
Gram positive bacteria (Actinobacteria, Firmicutes)	-2 to -10 MPa	Griffin 1981 Fierer et al. 2003 Zenova et al. 2007
Ectomycorrhizal fungi	-3 MPa	Coleman et al. 1989 Fernandez & Koide 2013
Basidiomycete decomposers	-4 to -7 MPa	Griffin 1977 Dix 1984
Arbuscular mycorrhizal fungi	-3 to -21 MPa	Allen et al. 1989 Jasper et al. 1989
Ascomycete (xerophilic) fungi	-7 to -60 MPa	Magan & Lynch 1986 Williams & Hallsworth 2009

Arbuscular Mycorrhizae

The diversity and abundance of fungi in drylands, like other terrestrial ecosystems, is also influenced by their associations with living plants. Several biotrophic fungal groups are found within tissues of dryland plant species, and I will start by describing the better-known root associates known as arbuscular mycorrhizal fungi or AMF (Phylum Glomeromycota). AMF are obligate symbionts that rely on living plant hosts for nutrition and form associations with ~80% of plant species (Johnson 2010). AMF hyphae penetrate root cortical cells via specialized infection structures (e.g., appressoria) and form an intraradical mycelium with characteristic intercellular branched structures called arbuscules where they bidirectionally exchange nutrients from the soil environment for photosynthetically derived carbon from plants (Allen 2009). AMF proliferate via aseptate (coenocytic) hyphae which are distinguishable by a lack of septa or

partitions dividing their hyphal cells and can store carbon in lipids, vesicles and hyphal coils within the intraradical mycelium (Smith & Read 2008). AMF can be transmitted horizontally between plants via the production of thick-walled, multinucleate spores, which can persist in soil surface layers and germinate in response to specific host plant exudates (Camargo-Ricalde et al. 2021; Requena et al. 2007). AMF also form an extraradical mycelium which can constitute a substantial proportion of soil microbial biomass in some environments, and these hyphae can produce exoenzymes to solubilize soil P complexes and to mineralize organic N such as proteins, peptides and amino acids, as well as compounds (i.e., glomalins) which aggregate soil particles (Johnson et al. 2010; Fierer et al. 2012). Mycorrhizae may transform organic N into inorganic forms before transferring it to host plant roots (Govindarajulu et al., 2005; Moe, 2013) and are significant conduits for C fluxes from plants to soils (Johnson et al., 2002). Some studies in semiarid grasslands have shown that AM fungi are abundant and ubiquitous in plant roots (Johnson et al. 2003, Allen et al. 1981), while others have found this group to be rare in comparison to other root-colonizing fungal endophytes (see below section; Barrow 2003, 1997, Porras-Alfaro et al. 2007, 2011, Green et al. 2008). Due to their expansion of the surface area and uptake capacity of roots, and their roles in transporting nutrients from the soil matrix to plants and among neighboring plants, AMF may play an important role in assisting plant acquisition of water and nutrients from nutrient-limited dryland soils (van der Heijden et al. 2015; Allen 2007).

Endophytes

In addition to mycorrhizal fungi in Glomeromycota, fungal endophytes belonging to Ascomycota and Basidiomycota are found in living tissues of most vascular plants, where they colonize intracellular spaces of root, stem and leaf cells alongside other endophytic microbes

including bacteria, microalgae, and protozoa (Porras-Alfaro and Bayman 2011; Baron and Rigobelo 2022). A polyphyletic group of facultative, root-associated fungi are the so-called "dark septate" endophytes or DSE, which are distinguished visually from other root inhabiting taxa by the presence of darkly pigmented, melanized, septate hyphae (Mandyam and Jumpponen 2005). These diverse fungi are facultative biotrophs that associate with ~600 plant species across the world and are prevalent in the roots of dryland plants (Porras-Alfaro and Bayman 2011) as well as found abundantly in dryland soil microbial communities (Bates et al. 2010). DSE form inter- and intracellular hyphae which grow between cortical and epidermal cells as well as on the root surface and into surrounding rhizosphere soil (Rodriguez et al. 2009; Barrow 2003). Dark-septate root endophytes also form intracellular microsclerotia, or dense, melanized clusters of thick-walled cells, but notably lack specialized structures for nutrient exchange such as arbuscules (Jumpponen and Trappe 1998). DSE are rarely known to form a teleomorphic (sexual) reproductive stage and reproduce via asexual conidia and hyphal fragments, although some can also form round chlamydospore-like cells within the root cortex (Rodriguez et al. 2009; Knapp et al. 2018). DSE are ubiquitous and prevalent in roots of grassland plants around the world (Romero-Jiménez et al., 2022; Rudgers et al., 2022), and prior studies have found high levels of root colonization in environments such as alpine, arctic, and arid ecosystems where they may facilitate greater stress tolerance to host plants (Kivlin et al. 2013; Mandyam and Jumpponen 2005; Li et al. 2018). In dryland ecosystems, these symbionts may affect the responses of plant communities to increased warming, drought, precipitation variability and other environmental stressors, and a better understanding of the dynamics between DSE and AMF within host plants and in soils are still needed (Bueno de Mesquita et al. 2018; Mack and Rudgers 2008).

Biological Soil Crusts

The distribution of soil fungi in drylands can be spatially heterogeneous, and their diversity, functioning, and activity depends on water availability as well as soil microsite characteristics (Austin, 2011; Ladwig et al., 2021; J. Zhang et al., 2023). Across global drylands, microbial diversity is concentrated in the topmost layers of soil due to the presence of biological soil crusts (biocrusts), which are consortia of micro- and macroscopic organisms including algae, cyanobacteria, fungi, bacteria, mosses and lichens that mediate nutrient inputs, outputs and exchanges in surface soils (Weber et al., 2022). Biocrusts contribute significantly to dryland net primary production and N-fixation and influence worldwide nutrient cycling patterns as they are estimated to cover 12% of Earth's land surface (Elbert et al. 2012; Rodriguez-Caballero et al. 2018). In addition to increasing surface soil fertility through C and N fixation, biocrusts affect the stability of surface soils which in turn controls erosion, water infiltration, seed germination and the capture and retention of nutrients from dust and organic matter (Belnap et al., 2016).

Biocrust Fungi

Biocrusts are hotspots for biodiversity and often support large communities of free-living, lichenized, and mycorrhizal fungi across spatial scales as well as different biocrust successional stages (Bates et al. 2012; Steven et al. 2015; Warren et al. 2019). Ascomycete fungi are the most common fungal biocrust constituents across broad biogeographic regions, including DSE taxa (Order Pleosporales) and other diverse fungal classes (e.g., Dothidiomycetes and Sordariomycetes). Both culture-based and fungal sequencing studies have consistently demonstrated the prevalence of DSE fungi in biocrust surface soils, which often make up 60-80% of identifiable taxa (Aanderud et al., 2018; S. T. Bates, Garcia-Pichel, et al., 2010; Ndinga-Muniania et al., 2021; Porras-Alfaro et al., 2011; T. Zhang et al., 2016). Basidiomycete taxa are

also commonly found across biocrusts, including saprotrophic taxa that are important decomposers of lignin, cellulose and other soil organic matter (Hudson et al., 2015) and there is at least some evidence of potentially ectomycorrhizal taxa, though they are likely low in abundance (Pombubpa et al., 2020; T. Zhang et al., 2016). AMF have received relatively less attention as biocrust constituents but are also detected in surface soils through use of phospholipid fatty acid analysis (PLFA; Omari et al. 2022), microscopic evaluation of soil spore abundance (Camargo-Ricalde et al. 2021), and DNA sequencing with AMF-specific primers (Hernández-Hernández et al. 2017). It is likely that these and other filamentous fungi contribute to microbial biomass, soil aggregation, and nutrient exchanges within biocrusts, but the precise functional roles of biocrust fungi are not well-defined (Bates et al. 2012; Maier et al. 2016).There is some evidence of geographic similarity in biocrust fungal community composition, particularly in lichen-dominated biocrusts within the same ecoregion (Bates et al. 2010; Bates et al. 2012; Pombubpa et al. 2020), and multiple studies have observed higher bacterial vs. fungal biomass and diversity (Bates et al. 2010; Mueller et al. 2015; Hansen et al. 2023; Steven et al. 2014), but more comparative studies are needed to betters understand the potential roles and interactions of biocrust-associated fungi.

DRYLAND NUTRIENT CYCLING

At a broader scale, the roles of dryland fungi, soil microbes, and plants in biogeochemical cycling are entwined with larger ecosystem functions in drylands, which are also considered in this dissertation. In dryland soils, variable inputs of water and organic matter also drive high spatial and temporal heterogeneity of essential compounds such as carbon (C), nitrogen (N) and phosphorus (P), and annual net primary productivity (ANPP) is considered co-limited by both

water and N availability (Hou et al. 2021; Schlesinger et al. 1996; Hooper and Johnson 1999). Dryland N limitation arises due to a number of interconnected biotic and abiotic factors: aboveground organic matter inputs are minimal due to photodegradation, wind erosion, and macrodetritivory, which remove litter before it can be redistributed and broken down in the soil (Collins et al. 2008; Throop and Archer 2009). Belowground nutrients also accumulate slowly because of soil characteristics such as high pH and low moisture content, which supports high oxidative enzyme potentials and prevents stable soil organic matter complexes from forming (Stursova et al. 2006; Sinsabaugh 2010). Soil N availability for plant uptake following a precipitation pulse is largely regulated by microbial processes, and bacteria and fungi can rapidly initiate N transformations like mineralization, ammonification, nitrification, and denitrification following soil rewetting (Krichels et al. 2022; Jackson et al. 1989; Huygens et al. 2016). However, the generally low availability of water and the asynchrony of precipitation inputs can also decouple microbial N mineralization from plant uptake (Augustine and McNaughton 2004), resulting in potential ecosystem N losses due to leaching and/or gaseous N emissions from soils (Leitner et al. 2017; Dijkstra et al. 2012; Brown et al. 2022).

The Fungal Loop Hypothesis

In dryland ecosystems, drought-tolerant, biocrust-associated fungi that also colonize plant roots have been hypothesized to form biogeochemical bridges that exchange nutrients and water between primary producers, an idea known as the "fungal loop hypothesis" (Collins et al. 2008; Green et al. 2008). Underlying this hypothesis are several lines of evidence in regard to dryland fungi, including the following assumptions: (i) due to their roles in N transformation in dryland soils, fungi rather than bacteria may dominate dryland nutrient cycling processes (H. Chen et al., 2015; Crenshaw et al., 2008; McLain & Martens, 2006). Due to their physiological and

metabolic adaptations for drought tolerance ((Allen, 2011; Stevenson et al., 2015), hyphae of dryland fungi may be (ii) active under dry conditions and/or (iii) more efficient at moving water and nutrients through dry soils compared to physical soil processes alone. Finally, (iv) fungi found in surface soil biocrust communities share some degree of similarity with DSE taxa that heavily colonize grass roots (Bates et al. 2012; Collins et al. 2008; Green et al. 2008), and taxa found in biocrust soils as well as plant roots could potentially be functionally integrated and may facilitate water and nutrient exchanges between the two producers.

DISSERTATION SUMMARY

To address some of the topics set out above, the overarching goal of this dissertation is to investigate the existence of connections between plants, fungi, and biocrusts and their importance in nitrogen (N) cycling and movement in grassland ecosystems in the Northern Chihuahuan Desert. In the following chapters, I provide a better understanding of several aspects of plant and microbial nutrient dynamics and begin to explore the mechanisms by which fungi might recouple critical nutrient cycling processes in these ecosystems by testing several of the mechanisms underlying the fungal loop hypothesis (outlined above). Here, I present three research studies that address nitrogen movement and uptake processes in dryland plants and microbes within a semiarid grassland ecosystem. Chapter 2 compares short-term N acquisition by different plant functional types and reviews the limited background literature describing dryland plant N uptake processes while testing assumption (iii) by providing clearer context for the expected rates of plant N uptake in absence of fungal translocation through soil. Chapter 3 explores the similarities and differences among fungi found in biocrust soils and roots of a dominant grass species and measures their responses to multiple global change factors while

testing assumption (iv) that taxonomic overlap in biocrust and root fungi could indicate potential functional overlap. Chapter 4 explicitly examines the role of fungal hyphal networks in connecting spatially separated biocrust and plant patches and tests assumptions (i-iii) to better understand the abiotic and biotic conditions under which fungi may mediate plant N uptake from surface soil communities. Altogether, this dissertation explores the various roles of plants and fungi in nutrient movement within drylands, and their responses to increased variability in N and water availability under predicted global change. The research presented here provides novel insights into rates of N movement and uptake by dryland plants and evaluates the diversity and functioning of dryland fungal communities and their potential importance in connecting nutrient cycling processes in these globally important ecosystems.

Chapter 2: Rapid foliar uptake of inorganic and amino acid nitrogen in three dryland plant species

ABSTRACT

Dryland primary production is often nitrogen (N) limited due in part to spatiotemporal decoupling of soil nutrient availability and plant uptake. Our aim is to quantify inorganic and organic N uptake at daily timescales to compare short-term nutrient acquisition patterns among dryland plant species. We assessed N uptake in three commonly co-occurring perennial plant species from a Chihuahuan Desert grassland (a C_4 grass, C_3 grass, and C_3 subshrub). In the greenhouse, we applied ^{15}N-ammonium, nitrate, or glutamate tracers to plant roots and quantified uptake and recovery in leaves after 12, 24, and 48 h. Plants took up inorganic and amino acid N to leaves as rapidly as 12 h following application, and uptake more than doubled between 24 and 48 h. Inorganic N uptake was 3-4x higher than glutamate in all three species, and plants took up ammonium and nitrate at 2-3x faster rates overall. On average, *Bouteloua eriopoda* had the highest inorganic N recovery and uptake rates, while *Gutierrezia sarothrae* had the highest glutamate uptake over time. *Achnatherum hymenoides* uptake was ~50% lower than the other two species after 48 h. Plants showed similar patterns of short-term foliar uptake and recovery indicating a lack of niche partitioning by N form among the three dryland species measured. Our results support that soil inorganic N, particularly nitrate, may comprise a greater proportion of plant N nutrition than amino acid-N and may be more widely exploited following a precipitation pulse in this habitat.

INTRODUCTION

In dryland ecosystems, aboveground primary production is constrained by the episodic availability of soil water and nitrogen (N) for plant uptake (Hooper & Johnson, 1999; Reichmann et al., 2013; Yahdjian, 2011). The amount and forms of plant-available soil N are restricted by low organic matter inputs (Hou et al., 2021; Stursova et al., 2006), high gaseous N losses (Homyak et al., 2016; Leitner et al., 2017; Whitford & Duval, 2019), and seasonal soil moisture fluctuations which impact rates of soil N cycling processes (Austin et al., 2004; Hartley et al., 2007; Lajtha & Schlesinger, 1986; Reynolds et al., 2003). Additionally, microbial N transformations (e.g., mineralization and nitrification) can happen within minutes following soil rewetting (Jackson et al., 1989; Krichels et al., 2022), and bioavailable sources of N can be depleted or lost to the atmosphere within < 24 hours of a precipitation event if plant uptake is decoupled from microbial release (Brown et al., 2022; Collins et al., 2008; Schimel & Bennett, 2004). Thus, knowing when and how rapidly different plants acquire different soil N forms for growth is important to understanding patterns of N availability and loss in dryland soils (Homyak et al., 2016).

Numerous studies indicate that roots of both mycorrhizal and non-mycorrhizal plants can acquire multiple forms of soil N, including inorganic compounds such as nitrate (NO_3^-) and ammonium (NH_4^+), as well as dissolved organic N forms like amino acids, peptides, and proteins (Daly et al., 2021; Farrell et al., 2013; Hill & Jones, 2019; Smith & Chalk, 2021; Warren, 2014; Wilkinson et al., 2015). For agricultural plant species, N uptake and recovery are well detailed and have been previously reviewed (Engels & Marschner, 1995; Farzadfar et al., 2021; Glass, 2003; Smith & Chalk, 2020; Vidal et al., 2020), but these rates are difficult to compare with dryland species since most agroecosystem-based experiments use irrigated crop plants and often

apply N fertilizers to soils at higher concentrations than what would be found in natural systems (Farzadfar et al., 2021; Jones et al., 2009). In non-cultivated plant communities, plant uptake of free amino acids can be significantly greater than inorganic N from soils (Bueno et al., 2019; Hill et al., 2011; Li et al., 2016; Näsholm & Persson, 2001), and soil organic N can make up a significant portion of plant nutrition in seasonally N-limited arctic, boreal and alpine ecosystems (Lipson & Näsholm, 2001; Miller & Bowman, 2003; Näsholm et al., 2009; Schimel & Chapin, 1996). Compared to these more mesic habitats, there is limited information on the concentrations and relative contribution of soil organic N to dryland plant N nutrition. Few comparative studies of dryland plants have generally found higher recovery and 1.5-5x greater rates of inorganic N uptake compared to amino acids like glycine (Aanderud & Bledsoe, 2009; Jin & Evans, 2010; Ouyang et al., 2016; Yang et al., 2022; Zhuang et al., 2020), although experimental methods and species vary. Understanding the limitations on soil N availability as well as the patterns of dryland plant N uptake may ultimately expand our knowledge of how resource-limited plants adapt different strategies for acquiring soil N and contribute to a better understanding of N cycling processes and ecosystem functioning in drylands.

In addition to gaining a more complete picture of the dryland N cycle, another reason to understand plant N uptake patterns is the potential for resource partitioning, or complementary uptake of different chemical N forms by different species, which has been suggested as one way for plants to maximize resource capture and species diversity in soils with limited N resources (J. Chen et al., 2015; Huygens et al., 2016; Jin & Evans, 2010; Ouyang et al., 2016). However, there is mixed evidence to support this phenomenon in drylands. Several soil-based dryland experiments found low relative uptake of amino acid-N tracers into plant tissues compared to inorganic N, which was attributed to strong microbial competition for organic N rather than

niche specialization among species (Chen et al., 2015; Huygens et al., 2016; Jin & Evans, 2010; Ouyang et al., 2016). An alternate understanding of resource use by N-limited plants is that co-occurring species exhibit niche plasticity – rather than specialization – and can take up multiple forms of N from shared soil pools wherever and whenever they are available (Chalk & Smith, 2021; Chesson et al., 2004; Hong et al., 2017; Miller & Bowman, 2002; Stahl et al., 2011). Differences in dryland plant uptake of NH_4^+, NO_3^-, and amino acid-N are more likely to be driven by individual growth strategies and competition for spatiotemporally variable local N sources than by species-specific "preferences" for N (Chalk & Smith, 2021; Chesson et al., 2004; Hong et al., 2017; James et al., 2009; James & Richards, 2007; Patrick et al., 2009; Stahl et al., 2011), and it is possible that dryland plant species may exhibit resource use plasticity, but more comparative studies of N uptake dynamics among species with different growth strategies are needed, especially if soil water and nutrient uptake are asynchronous following a moisture pulse to these systems (BassiriRad & Caldwell, 1992b; Gebauer & Ehleringer, 2000).

To explore dryland plant N uptake capabilities, we here investigate the timing of root-to-leaf N uptake in 2 perennial grasses and 1 subshrub species from a semiarid grassland-shrubland transition zone in the Northern Chihuahuan Desert. We conducted a greenhouse experiment to compare N uptake of ^{15}N-labeled ammonium (NH_4^+), nitrate (NO_3^-), and glutamate (an amino acid) over 12 to 48 hours. Our study examined three main questions: **(1)** How rapidly do these dryland plants take up available soil N? Based on prior studies, we predicted that 24 h would be sufficient for observing foliar ^{15}N uptake as other studies have documented increased photosynthetic response, leaf transpiration, and root proliferation within 24 h following natural and experimental precipitation events in drylands (Gebauer et al., 2002; Lauenroth et al., 1987; Sala & Lauenroth, 1982; Thomey et al., 2011). Prior experiments have also observed that 48 h (2

days) is a reasonable measured limit after which evapotranspiration and soil diffusion rates (and thus root N influx) decline in dryland grassland communities (Ivans et al., 2003; James & Richards, 2006; Kurc & Small, 2004). **(2)** Does leaf N uptake differ among inorganic and amino acid N forms? We hypothesized that N uptake patterns would reflect the plant-available soil N pool in this habitat, which is dominated by ammonium over nitrate in the uppermost layers where plant roots are located (Adelizzi et al., 2022; Brown et al., 2022; Kurc & Small, 2004), and that both NH_4^+ and NO_3^- would be taken up at greater rates than glutamate based on our review of past comparative studies which demonstrated greater inorganic versus amino acid N uptake (Bueno et al., 2019; Kuster et al., 2016; Thornton & Robinson, 2005; Yang et al., 2022; Zhuang et al., 2020). **(3)** Do plant species differ in the rate or form of short-term N uptake? We expected that individuals of all three species in this study would ultimately transport similar amounts of ^{15}N to leaves within 12 – 48 h based on evidence from prior dryland ^{15}N tracer experiments that reported recovery of NH_4^+, NO_3^-, and amino acid-N forms in leaves of similar perennial grass and woody shrub/subshrub species < 72 h following application of water and N (Aanderud & Bledsoe, 2009; BassiriRad et al., 1999; Carvajal Janke & Coe, 2021; Ivans et al., 2003; James et al., 2008; Zhuang et al., 2015, 2020). Finally, much of the key background literature comparing inorganic and organic N uptake among different plant functional types comes from studies performed in non-dryland ecosystems such as temperate grasslands (Bardgett et al., 2003; Näsholm et al., 2000; Weigelt et al., 2003; Wilkinson et al., 2015) and tundra ecosystems (Ashton et al., 2008, 2010; McKane et al., 2002; Miller & Bowman, 2003; Miller et al., 2007; Näsholm et al., 2009). Thus, to add context to the methods and results of our study, we also compiled published data from experiments that specifically measured N uptake in dryland plant species.

METHODS

Site description

We studied two grassland locations within the Sevilleta National Wildlife Refuge (SNWR) in central New Mexico, USA. Mean annual precipitation at the SNWR is ~250 mm, with two distinct growing seasons: C_3 shrubs and forbs in the spring, and C_4 grasses during the summer monsoon (July-September) when more than half of annual precipitation occurs (Notaro et al., 2010; Pennington & Collins, 2007). Soil pH is basic (> 8). Total soil N pools at SNWR are 20 g m^{-2}, (Collins et al., 2010), and atmospheric N deposition occurs at an average rate of 0.2 g m^{-2} yr^{-1} at this site, with over half (57%) deposited as NH_4^+ (Burnett et al., 2012; Gibbens & Lenz, 2001; Kurc & Small, 2004). Previous N fertilization experiments indicated that N can be limiting to primary productivity in grasslands at this site (Báez et al., 2007; Collins et al., 2010; Muldavin et al., 2008).

Species descriptions

We sampled three species within the SNWR: *Bouteloua eriopoda* (Torr.) Torr. (black grama), *Achnatherum hymenoides* (Roem. & Schult.) Barkworth (Indian ricegrass), and *Gutierrezia sarothrae* (Pursh) Britton & Rusby (broom snakeweed). These plants overlap within grassland ecotones at SNWR, where graminoids and sub-shrubs make up >75% and 13% of ANPP, respectively (Muldavin et al., 2008; Peters & Yao, 2012; Thomey et al., 2014). These three species also differ in physiology and phenology, and thus may have distinct growth demands and nutrient acquisition strategies. Among the two perennial grass species, *B. eriopoda* is a long-lived, stoloniferous C_4 grass with fibrous, finely divided roots concentrated in the upper 5 – 10 cm of soils (Burnett et al., 2012; Gibbens & Lenz, 2001; Kurc & Small, 2004), and

Achnatherum hymenoides, an early-season C_3 bunchgrass, grows fibrous roots up to 0.8 – 1.5 m below the soil surface (DeFalco et al., 2007; Reynolds & Fraley, 1989; Yoder et al., 2000). *G. sarothrae* is a woody, perennial C_3 subshrub with a taproot extending as far as 1–2 m below the soil surface that allows for rapid subsoil water uptake (Gibbens & Lenz, 2001; Wan et al., 1995). Within grasslands at SNWR, *B. eriopoda* is considered a foundation species and has decreased in abundance under N fertilization treatments (Ladwig et al., 2012). *A. hymenoides* reaches the southernmost limits of its range in mixed grasslands at SNWR (Muldavin et al. 2008), and has not shown strong responses in aboveground cover or foliar N content in N fertilization experiments from the Colorado Plateau (Osborne et al., 2022; Petersen et al., 2004; Phillips et al., 2021). *G. sarothrae* is a sub-dominant species found throughout *B. eriopoda*-dominated grasslands that has shown marginal cover increases in response to N fertilization at 2 g N m^{-2} yr^{-1} (Collins et al., 2010; Ladwig et al., 2012; Muldavin et al., 2008; Thomey et al., 2014). In this habitat, belowground resource competition during the growing season is likely highest in the uppermost 10 – 20 cm of soils where extensive intermixing of grass and shrub roots can occur (Caldwell et al., 1991; Casper & Jackson, 1997; Gibbens & Lenz, 2001; Kurc & Small, 2004; Ogle & Reynolds, 2004; Thomey et al., 2011).

Plant collection

On February 3rd, 2017, we collected 25 individuals of *B. eriopoda,* 75 individuals of *G. sarothrae* from a Chihuahuan Desert grassland site (34.338 N, -106.735 W, 1605 m), and 25 individuals of *A. hymenoides* from a Great Plains/Chihuahuan Desert grassland ecotone site (34.404 N, -106.683 W, 1560 m) within the SNWR. We sampled prior to the start of the spring growing season while plants were still senescent to reduce transplant shock. We selected vegetative individuals < 30 cm in height to better facilitate individual growth in pots, and we

attempted to extract the major roots of each plant up to ~20 cm below the soil surface. Any loosely attached rhizosphere soil was gently shaken from roots prior to potting. Immediately following field collection, we transplanted plants into D40L Deepots (7 x 25 cm, 656 mL, Stuewe & Sons, Tangent, OR, USA) using a 1:1 mixture of sand and Metro-Mix® (SunGro, Agawam MA, USA). Each individual *B. eriopoda* and *A. hymenoides* bunchgrass was split into three different pots so that genetically identical individuals would receive an addition of each ^{15}N tracer (see section below), and grasses were trimmed to the crown to remove past season leaves.

Greenhouse set-up

We divided up the total individuals of each species to be maintained in greenhouses at the University of New Mexico (150 pots) and the University of Texas at El Paso (75 pots). Plants in both greenhouses had identical supplemental overhead lighting (10 h light, 14 h dark) and were hand-watered to soil water holding capacity 1-3 times per week for ~6 weeks following harvest to stimulate growth. Of the total plants collected (N = 225 individuals), 60 of *B. eriopoda*, 63 of *A. hymenoides* and 42 of *G. sarothrae* (N = 165) plants survived to tracer application (see next section). We positioned pots in trays > 20 cm apart so that no leaves touched between individuals. Prior to tracer application, we removed each individual from their pot and gently wrapped aluminum foil around all roots and soils below the stem to better constrain the contents of the pot while accessing the roots. A small opening was left at the bottom of each aluminum wrap for water to drain, and wrapped plants were placed back in their respective pots. One day prior to tracer application, we watered all pots to free drainage and collected green leaf samples to measure natural abundance of stable isotopes for each species.

^{15}N tracer application

Plants were randomly selected to receive one of three ^{15}N-labelled isotopic tracers (all at 98 atom % ^{15}N): i) ammonium chloride ($^{15}NH_4Cl$); ii) potassium nitrate ($K^{15}NO_3$); or iii) L-glutamic acid ($HO_2C(CH_2)_2CH(^{15}NH)CO_2H$; Sigma-Aldrich, Inc., St. Louis MO, USA). Each solid ^{15}N tracer was mixed into 25 mL of Milli-Q® purified water (MilliporeSigma, Burlington, MA, USA) to create three aqueous solutions at the following concentrations: 0.057 *M* $^{15}NH_4Cl$, 0.057 *M* ^{15}N-glutamate (both 0.43 mg ^{15}N per plant), or 0.048 *M* of $K^{15}NO_3$ (0.36 mg ^{15}N per plant). While the latter was added at a slightly lower solution concentration (due to a minor miscalculation), the mass of ^{15}N detected in leaves indicated that the total amount of $^{15}NO_3^-$ added per plant (0.36 mg) was enough to exceed the detection limits for each species. We chose these ^{15}N solution concentrations to enable detection of plant uptake and allocation without significantly exceeding background soil inorganic N concentrations measured in unamended soils at this site (Table S2.3). Each individual plant received only one type of ^{15}N tracer to avoid the potentially inhibitory effects of combining chemical N forms (Miller et al., 2007; Thornton & Robinson, 2005).

All ^{15}N tracer solutions were applied to roots and rhizosphere soils between 8:00 – 9:00 AM. Immediately prior to tracer application, we securely covered aboveground stems and leaves with a sealable plastic bag to prevent ^{15}N solutions from inadvertently contacting leaf surfaces. We then removed each plant from its pot, opened the aluminum foil wrap to access the roots, and applied 0.5 mL of ^{15}N tracer solution directly to the outer surface of all visible roots and soils using a 2.5 mL glass atomizer bottle. The aluminum foil wrap was then re-secured around the roots to keep the soils in place before reinserting into pots, and the aboveground plastic bag was removed and discarded.

Sample collection and processing

We collected 5 leaves from each plant at 12, 24, and 48 hours post-application in order to capture two day/night cycles when plant stomata would be open to facilitate transpiration-driven water movement from roots to leaves. This timescale was chosen based on prior dryland experiments that reported N recovery in leaves of similar species within 24 – 48 hours following application of aqueous ^{15}N tracer solutions to soils (Adelizzi et al., 2022; BassiriRad et al., 1999; Green et al., 2008; Ivans et al., 2003; James & Richards, 2006). For some individuals, we could not harvest sufficient leaf material at every time point (0, 12, 24, and 48 h) due to poor aboveground condition and/or small size of leaves. At the end of the experiment, we clipped all shoots, rinsed roots clean from soil using tap water, and separated above- and belowground biomass for drying. All plant samples were dried for 3 d at 60 °C and then weighed to the nearest 0.1 mg following collection.

Leaf samples from each time point were ground for 24 to 32 h in 1.5 mL plastic scintillation vials using stir bars to homogenize tissue. Approximately 4.5 mg of ground leaf material was packed in aluminum capsules (CE Elantech, Lakewood, NJ) for ^{15}N analysis. Samples were analyzed at the Center for Stable Isotopes (University of New Mexico) on an ECS 4010 Elemental Analyzer and a Delta V Isotope Ratio Mass Spectrometer (Thermo Fisher Scientific, Waltham, MA, USA), at the University of California-Davis Stable Isotope Facility using a PDZ Europa ANCA-GSL elemental analyzer interfaced to a PDZ Europa 20-20 isotope ratio mass spectrometer (Sercon Ltd., Cheshire, UK), or at the EaSI Lab in the Department of Geological Sciences at the University of Texas at El Paso, in which samples were combusted using a PyroCube® (Elementar, Langenselbold, Germany), followed by isotope analysis with a continuous-flow isotope ratio mass spectrometer (IsoPrime GeovisION, Elementar,

Langenselbold, Germany). Samples were sent to different facilities to increase data turnaround time, and facility location had no significant influence on isotope values because standards sent to each facility did not significantly differ in nitrogen content ($N = 17$; $P = 0.18$) among facilities.

Response variables

Nitrogen isotope ratios were expressed in δ notation (‰) using atmospheric N_2 as the standard (Mariotti, 1983). Leaf samples collected prior to ^{15}N tracer addition (Time 0) were used to calculate natural abundance or background $\delta^{15}N$ values for each species (*B. eriopoda*, *A. hymenoides*, and *G. sarothrae*) at each greenhouse location where plants were grown (see Table 2.1). We used the average $\delta^{15}N$ natural abundance values to estimate six "enrichment cutoff" values by fitting a kernel density function to each set (one set per species × location; Warren & Silverman, 1987) and selecting the 99.9^{th} percentile as the cutoff value. We chose a conservative threshold for the cutoff estimate to be certain that the ^{15}N tracers we applied at the roots had indeed been assimilated into aboveground tissues. We considered post-addition samples with $\delta^{15}N$ values above the respective species cutoff value to be "enriched", and those with $\delta^{15}N$ values equal to or below the species cutoff as "unenriched". For our analyses, we used a subset of 220 enriched leaf samples out of the total 278 collected, excluding 23 Time 0 samples (leaves collected prior to ^{15}N tracer addition) and 35 non-Time 0 samples that were unenriched, or had enrichment values below their respective species cutoff value.

For enriched samples only, we first determined the total mass of all N (M_{sample}) in leaves using the following equation:

$$M_{\text{sample}} = \%\text{N}_{\text{plant}} \times \text{adw}_{\text{plant}}$$

where $\%N_{plant}$ is the average %N across all leaf samples of the same plant, and adw_{plant} is the total aboveground dry weight (dw) of all leaf samples plus the final harvested biomass from the plant (mg). We then determined the proportion of ^{15}N measured in each leaf sample (F) using the following equation:

$$F = \frac{R}{(1 + R)}$$

where R = sample $\delta^{15}N$ value converted to atom %. We then calculated the total mass of ^{15}N in each post-addition sample ($M_{labeled}$) using the following equation (Robinson, 2001):

$$M_{labeled} = M_{sample} \times F$$

We did the same for all leaves collected at Time 0 to calculate the total mass of ^{15}N in each natural abundance sample ($M_{background}$). We then subtracted $M_{background}$ (mg) from $M_{labeled}$ (mg) to determine *leaf N uptake*, or the total mass of ^{15}N recovered in leaves in excess of natural abundance (mg ^{15}N per g leaf dw). We converted this value to µg and then to µmol ^{15}N by dividing it by the atomic mass of N (14.0067 u) for ease of comparison with other studies.

To answer Question 1, we calculated the mean *N uptake rate* (µmol ^{15}N per g dw per h) by dividing leaf N uptake by time (h) since tracer addition for each sample, and then averaged values across samples in each tracer, species, or tracer × species group to determine the speeds at which plants took up applied ^{15}N to leaves (Table 2.3, Table S2.1).

Other responses

For individuals that were sampled at all three post-addition time points, we calculated percent (%) N recovery per plant using the following equation:

$$\%\text{ N recovery} = \frac{\text{Total mass of } ^{15}N \text{ recovered in leaves}}{\text{Total mass of } ^{15}N \text{ applied to plant}} \times 100$$

where the total mass of ^{15}N recovered in leaves equals the cumulative sum of leaf N uptake from all samples collected from the same plant (mg), and the total amount of ^{15}N applied equals 0.43 mg (or 0.36 mg for plants given $K^{15}NO_3$).

We also calculated the percentage of leaf samples enriched for each ^{15}N tracer × species group by dividing the total number of enriched samples by the total number of samples collected at each time point and multiplying by 100.

Table 2.1 Leaf natural abundance ± standard error and calculated enrichment cutoff $\delta^{15}N$ values (permille, ‰) for three plant species (*B. eriopoda*, *A. hymenoides*, and *G. sarothrae*) maintained at two different greenhouse locations at the University of New Mexico (UNM) or University of Texas at El Paso (UTEP). For *G. sarothrae*, natural abundance $\delta^{15}N$ values were only measured from plants at UNM, so one cutoff value was applied for that species.

Plant Species	Institution	Natural Abundance (‰)	Enrichment Cutoff (‰)
Bouteloua eriopoda	UNM	1.90 ± 1.01	8.63
	UTEP	1.47 ± 0.36	2.74
Achnatherum hymenoides	UNM	0.25 ± 0.83	5.15
	UTEP	-0.17 ± 1.17	4.25
Gutierrezia sarothrae	UNM	-1.30 ± 0.29	-0.06

Analysis

We performed all statistical analyses in R version 4.0.5 (R Core Team 2021). To answer Questions 2 and 3, a linear mixed-effects (lme) model was fit by maximum likelihood using the 'lmer' function in the *lme4* package version 1.1-27 (Bates et al., 2015) to compare leaf N uptake among different ^{15}N tracers and plant species over time. Response data were log-transformed in order to improve the normality of residuals. The full lme model included ^{15}N tracer (3 levels: NH_4^+, NO_3^-, or glutamate), plant species (3 levels: *B. eriopoda, A. hymenoides,* or *G. sarothrae*), and time point (3 levels: 12, 24, or 48 h) as categorical fixed effects, and plant genotype (n = 58;

nested within plant species), and pot ID (n = 86; nested within plant species and genotype) as random effects to account for repeated measures of the same plant genotype and individual.

The significance of main effects and interactions was assessed via analysis of deviance Type II tests using the 'Anova' function in the *car* package version 3.0–10 (Fox et al., 2012). Results were visualized using the *visreg* package version 2.7.0 (Breheny & Burchett, 2017) and the amount of variance explained by our whole model was substantial (marginal R^2 = 0.29, conditional R^2 = 0.88; see Table S2.2). We checked model fit by performing a backwards model selection process where terms were sequentially removed and compared the reduced models to the full model using analysis of variance (ANOVA) via the 'anova' function in the R *stats* package version 4.2.2 (R Core Team 2022) and the Akaike Information Criterion (AIC). The final model included all 3 fixed effects but removed the random effect of plant genotype, which obtained statistically similar results to the full model (LRT: X^2 = 1.0, P = 0.32) with a slightly smaller AIC value. Including time as a categorical vs. continuous variable did not significantly affect model fit (LRT: X^2 = 8.7, P = 0.47), and results using categorical time are reported below to allow for nonlinear change through time. We checked the normality of model residuals via a Kolmogorov-Smirnov test using the 'km.test' function in the *R stats* package version 4.2.2 (R Core Team 2022), which indicated that the residuals were normally distributed (D = 0.08, P = 0.13). We assessed homogeneity of variance across groups by performing a Levene's test on model residuals using the 'leveneTest' function in the *car* package version 3.0–10 (Fox et al., 2012) and found that the assumption of equal variances was met for tracer (F = 0.71, P = 0.49), species (F = 0.40, P = 0.67), and timepoint (F = 0.77, P = 0.46). We also checked the final model for uniformity, over- and under-dispersion, outliers, and zero inflation (none detected) of fitted vs. simulated residuals using tests within the *DHARMa* package version 0.4.5 (Hartig,

2022). *Post hoc* pairwise comparisons of treatment means for main effects and interactions among ^{15}N tracer × time, species × time, and ^{15}N tracer × species × time were performed in the *emmeans* package version 1.6.1 (Lenth, 2021). *P* values were adjusted for multiplicity using the Tukey method for comparing a family of 3 estimates, and all pairwise comparisons of means used the Kenward-Roger degrees-of-freedom method and a 0.95 confidence level.

Literature search and review

To help place our results in context and compare broader trends of plant N uptake in dryland habitats, we compiled existing data from 30 experiments in 28 published studies that quantified uptake of inorganic and/or organic ^{15}N tracers in uncultivated dryland plant species. We used a combination of Google Scholar (https://scholar.google.com) and Connected Papers (https://www.connectedpapers.com) to search for publications that included more than one chemical N form and/or plant species from dryland ecosystems only. We derived study data directly from main text data tables and figures and supplementary materials as necessary, using ImageJ (Schindelin et al., 2012) to determine values from graphical data. We report values from 20 soil-based experiments from field (n = 16), greenhouse (n = 2), and growth chamber (n = 2) settings, and 10 laboratory assay experiments in which plant N uptake was quantified via depletion of assay solutions by either roots of "intact" plants (those still connected to aboveground tissues) or excised roots only. For experiments that measured plant N uptake from soils, the application of ^{15}N tracer solutions occurred either at the soil surface (i.e., to biological soil crust patches, or to the entire plot surface in a simulated rainfall event) or in the upper ~10 cm of soils, where solutions were injected directly into the soil at one or more points surrounding a target plant. In studies that applied N at multiple soil depths (e.g., 0-5 cm and 5-10 cm), we averaged values across depth. In solution-based experiments where solutions of varying N

concentrations were used, we reported the median concentration (i.e., if solutions ranged from 0 to 1000 μM ^{15}N, we reported results from plants in 500 μM solutions only). Details on the chemical form and concentration of N added were simplified by converting concentrations to similar molar (*M*) units where possible. In studies that featured other experimental manipulations (e.g., elevated CO_2, drought or warming treatments, etc.), we reported data from non-treated control or ambient conditions only and averaged across technical replicates, if applicable. In some studies, the authors combined results from NH_4^+ and NO_3^- applications although they were applied to plants separately, and this is noted in Table 2.5.

We grouped data based on the most common N uptake responses measured across studies: (i) percent N recovery, or the percentage (%) of ^{15}N recovered in plant tissues out of the total amount applied; (ii) N uptake rate, or the amount of ^{15}N in excess of natural abundance per gram plant dry weight (dw) per unit time, most often expressed as micromoles ^{15}N per gram root dw per hour; and (iii) aboveground plant $\delta^{15}N$ values following isotopic tracer application, expressed as permille (‰). Note that $\delta^{15}N$ values alone are not directly comparable among different studies without additional information about the total mass of the elemental N pool in those study systems (Chen et al., 2015; Daly et al., 2021; Owen & Jones, 2001). If the amount of foliar ^{15}N recovery by mass (excess N) was the only result reported, we converted values to micromoles ^{15}N for ease of comparison and divided these values by the time since application to calculate rates of N uptake per hour. In one case, we include N uptake rates measured in terms of soil surface area (e.g., milligrams N per square meter per hour) instead of by plant mass (Jackson et al., 1989). For studies using more than one N form, we also calculated two unitless ratios to compare proportional N uptake and recovery among chemical forms (NH_4^+ vs. NO_3^- and inorganic vs. organic N) regardless of addition amount. For studies that included at least one

inorganic and one organic form, we divided inorganic N values (averaged across both NH_4^+ and NO_3^- when applicable) by those from amino acid-N to calculate the inorganic:organic ratio.

RESULTS

How rapidly do these dryland plants take up available N?

Rapid N transport from roots to leaves occurred within 12 h of tracer application (mean ± SE leaf uptake at 12 h = 0.27 ± 0.05 μmol ^{15}N g^{-1} dw) and more than doubled between 24 h (mean ± SE = 0.34 ± 0.07 μmol ^{15}N g^{-1} dw) and 48 h (mean ± SE = 0.86 ± 0.13 μmol ^{15}N g^{-1} dw) across all ^{15}N tracers and species (time point main effect: $X^2 = 215.94$, $P < 0.001$; pairwise comparisons of 12 vs. 24 h: $t = -4.71$, $P < 0.001$, and 24 vs. 48 h: $t = -10.13$, $P < 0.001$; Table 2.2, Fig. 2.1). Overall minimum and maximum rates of N uptake ranged from 0.002 to 0.045 μmol ^{15}N g^{-1} dw h^{-1} over the course of the experiment, and mean N uptake rates were ultimately similar across 48 h for all species and tracer types (mean ± SE = 0.017 ± 0.002 μmol ^{15}N g^{-1} dw h^{-1}; Table 2.3), matching our statistical model results which did not find a significant difference in the three-way interaction of ^{15}N tracer × Species × Time: $X^2 = 2.73$, $P = 0.950$; Table 2.2). Mean percent N recovery after 48 h was 6.0 ± 1.1% across all plant individuals, which was ~6x higher at the conclusion of the experiment versus after 12 h post-application (mean ± SE = 1.0 ± 0.2%; Table 2.4).

Table 2.2 Results from generalized linear mixed effects ANOVA model testing for main and interacting effects of ^{15}N tracer type (ammonium, nitrate, and glutamate), plant species (*B. eriopoda, A. hymenoides*, and *G. sarothrae*) and time (12, 24, and 48h post-application) on leaf N uptake. Significant predictors ($P < 0.05$, Type II Wald Chi-square tests) are bolded.

	Leaf N Uptake		
Predictors	df	X^2	P

^{15}N Tracer	2	**19.05**	**< 0.001**
Species	2	3.25	0.197
Time	2	**215.94**	**< 0.001**
^{15}N Tracer × Species	4	1.79	0.774
^{15}N Tracer × Time	4	**14.94**	**0.005**
Species × Time	4	**17.53**	**0.002**
^{15}N Tracer × Species × Time	8	2.73	0.950

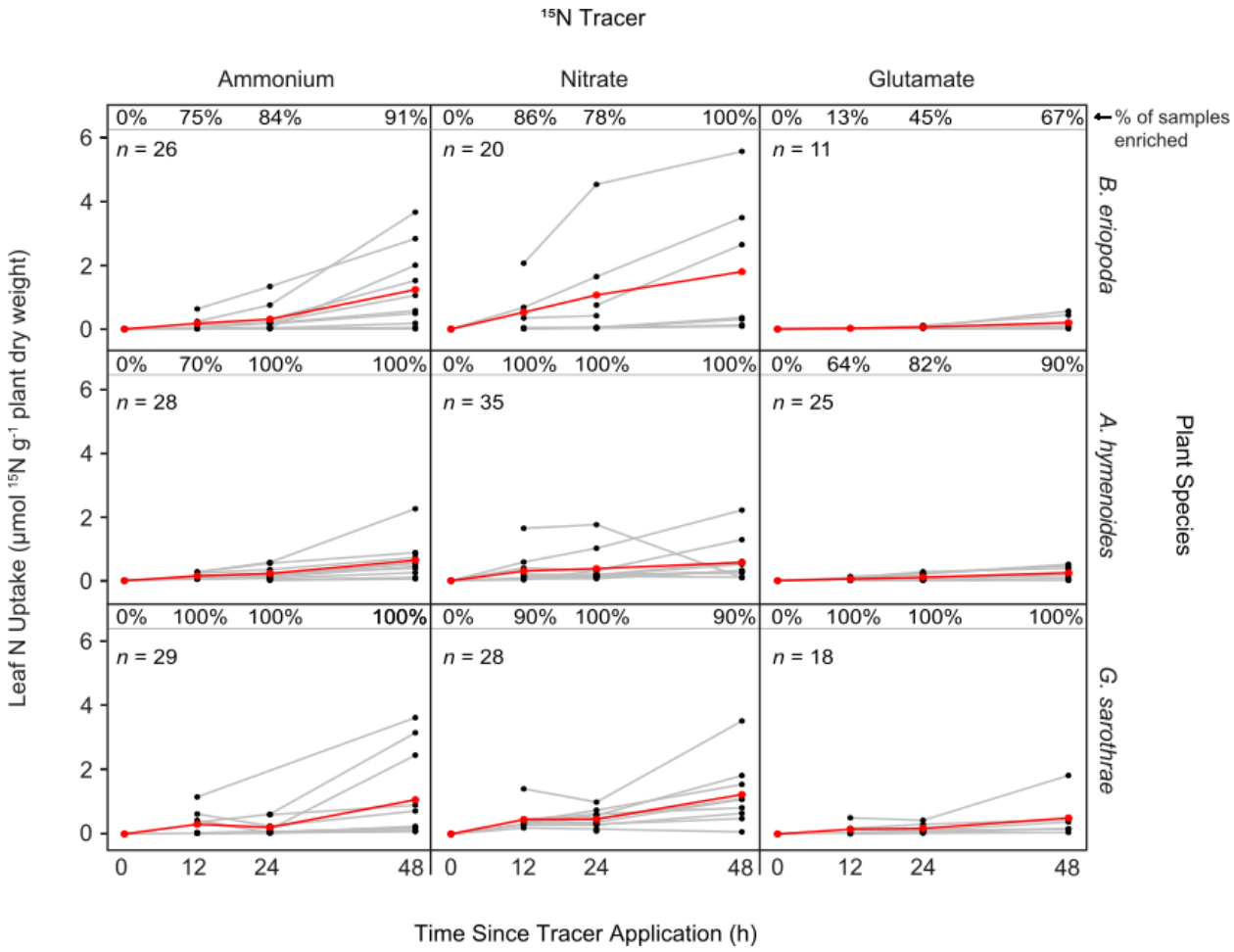

Fig. 2.1 Leaf N uptake (μmol ^{15}N per g plant dw) over time (h) of ^{15}N-enriched samples only (*N* = 220) collected from individuals of *B. eriopoda*, *A. hymenoides,* and *G. sarothrae* before and after application of one of three ^{15}N tracers (ammonium, nitrate, or glutamate) to root and rhizosphere soils. Grey lines connect samples from the same plant individual while red lines show mean N uptake rates (μg ^{15}N per g plant dw per h) for each tracer and species group. The percentage (%) of leaf samples considered N-enriched out of the total number of samples (*n*) for each ^{15}N tracer × species × time point group is displayed at the top of each panel.

Table 2.3 Leaf N uptake (μmol ^{15}N per g plant dw) and N uptake rate (μmol ^{15}N per g dw per h) for ^{15}N-enriched samples only (N = 220). Mean ± standard error (SE) values are averaged across n samples for each ^{15}N tracer or plant species level, and overall mean is averaged across the 3 post-addition time points (12, 24, and 48 h). Significant predictors ($P < 0.050$, Type II Wald tests) are bolded; superscript letters indicate significant *post hoc* differences among levels ($P < 0.05$).

			Leaf N Uptake (μmol ^{15}N g^{-1} plant dw)				
	Levels	n	12	24	48	Overall Mean	N Uptake Rate
^{15}N Tracer	Ammonium[a]	83	0.23 ± 0.07	0.26 ± 0.06	0.99 ± 0.20	0.53 ± 0.09	0.017 ± 0.002
	Nitrate[a]	83	0.41 ± 0.10	0.59 ± 0.17	1.13 ± 0.27	0.70 ± 0.11	0.027 ± 0.004
	Glutamate[b]	54	0.10 ± 0.04	0.13 ± 0.03	0.32 ± 0.09	0.19 ± 0.04	0.006 ± 0.001
Species	*B. eriopoda*[c]	57	0.34 ± 0.17	0.53 ± 0.23	1.16 ± 0.33	0.73 ± 0.16	0.024 ± 0.005
	A. hymenoides[c]	88	0.20 ± 0.07	0.26 ± 0.07	0.51 ± 0.10	0.33 ± 0.05	0.012 ± 0.002
	G. sarothrae[c]	75	0.33 ± 0.08	0.31 ± 0.06	1.01 ± 0.23	0.56 ± 0.09	0.020 ± 0.003

Table 2.4 Percent (%) N recovery of NH_4^+, NO_3^-, and glutamate in leaves of *B. eriopoda*, *A. hymenoides*, and *G. sarothrae* plants over 48 h. Mean and standard error (SE) values are averaged for species × ^{15}N tracer combination across the 3 post-addition time points for ^{15}N-enriched samples only (N = 220).

	B. eriopoda		*A. hymenoides*		*G. sarothrae*	
^{15}N Tracer	Mean	Max	Mean	Max	Mean	Max
NH_4^+	3.79 ± 1.28	15.85	2.00 ± 0.52	10.22	1.81 ± 0.61	15.85
NO_3^-	8.36 ± 3.42	47.96	2.91 ± 0.85	15.00	4.72 ± 1.00	23.44
Glu	0.85 ± 0.28	2.16	0.76 ± 0.19	2.70	1.42 ± 0.45	9.12

Does leaf N uptake differ among inorganic and amino acid N forms?

On average across species, plants took up 3-4x more of the two inorganic N forms (NH_4^+ and NO_3^-) than the amino acid glutamate (^{15}N tracer main effect: $X^2 = 19.05$, $P < 0.001$; pairwise comparisons of glu vs NH_4^+: $t = 2.74$, $P = 0.021$; vs NO_3^- $t = -4.39$, $P < 0.001$) from roots to leaves (Table 2.2). Across all species and timepoints, plants given NO_3^- had the highest leaf N uptake on average (mean ± SE = 0.70 ± 0.11 μmol ^{15}N g^{-1} dw), followed by NH_4^+ (mean ± SE = 0.53 ± 0.09 μmol ^{15}N g^{-1} dw), and then glutamate (mean ± SE = 0.19 ± 0.04 μmol ^{15}N g^{-1} dw; Table 2.3). Plants took up 2-3x more NH_4^+ than glutamate after 12 and 48 h on average (pairwise comparison of NH_4^+ vs. glu at 12 h: $t = 2.84$, $P = 0.014$; 24 h: $t = 1.73$, $P = 0.198$; and 48h: $t = 2.81$, $P = 0.017$), and 3-4x more NO_3^- than glutamate at every post-application time point (pairwise comparisons of glu vs. NO_3^- at 12 h: $t = -4.68$, $P < 0.001$; 24 h: $t = -3.73$, $P < 0.001$; and 48 h: $t = -3.44$, $P = 0.002$; Table 2.3, Fig. 2.2a). Similarly, plants transported NO_3^- 3x faster and NH_4^+ 2x faster (mean rate for both inorganic N forms = 0.02 μmol ^{15}N g^{-1} dw h^{-1}) than glutamate, which moved at an average rate of 0.01 μmol ^{15}N g^{-1} dw h^{-1} across all species (Table 2.3, Fig. 2.1). Plants given inorganic N also had 2-4x higher percent N recovery than those given glutamate and mean ± SE and maximum N recovery, respectively, for each tracer type were NH_4^+: 5.1 ± 1.2% and 16%; NO_3^-: 8.6 ± 2.2% and 48%; and glu: 2.2 ± 0.6% and 9% at the conclusion of the experiment (Table 2.4). The overall highest percent N recoveries were from individuals given NO_3^- at the roots.

Do plant species differ in the rate or form of N uptake?

According to our model, plant species alone was not a significant predictor of the amount of leaf N uptake (species main effect: $X^2 = 3.25$, $P = 0.197$) when averaged across ^{15}N tracers and time (Table 2.2). However, some species-level differences emerged over time (species × time: X^2

= 17.53, $P = 0.002$), and N uptake for each species doubled on average across all tracer types between 24 and 48 h (pairwise comparisons of 24 h vs. 48 h: *B. eriopoda*: $t = -6.74$, $P < 0.001$; *A. hymenoides*: $t = -5.14$, $P < 0.001$; and *G. sarothrae*: $t = -5.56$, $P < 0.001$; Table 2.3, Fig. 2.2b). Overall, *B. eriopoda* N uptake increased the most over time with 3.4x higher uptake after 48 h compared to 12 h post-application (Table 2.3). Across all tracer types, *B. eriopoda* also had ~2-3x greater percent N recovery than *A. hymenoides* and *G. sarothrae*, and overall mean and maximum N recovery, respectively, for each species were *B. eriopoda*: 12.2 ± 4.6% and 48%; *A. hymenoides*: 3.9 ± 0.8% and 15%; and *G. sarothrae*: 5.4 ± 1.2% and 23% (Table 2.4). Differential uptake among species were also apparent at individual time points. For example, *B. eriopoda* and *G. sarothrae* individuals had similar N uptake amounts after 12 h, but *B. eriopoda* tended to take up 1-1.5x more N (across all tracer types) after 24 and 48 h than *G. sarothrae* (Fig. 2.2b), and *A. hymenoides* took up 1-2x less N than the other two species at 12, 24, and 48 h post-application (Fig. 2.2b). *B. eriopoda* and *G. sarothrae* also had marginally faster N uptake rates (mean value = 0.02 μmol ^{15}N g^{-1} dw h^{-1}) than *A. hymenoides*, which had a mean rate of 0.01 μmol ^{15}N g^{-1} dw h^{-1} across all tracers (Table 2.3). Although the interactive effects of N form and species were not considered significant predictors of N uptake in our model (^{15}N tracer × species $P = 0.774$; Table 2.2), *B. eriopoda* plants given NO_3^- had the overall fastest uptake rates (0.04 ± 0.01 μmol ^{15}N g^{-1} dw h^{-1}) and *G. sarothrae* plants took up glutamate ~2x faster than the other two species. The three-way interaction of ^{15}N tracer × species × time was also not significant in our model ($P = 0.950$; Table 2.2), however *G. sarothrae* took up 2.5-5x more glutamate than *B. eriopoda* and 1.6-2.5x more glutamate than *A. hymenoides* at each time point, and the two grass species took up similar amounts of NH_4^+ and glutamate over time (Table S2.1). Overall, each of

the three species followed a similar pattern of NO_3^- > NH_4^+ > glutamate uptake over time (Fig. 2.1; see Table S2.1).

While we did not statistically compare the percentage (%) of leaf samples that were enriched for each ^{15}N tracer × species group over time (top of each panel in Fig. 2.1; see Fig. S2.1), we also note some patterns that emerged among species. For *G. sarothrae*, plants had 100% of leaves enriched at nearly every timepoint across all N tracer types, except for plants given NO_3^- after 12 and 48 h, which both had 90% of samples enriched. The percent of leaves enriched for *B. eriopoda* plants given NO_3^- also decreased from 86% to 78% between 12 and 24 h, but then increased to 100% after 48 h. This seemingly anomalous pattern is likely due to the fact that most plants do not assimilate root N into all leaves in a consistent pattern (Chen et al., 2015; Daly et al., 2021; Owen & Jones, 2001), and that we collected a different set of leaves from each individual at each time point to account for this potential variation in leaf N uptake. *B. eriopoda* plants given glutamate also had the overall lowest percentage of leaves enriched (13%) after 12 h, and only 67% enriched after 48 h, which was ~40% lower than *B. eriopoda* plants given NH_4^+ and NO_3^- which had 91% and 100% leaf enrichment after 48 h, respectively. At each time point, *A. hymenoides* plants given glutamate also tended to have ~10-20% lower leaf enrichment compared to those given inorganic N tracers, and *A. hymenoides* individuals given NO_3^- were 100% enriched at every time point.

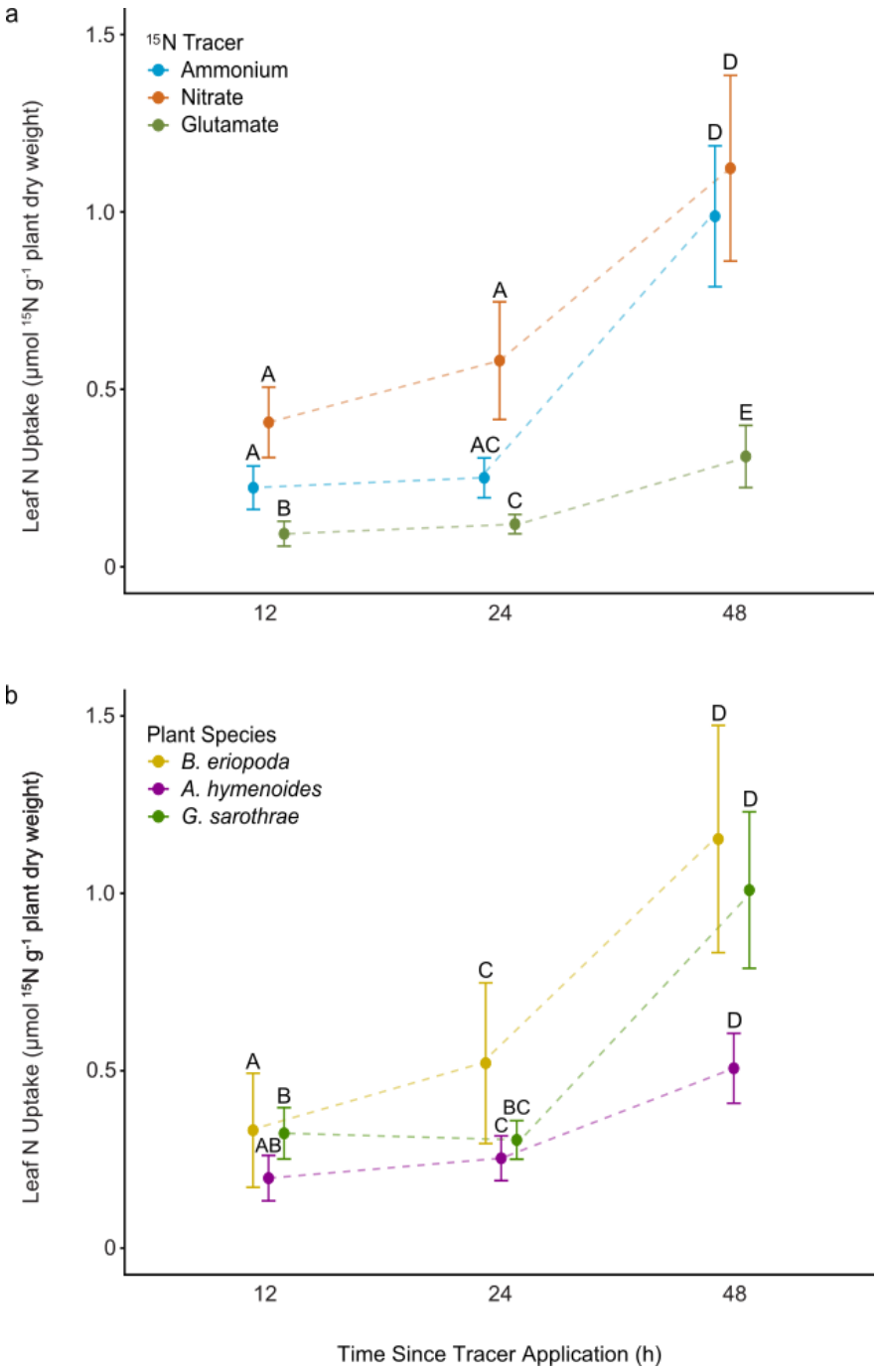

Fig. 2.2 Mean leaf N uptake ± standard error (µmol ^{15}N per g plant dw) of (a) ^{15}N tracer types (ammonium, nitrate, glutamate) averaged across species, and (b) plant species (*B. eriopoda*, *A. hymenoides,* and *G. sarothrae*) averaged across tracer types at each time point measured (12, 24, and 48 h). Letters indicate significant *post hoc* differences ($P < 0.050$) among (a) ^{15}N tracers at each time point, and across time for each ^{15}N tracer type; and (b) species at each time point, and across time for each species. Values are reported in Table 2.3.

Literature review

All of the 30 dryland N uptake experiments we found included at least one form of inorganic N (NH_4^+ and/or NO_3^-). Nine experiments only compared both inorganic N forms (NH_4^+ *and* NO_3^-), 11 experiments only used one inorganic form (NH_4^+ *or* NO_3^-), 3 experiments used a combined inorganic form (NH_4NO_3), and 7 studies compared at least one inorganic N form with an organic amino acid form (see Table S2.4 for study details). Percent N recovery results reported from 8 soil-based experiments were the simplest response to compare across studies with different methodologies, and we found that percent recovery of NH_4^+ ranged from 1.2% to 73.5% (median = 12.5%) and of NO_3^- ranged from 0.8% to 85.1% (median = 30.8%; Table 2.5) across 7 studies that injected each tracer individually into soils surrounding plants. One study used $^{15}NH_4{}^{15}NO_3$ and found 0.3% to 6.7% recovery in two subshrub species from 8 – 48 h (James & Richards, 2006). In experiments that compared inorganic and organic N uptake, ^{15}N-glycine was the most widely used amino acid, and percent recovery of glycine ranged from 0.6% to 41.6% (median = 7.8%) across 6 studies. One experiment applied ^{13}C-^{15}N-glutamate to biocrust soil patches < 1 m away from perennial bunchgrass tussocks (Green et al., 2008) and found 0.2% to 0.4% N recovery in leaves between 1 and 4 d following application (Table 2.5). Results from studies measuring both inorganic and organic N uptake consistently found higher percent recovery of NO_3^- compared to amino acid-N, and similar or lower percent recovery of NH_4^+ compared to amino acid-N recovery. Overall, all reported studies that compared inorganic and organic N forms had recovery ratios > 1 (Table 2.5).

Prior dryland studies that quantified N uptake rates per unit time were primarily laboratory assay experiments which measured inorganic N depletion from nutrient solutions of known concentrations within a range of ~0.5 to 4 hours (see Table S2.4). The 10 solution-based

experiments that we reviewed documented the highest uptake rates overall, ranging from 4.6 to 25.2 μmol ^{15}N g^{-1} dw h^{-1} for NH_4^+ (median = 9.8), and 2.1 to 17.8 μmol ^{15}N g^{-1} dw h^{-1} for NO_3^- (median = 5.9; Table S2.5). One study (James et al., 2009) combined results from both inorganic forms, and these rates ranged from 1.6 to 9.1 μmol ^{15}N g^{-1} dw h^{-1} (median = 7.3). We only found one dryland experiment that measured organic N uptake from solution of an aquatic plant species (Schiller et al., 1998), but it was not included due to differences in physiology and habitat. For soil-based experiments, regardless of the N addition method, inorganic N uptake rates were much lower than those measured in solution-based experiments, with values ranging from 0.002 to 2.1 μmol ^{15}N g^{-1} dw h^{-1} for NH_4^+ (median = 0.20) and from 0.05 to 14.9 μmol ^{15}N g^{-1} dw h^{-1} for NO_3^- (median = 0.42; Table S2.5). Foliar uptake rates of amino acid-N from soils were reported from ^{15}N-glycine in 4 studies (Jin & Evans, 2010; Ouyang et al., 2016; Yang et al., 2022; Zhuang et al., 2020) and ranged from 0.01 to 1.98 μmol ^{15}N g^{-1} dw h^{-1} (median = 0.19). Results from 6 field-based experiments that only reported leaf $\delta^{15}N$ values at more than one timepoint indicate that overall, foliar $\delta^{15}N$ enrichment from NH_4^+, NO_3^-, or NH_4NO_3 increased significantly over time (> 48 h) following water and ^{15}N tracer application (Table S2.5).

Table 2.5 Percent (%) N Recovery results from published studies measuring soil inorganic and organic N uptake in dryland plant species. Values are reported as percent (%) of applied ^{15}N recovered in plant shoots. The ratio of NH_4^+:NO_3^- recovery represents %NH_4^+ recovery divided by %NO_3^- recovery (unitless). The ratio of inorganic:organic N recovery represents the average % recovery of NH_4^+ and NO_3^- (if both forms were applied in the study) divided by the % amino acid recovery (unitless). Data are from control (no treatment) plots only. An "--" indicates that the variable was not measured in the study. An "NA" indicates that the variable could not be determined or calculated based on the data provided in the study.

			%N Recovery			Recovery Ratio	
Reference	Plant Species	Time	NH_4^+	NO_3^-	AA[d]	NH_4^+:NO_3^-	Inorg:Org
Jackson, Schimel & Firestone 1989	*Avena barbata, Bromus mollis, Lolium multiflorum*	24 h (Feb)	8.7	19.6	--	0.44	--
		24 h (Apr)	10.7	25.9	--	0.41	--
James & Richards 2006	*Atriplex confertifolia*	8 h	3.8	**	--	NA	--
		12 h	3.1	**	--	NA	--
		24 h	5.3	**	--	NA	--
		48 h	6.7	**	--	NA	--
	Atriplex parryi	8 h	0.3	**	--	NA	--
		12 h	0.3	**	--	NA	--
		24 h	1.9	**	--	NA	--
		48 h	3.3	**	--	NA	--
James et al. 2008	*Bromus tectorum*	72 h	22.0	49.3	--	0.45	--
	Taeniatherum caput-medusae		17.4	43.5	--	0.40	--
	Elymus elymoides		10.2	35.7	--	0.29	--
	Pseudoroegneria spicata		17.0	21.3	--	0.80	--
	Poa secunda		14.9	24.8	--	0.60	--
	Crepis intermedia		20.4	48.7	--	0.42	--
	Lomatium triternatum		20.8	52.8	--	0.39	--
Green et al. 2008	*Bouteloua* spp.	24 h	--	5.1	Glu: 0.2	--	21.11
		4 d	--	9.4	Glu: 0.3	--	28.01

Aanderud & Bledsoe 2009	*Bromus diandrus*	72 h	73.5	51.4	Gly: 38.6	1.43	1.62
	Bromus hordeaceus		48.7	47.4	Gly: 41.6	1.03	1.16
	Elymus glaucus		23.3	52.5	Gly: 29.3	0.44	1.29
	Nassella pulchra		21.8	45.0	Gly: 23.5	0.48	1.42
Wang et al. 2016	*Leymus chinensis*	3 h (Aug)	1.2	0.9	Gly: 0.6	1.42	1.90
	Stipa grandis		1.3	0.8	Gly: 0.8	1.57	1.39
Zhuang et al. 2020	*Erodium oxyrrhynchum*	24 h (May)	2.7	3.3	Gly: 2.2	0.80	1.35
	Hyalea pulchella		3.4	3.6	Gly: 2.5	0.95	1.41
	Nonea caspica		6.6	5.8	Gly: 3.8	1.15	1.65
	Lactuca undulata		3.4	5.4	Gly: 2.8	0.62	1.60
Yang et al. 2022	*Cleistogenes squarrosa*	3 h	11.1	76.5	Gly: 13.1	0.15	3.34
	Leymus chinensis		8.1	85.1	Gly: 7.8	0.10	6.00
	Stipa grandis		13.9	75.5	Gly: 11.4	0.18	3.91
Present Study	*Achantherum hymenoides*	12 h	0.5	1.2	Glu: 0.2	0.41	4.67
		24 h	1.5	2.7	Glu: 0.6	0.54	3.39
		48 h	4.0	5.0	Glu: 1.6	0.80	2.80
	Bouteloua eriopoda	12 h	0.6	2.1	Glu: 0.1	0.28	16.69
		24 h	2.4	7.8	Glu: 0.3	0.31	15.83
		48 h	9.1	18.5	Glu: 2.2	0.49	6.39
	Gutierrezia sarothrae	12 h	1.0	1.8	Glu: 0.5	0.56	2.90
		24 h	1.2	3.8	Glu: 1.1	0.33	2.36
		48 h	3.4	8.6	Glu: 2.7	0.40	2.23

*Study combined results from $^{15}NH_4^+$ and $^{15}NO_3^-$ treatments **Study added ammonium nitrate ($^{15}NH_4{}^{15}NO_3$)

DISCUSSION

Our experiment resulted in three main findings: 1) dryland plants transported all sources of available nitrogen to leaves as rapidly as 12 h following ^{15}N tracer application to roots; 2) plants given NH_4^+ and NO_3^- took up 3-4x more N to leaves and had 2-4x higher percent N recovery than those given glutamate; 3) each of the three plant species took up inorganic N sources 2-3x faster than glutamate, with a similar pattern of $NO_3^- > NH_4^+ >$ glutamate uptake over time.

How rapidly do these dryland plants take up available soil N?

Overall, these results indicate that inorganic and organic forms of ^{15}N can be translocated from roots to aboveground shoots on the scale of 12 to 48 hours in wild-harvested plants of *B. eriopoda*, *A. hymenoides*, and *G. sarothrae* under non-water-limiting conditions. We observed the highest N recovery 48 h following tracer application, and mean N uptake rates more than doubled between 24 and 48 h, suggesting that these plants may continue to take up available inorganic and/or organic N within several days of a pulse event until nutrient supply and soil moisture decline. We found less N recovery compared to some other soil-based dryland experiments, which could be due to the relatively lower concentrations and solution amounts (0.5 mL) that we used in order to reflect realistic soil nutrient availability at the roots of plants in this ecosystem. We intentionally used tracer amounts of N so as not to exceed background soil levels, which could likely disrupt plant-soil-microbial feedbacks responsible for growth responses and N cycling processes under otherwise natural conditions (Knops et al., 2002; Reynolds et al., 2003). However, these results matched with other dryland experiments that found < 20 % inorganic N recovery and < 5% amino acid-N recovery within 24 to 48 hours of N and water application (James & Richards 2006; Wang et al., 2016; Zhuang et al. 2020), including one field

study in the same Chihuahuan Desert grassland where our plants were collected (Green et al., 2008). On average, the N uptake rates we measured were comparable to several other soil-based experiments that quantified N uptake by roots of intact plants within < 24 to 72 hours (Booth et al., 2003; James et al., 2008; Ouyang et al., 2016), although they were much lower than those measured in solution-based experiments where roots were removed from soils. For example, in one hydroponic experiment, *Bouteloua eriopoda* uptake of NO_3^- after 4 h was 30.98 μmol ^{15}N g^{-1} dw h^{-1} (BassiriRad et al., 1997), which was more than 600x the highest NO_3^- uptake rate we measured from this species (~ 0.05 μmol ^{15}N g^{-1} dw h^{-1}). In a different experiment, NH_4^+ uptake by *A. hymenoides* plants was measured up to 5.6 μmol ^{15}N g^{-1} dw h^{-1} after 30 minutes (Yoder et al., 2000), which was ~250x the highest N uptake rate we measured for *A. hymenoides* in our study (~0.02 μmol ^{15}N g^{-1} dw h^{-1}). We did not find any background reference values for *G. sarothrae*, and we believe that our study is the first to document N uptake rates for this species. These solution-based experiments provide valuable insight into potential short-term nutrient uptake kinetics at timescales ranging from minutes to hours, however they may not capture realistic rates of N uptake from within the soil matrix nor reflect the complexity of rhizosphere interactions (Owen & Jones, 2001; Wang & Macko, 2011). For example, some root-associated mycorrhizae mediate acquisition and biochemical transformation of inorganic and organic soil N before root transfer occurs (Govindarajulu et al., 2005; Leigh et al., 2009; Moe, 2013). Excluding the influence of fungi and other microbes would not accurately capture the feedbacks that regulate root N uptake in soils under more natural conditions, and could ultimately alter the rate and form(s) by which N enters into internal plant uptake pathways over the course of hours to days (Dijkstra et al., 2010; Kuypers et al., 2018; Näsholm et al., 2009; Wen et al., 2022). In our experiment, we did not remove soils attached to fine roots or rhizosheaths prior to potting the

field-collected plants, and it is possible that these types of rhizosphere microbe interactions were preserved. Ultimately, our results support our hypothesis and confirm that 24 h following water and N application is a reasonable study period for observing foliar uptake of different N forms from roots and rhizosphere soils in this plant community.

Does leaf N uptake differ among inorganic and amino acid N forms?

We found significantly greater uptake of NH_4^+ and NO_3^- versus glutamate, an amino acid form, which was transported 3-4x slower from roots to leaves than either inorganic form within 48 hours of this study. These findings are consistent with prior studies where desert shrub/subshrub, grass and herbaceous species acquired more NO_3^- than dissolved organic N from the amino acid glycine (Aanderud & Bledsoe, 2009; Jin & Evans, 2010; Ouyang et al., 2016; Yang et al., 2022; Zhuang et al., 2020), and also matches experiments of woody and grass species from subtropical ecosystems where one experiment found higher NO_3^- uptake relative to glycine after 72 h (Wei et al., 2015), and another found greater NO_3^- uptake compared to glutamine and arginine-N following a 2 h root incubation (Bueno et al., 2019). Plants in most terrestrial ecosystems acquire soil N from mixed pools where mineral and organic N cycling are biologically coupled (J. Chen et al., 2015; Daly et al., 2021; Owen & Jones, 2001), and soil amino acid-N pools are highly dynamic with a half-life of < 1 h in some locations (Chen et al., 2015; Daly et al., 2021; Owen & Jones, 2001). These and other organic N forms can be rapidly depleted and/or mineralized by microbes prior to root uptake (Hodge, Robinson, et al., 2000; Jones et al., 2005) and so mineral N forms are commonly considered the most abundant sources of N for plants in most terrestrial ecosystems (Cramer & Miller, 2005; Kraiser et al., 2011). The significantly slower rates of glutamate uptake in our study could be due in part to short-term microbial competition, since we did not sterilize nor fertilize potting soils during the experiment,

and some of the rhizosphere soils may have contained active microbes that immobilized glutamate-N before it could be transported across root cell membranes (J. Chen et al., 2015; Kwiecinski et al., 2020). On an even shorter timescale, a previous field study evaluating amino acid uptake in *Bouteloua gracilis*, ~50% of applied alanine was recovered in microbial biomass and only 0-1% in plant tissues after 3 h, which they hypothesized was due to rapid fungal uptake and immobilization (Chen et al., 2015; Kwiecinski et al., 2020). Although beyond the scope of our study, it is also possible that applied glutamate was converted into inorganic N forms by rhizosphere microbes prior to root uptake (Rothstein 2014). Using double-labelled (^{13}C and ^{15}N) glutamate and measuring C recovery in roots would provide further insight into potential factors affecting uptake speed of intact amino acid-N to leaves of these species.

Background soil N pool sizes are also an important consideration for making accurate comparisons of plant N uptake across and within ecosystems. For example, although our results demonstrate that these plant species are capable of taking up amino acid-N from glutamate when added as a single N source to roots, soils at our study site have high pH and oxidative enzyme activity and low levels of organic matter accumulation, thus organic N may not be a consistent source for plant N nutrition in this habitat (Stursova & Sinsabaugh, 2008). N from amino acids like glutamate could potentially meet a portion of these species' N demands if NO_3^- and NH_4^+ were not immediately available, but further details on the concentrations and distribution of soil organic N at this site are still needed to clarify these findings.

Among the two inorganic N forms applied, we expected that plants given NH_4^+ would have the highest N uptake based on background measurements of soil N pools at the SNWR (see Table S2.3), but we found consistently higher NO_3^- vs. NH_4^+ uptake across species over time, although the differences were not statistically significant at $P < 0.05$. From our review of other

dryland studies, NO_3^- uptake tends to be higher than NH_4^+ when both were added to soil-based, intact plant systems (NH_4^+: NO_3^- ratio < 1.00), while NH_4^+ uptake tends to be higher than NO_3^- in solution-based experiments where N was consistently provided to roots in nutrient solutions (NH_4^+: NO_3^- ratio > 1.00). These trends may be attributable to solubility of the two mineral forms: NO_3^- is negatively charged and has a much higher soil diffusion rate (effective soil diffusion coefficient = 2.82×10^{-1} cm^2 d^{-1}; Owen & Jones, 2001) than NH_4^+, which can be sorbed to soil particles and becomes less accessible to roots and microbes as soil moisture declines (Wang & Macko, 2011). Additionally, while NO_3^- is more energy intensive for plants to assimilate, it can be stored in plant tissues unlike NH_4^+, which can be phytotoxic if it accumulates in cells (Britto & Kronzucker, 2002; Engels & Marschner, 1995; Moreau et al., 2019). Our results indicate that these grassland species can take up multiple inorganic and organic forms of N locally within 24 h of N reaching the roots, and the clear patterns of greater inorganic N uptake versus glutamate observed across species offer partial support for our hypothesis of $NH_4^+ > NO_3^- >$ glutamate uptake.

Do plant species differ in the rate or form of N uptake?

In our experiment, we did not observe statistically significant differences in N uptake at $P < 0.05$ among the three plant species tested. However, there were a few distinguishable patterns over the 48 h timespan that could likely be attributed to differences in life history strategies and physiology. *B. eriopoda* plants had the overall highest rates of N uptake and recovery in our experiment, which might be expected for a dominant species that forms large monospecific patches at SNWR compared to the other two subdominant C_3 species in our study (Kurc & Small, 2004). The lowest N uptake overall was observed in *A. hymenoides* individuals, which had ~50% less mean N uptake than the other two species after 48 h. This cold desert grass

species reaches the southernmost limits of its range at the SNWR where we sampled (Muldavin, 2002), and it is possible that plants required a different set of environmental conditions to break winter dormancy and/or were experiencing stress when transplanted into the greenhouse. Although the percentage of samples enriched for each species × tracer group do not equate to the amount of N uptake by mass, they indicated that *G. sarothrae* leaves were 100% N-enriched at every timepoint in contrast to the two grass species, particularly noticeable for plants given glutamate at 12 h following application (Fig. 2.1). *G. sarothrae*, a ruderal subshrub, also had higher glutamate uptake than the two grasses at each time point and took up glutamate twice as fast as the other species overall. In the greenhouse pots, *G. sarothrae* individuals had 3-4x higher mean aboveground biomass than either *B. eriopoda* or *A. hymenoides* (data not shown), and potentially greater photosynthetic demands may have driven root uptake in this woody species compared to the two perennial grass species, which could explain the higher percentages of leaves enriched for nearly all N forms for *G. sarothrae*.

Plants in resource-limited habitats may also adopt different belowground strategies to increase the solubility and mobilization of mineral and organic N forms to roots, such as altering root architecture and foraging behaviors (Forde & Walch-Liu, 2009; Jumpponen et al., 2002), or exuding carbon from roots to boost local microbial activity and enzyme production in the rhizosphere (Ladwig et al., 2015). Shallow-rooted dryland grasses can have greater radial root spread to capture soil water from small rain events (Sala & Lauenroth, 1982; Thomey et al., 2014), whereas woody plants can extend lateral and vertical roots to access water and/or nutrients in deeper soil layers (Lee & Lauenroth, 1994; Wan et al., 1995). While these adaptations could also allow coexisting plants to partition resources based on soil depth, the similarities in N uptake observed among *B. eriopoda*, *A. hymenoides* and *G. sarothrae* indicate

that rather than specializing in a certain chemical N form to avoid competing for the same limiting resource, these species may employ similarly flexible strategies for acquiring whichever soil N source is most available when water limitation has been lifted and growth conditions are favorable (Ashton et al., 2008; Chalk & Smith, 2021; Stahl et al., 2011).

While our study quantifies baseline information about relative N uptake in intact plants once water limitation is lifted, inter- and intra-species competition for shared soil nutrients are nuanced and likely more complex than what we were able to measure in a single study. In the greenhouse, roots were constrained to 25 cm depth and had limited lateral spread, pots were watered to field capacity prior to N additions, and individuals were evenly spaced in the greenhouse to receive equal amounts of light and water. These growth alterations, as well as removing individuals from direct competition for local resources, may have muted species-specific N uptake responses that might be more clearly observed under field conditions during their respective growing seasons (James & Richards, 2007; Miller et al., 2007). Under non-water-limiting conditions, our hypothesis was supported as N uptake did not statistically differ among the three species. However, BassiriRad et al., 1999 observed species-level differences in $^{15}NO_3^-$ uptake of two Chihuahuan Desert shrub species in watered vs. unwatered treatments, which supports that co-occurring plants in this system may have differential nutrient uptake responses under more limited soil moisture conditions. In future experiments tracing inorganic or organic N uptake in these species, we may expect that any divergence from rapid (24 to 48 h) root to leaf uptake could be due to other physical, biological, or competitive interactions when N is applied directly to roots or rhizosphere soils.

CONCLUSIONS

Plants of all three grassland species opportunistically took up all forms of available N within 48 h following application of ^{15}N tracers to roots and rhizosphere soils. Our results confirm the occurrence of rapid N uptake in these grassland species once water limitation is lifted, lending support to the concept of serial resource limitation in this dryland ecosystem. Although average percent recovery and root-to-leaf N uptake rates were lower than those measured in some prior experiments, overall we were able to detect a consistent trend across species that showed significantly higher uptake of inorganic N sources (NH_4^+ and NO_3^-) versus an organic amino acid form (glutamate). Since we did not observe significant differences in N uptake by species, the similar uptake pattern and rates indicate that they may have similar capacity for exploiting inorganic soil N sources and suggests they may compete for the same plant-available N pools (e.g., inorganic N and amino acid-N in excess of microbial demand) in their shared habitat. From our review of published N uptake experiments, we can conclude that inorganic N, particularly NO_3^-, is generally taken up at faster rates than amino acid-N in studies that included both inorganic organic N uptake. We also observed that there is a wide range of methods for testing different N forms and plant species, and greater standardization of N application and sample collection methods may facilitate more effective comparisons of short-term uptake among studies and habitats. Assessing nutrient uptake patterns in dryland-adapted plants will improve our understanding of their responses to current and predicted environmental changes, and how asynchronous water and N availability may influence biotic interactions and nutrient retention in these globally important communities. As increasing N deposition and changing climate variables shift the balance of N inputs to dryland soils (Báez et al., 2007;

Ramond et al., 2022), interpreting short-term responses of individuals and the effects on plant community dynamics will be key to mitigating N losses from these ecosystems.

Chapter 3: Responses of biocrust and root-associated fungal communities to nitrogen and water additions in a semiarid grassland

ABSTRACT

Increasing variability in climate factors such as precipitation and nitrogen (N) deposition in drylands may drive changes in diversity and functioning of soil microbial communities. Fungi have been shown to play key roles in soil biogeochemical processes in drylands, but more information is needed on their responses to global change factors and their associations with keystone plant species sensitive to drought and other natural disturbance. We investigated the responses of fungal communities in soils and in roots of a dominant grass species among three long-term experiments in a semiarid grassland ecosystem. We extracted DNA from biocrust soils and roots and sequenced the fungal ITS region to determine the degree of similarity between communities and how different levels and legacies of N fertilization, water addition, or combined water and N additions may influence fungal community composition and structure, fungal functional guilds, soil fungal biomass, and fungal root colonization. Sequencing of the fungal ITS2 region demonstrated that biocrust and root communities are relatively dissimilar and each have more unique OTUs than shared, with 8-12% overlap of mostly saprotrophic taxa. Roots contained distinct functional guilds including symbiotrophs and were heavily colonized by dark-septate endophytic (DSE) taxa. Overall, we found that richness, diversity, and evenness of fungi in roots declined in response to N additions in two experiments (MRME and NutNet) and decreased under water addition treatments at one experiment (MRME) compared to controls, while biocrust community structure, but not richness/diversity, tended to respond more strongly to experimental N and water additions. Soil fungal biomass and the ratios of bacterial:fungal biomass were overall fairly low and did not show significant changes in response to N treatments

across the three experiments. Fungal root colonization was consistently high for septate hyphal morphotypes and only aseptate colonization showed declines under N additions. Fungal communities in biocrust and root microsites may share some functional overlap but are taxonomically distinct. Richness and diversity, but not composition of root fungal communities may be highly sensitive to changes in N inputs and decline under multiple changing environmental conditions such as longer-term water + N fluctuations, while biocrust soil communities may become more similar in composition under increased precipitation variability.

INTRODUCTION

Fungi are considered major microbial drivers of biogeochemical cycles of essential nutrients like carbon (C), nitrogen (N) and phosphorous (P) in every terrestrial ecosystem on Earth. They provide essential ecosystem functions by decomposing organic matter, mobilizing soil nutrients, and enhancing plant root acquisition of water and nutrients (Romero et al. 2023; van der Heijden et al. 2006; Johnson et al. 2013). In dryland ecosystems, fungi can access water and dissolved nutrients at lower water potentials than plant roots (Manzoni et al. 2012; Allen 2007) and can be significant drivers of soil N transformations like denitrification under low soil moisture conditions (Crenshaw et al. 2008; McLain and Martens 2006). Despite these important functions, systematic studies of dryland fungal communities have received infrequent attention, and it is likely that fungal diversity and functioning remains underestimated and underexplored at various scales in these ecosystems (Hawksworth and Lücking 2017).

Prior studies in drylands have detected a wide range of fungal functional guilds in soils, including pathogenic, endophytic, saprotrophic, and symbiotic taxa such as mycorrhizal fungi (Johnson et al. 2003; Camargo-Ricalde et al. 2021; Hamm et al. 2020). In these ecosystems, free-

living fungi can also be part of surface soil communities known as biological soil crusts (biocrusts), which form an assemblage of cyanobacteria, algae, fungi, lichen, bryophytes, and other taxa in the upper 0-2 cm of soils, where they play important roles in C and N cycling and can substantially increase soil N fixation and retention (Barger et al. 2016; Pointing and Belnap 2012). Biocrusts also support a diversity of free-living fungi, and these communities can vary across small spatial scales as well as stages of crust complexity (Abed et al., 2019; Steven et al., 2015). Ascomycetes are the most common fungal biocrust constituents across different dryland regions, particularly those in the order Pleosporales, some of which are also referred to as "dark-septate" fungi or dark-sepatate endophytes – DSE (Bates et al. 2010; Steven et al. 2013; Porras-Alfaro et al. 2008; Green et al. 2008). These fungi are notable for the presence of melanin in cell walls and their tolerance of environmental stressors such as high heat, UV radiation and desiccation (Gostinčar et al. 2012), which are conditions likely experienced by biocrust microbes near the soil surface. Despite their ubiquity, the precise identities and functions of Pleosporalean fungi in biocrusts are not well-defined. Interestingly, these same taxa are also prevalent in roots and rhizosphere soils of different perennial grasses (Kazarina et al., 2023; Lagueux et al., 2021; Rudgers et al., 2022), and may aid in plant growth and survival under stressful abiotic conditions, although their roles as plant mutualists remain relatively understudied compared to groups like arbuscular mycorrhizal fungi (Newsham 2011; Havrilla et al. 2020).

In addition to broadening our knowledge of fungal biodiversity, a better understanding of fungal responses to global change factors is also needed, especially in dryland regions where plant and microbe communities may be highly sensitive to potential changes in drought and climate variability (Maurer et al. 2020). Prior studies of fungal responses to changes in one or more environmental factors have found diverging responses among fungal community

composition and measures of diversity and abundance. For example, a survey of root-associated fungi in grass species under experimental drought treatments found that fungal diversity, richness and evenness and root colonization did not show strong decreases under drought conditions, but the abundance of specific taxa and the structure of fungal communities changed significantly (Lagueux et al. 2021). While some dryland microbes do not show strong diversity responses to N fertilization alone (McHugh et al. 2017; Mueller et al. 2015; Jumpponen et al. 2005), other responses like fungal biomass, root colonization, and interactions with plant hosts can be impacted depending on the rates and duration of N fertilization (Nancy Collins Johnson et al., 2010; Treseder, 2008; Zhou et al., 2017). Studies of altered precipitation regimes in drylands have found that water additions also shift fungal community composition, and fungal biomass can show differing responses based on the frequency and size of rainfall manipulations (Nielsen and Ball 2015; Zelikova et al. 2012; Kwiecinski et al. 2020). Similarly, changes in community composition, but not diversity, followed experimental additions of both water and water + N together due to shifts in the relative abundances of stress-tolerant fungal taxa (She et al. 2018). Improving our knowledge of the effects of multiple environmental factors on the abundance and composition of dryland fungi will better inform our understanding of ecosystem processes and help predict patterns of change in drylands globally.

In this study, we investigate responses of fungi in surface biocrust soils and in roots of black grama (*Bouteloua eriopoda*), a dominant perennial C_4 grass species from the Chihuahuan Desert, to answer the following questions: **(1)** How similar or different are biocrust- and black grama root-associated fungal communities, and which taxa dominate these communities? We expect there to be moderate to high taxonomic overlap with a large proportion of taxa in Pleosporales (Ascomycota) in both biocrust soils and roots, as they have been previously

detected in biocrust soils and within roots of various perennial grass species, including other *Bouteloua* grasses. **(2)** How does N fertilization alter the diversity, composition and abundance of biocrust- and root-associated fungi? We expect that N addition alone may not strongly affect the composition of biocrust and root communities, since responses to N additions without addition of water or C source have been found to be minimal in previous studies. However, there may be decreases in soil fungal biomass and root colonization in response to N addition, especially in experiments on the relatively higher end of N fertilization (i.e., 10 g N m^{-2} yr^{-1}). **(3)** How do changes in rainfall regime alone, and combinations of water and N addition alter biocrust and root-associated fungal communities? We predict that both biocrust and root communities may show greater changes in composition, biomass, and increased diversity under water addition treatments and water + N treatments compared to N treatments alone. We expect that biocrust fungi will show the strongest compositional changes in response to water additions compared to root-associated fungi, due to potentially greater shifts in the abundance of drought-tolerant taxa in microhabitats at the soil surface where soil moisture conditions declines more rapidly than in plant roots.

METHODS

General site description

In this study, we sampled three semiarid grassland locations at the Sevilleta Long-Term Ecological Research program site (SEV-LTER) located within the Sevilleta National Wildlife Refuge (SNWR) at the northern boundary of the Chihuahuan Desert in central New Mexico, USA. Mean annual precipitation at the SNWR is ~250 mm, with 50% or more occurring during the summer monsoon season (July-September) when C_4 grass production peaks (Notaro et al.,

2010; Pennington & Collins, 2007). In 2019, rainfall measurements at one ongoing experiment site totaled 210 mm for the year, ~57 mm (27%) of which occurred from July to mid-September prior to our sampling dates on Sept. 13-14th (Collins 2023). Overall edaphic characteristics are similar among the three sampling sites: pH of sandy loam soils is basic (8.1-8.7) and oxidative enzyme potentials are high in the upper < 20 cm of soils where root biomass is highest (Muldavin et al. 2008; Kieft et al. 1998; Stursova et al. 2006). Atmospheric N deposition occurs at an average rate of 0.2 g m^{-2} yr^{-1} at SNWR, with over half (57%) deposited as NH_4^+ (Báez et al., 2007). Grassland N fertilization experiments within SNWR indicate that N is limiting to primary productivity, and the strength and direction of plant responses depend on the size of seasonal rainfall pulses (Báez et al., 2007; Collins et al., 2010; Ladwig et al., 2012; Muldavin et al., 2008).

Overview of SEV-LTER experiments

Sampling was conducted within three ongoing global change/resource manipulation experiments included in the SEV-LTER program (https://sevlter.unm.edu). The full design and objectives of each experiment have been detailed in several previous publications (Baldarelli et al., 2021; Collins et al., 2010; Thomey et al., 2011); and are described briefly below (Table 3.1).

Monsoon Rainfall Manipulation Experiment

The MRME (34.3441, -106.7268, 1603 m) was established in 2006 and was designed to understand changes in grassland ecosystem structure and function caused by increased precipitation variability (https://sevlter.unm.edu/monsoon-rainfall-manipulation-experiment). MRME includes thirteen 8 m × 14 m plots, ten of which receive additions of reverse osmosis water from overhead sprinklers in addition to ambient precipitation as either monthly "large/infrequent" (L) rainfall events (3 × 20 mm, n = 5) or weekly "small/frequent" (S) rainfall

events (12 × 5 mm, *n* = 5) during the monsoon season from July-September each year (total supplemental water addition= 60 mm yr^{-1}). Three control plots receive ambient precipitation only (no water additions). Nitrogen is added annually to 2 m × 2 m N fertilization subplots nested within each small (SN) and large (LN) rainfall treatment plot (*n* = 13) at the beginning of the monsoon season as NH_4NO_3 at a rate of 5 g N m^{-2} yr^{-1} (50 kg N ha^{-1} yr^{-1}). We sampled all experimental rainfall plots (*n* water addition only; S = 5, L = 5) and their nested N fertilization subplots (*n* water + N addition; SN = 5, LN = 5) along with control plots (no treatment; *n* = 3) and their respective N fertilization subplots (N addition only; *n* = 3). We sampled 2 additional controls from untreated soils outside of the experimental plots but within the fenced project boundary at the MRME site (*N* = 30). Plant cover is dominated by *Bouteloua eriopoda* (70% of total) and subdominant species including *Sphaeralcea wrightii*, *Sporobolus* spp., and *Gutierrezia sarothrae* (Thomey et al. 2011).

Nutrient Network Experiment

The NutNet experiment (34.3597, -106.6914, 1597 m) was established in 2007 and examines the effects of multiple resource additions on plant species composition and soil nutrient concentrations within a grassland ecosystem (https://sevlter.unm.edu/nutrient-network-experiment). Nitrogen is added alone or in combination with other nutrient treatments (P, K, micronutrients) annually to 5 m × 5 m treatment plots at the beginning of the monsoon season as NH_4NO_3 at a rate of 10 g N m^{-2} yr^{-1} (100 kg N ha^{-1} yr^{-1}). Water additions are not included in the NutNet experimental design, and we only sampled N fertilization (N addition only, *n* = 5) and control plots (no treatment, *n* = 5) at this site (*N* = 10). Plant cover is dominated by *B. eriopoda* (50-70% of total), *Gutierrezia sarothrae*, and *Salsola tragus* (Baur et al., 2021a).

Warming-El Nino-Nitrogen Deposition Experiment

The WENNDEx (34.3597, -106.6906, 1598 m) was also established in 2006 and tests the effects of multiple global change drivers (increased temperature, N deposition, and precipitation variability) on species reordering and associated ecosystem functioning in grassland communities (https://sevlter.unm.edu/wenndex). Nitrogen is applied alone or in combination with precipitation and/or nighttime warming treatments annually to 3 m × 3.5 m plots at the beginning of the monsoon season as NH_4NO_3 at a rate of 2 g N m^{-2} yr^{-1} (20 kg N ha^{-1} yr^{-1}). Water treatments are added alone or crossed with other treatments in six winter precipitation events (4 × 5 mm, 1 × 10 mm, and 1 × 20 mm) during January-March for a total supplemental water addition of 50 mm yr^{-1}. We sampled N fertilization (N addition only, n = 5) or water addition (water addition only, n = 5) plots as well as those receiving combined water + N treatments (water + N addition, n = 5) plus control plots (no treatment, n = 5) at the WENNDEx site (N = 20). Plant cover in these plots is dominated by *Bouteloua eriopoda* (25-60% of total), *B. gracilis*, *Pleuraphis jamesii*, and *Gutierrezia sarothrae* (Baur et al., 2021b).

Table 3.1 Sample sizes from three experiments (MRME, NutNet, WENNDEx) sampled within the SEV-LTER site, including the number of plots sampled (*n*) and total annual additions of the following experimental treatments: control (no treatment), N addition only (g N m^{-2} y^{-1}), water addition only (mm y^{-1}), and combined water + N additions. Also included are the total number of biocrust (B) and root (R) samples collected per experiment × treatment. An "--" indicates that water additions were not part of the experimental design (NutNet).

	MRME		NutNet		WENNDEx		*N* samples	
Treatment	*n*	Addition[1]	*n*	Addition	*n*	Addition[2]	B	R
Control	5	None	5	None	5	None	15	15
N only	5	5 g N m^{-2}	5	10 g N	5	2 g N m^{-2}	15	13
Water only	10	S: 60 mm (5) L: 60 mm (5)	--	--	5	50 mm	15	15
Water + N	10	S + 5 g N m^{-2} (5) L + 5 g N m^{-2} (5)	--	--	5	50 mm + 2 g N m^{-2}	15	15
Total	30		10		20		60	58

[1]MRME: Small/frequent (S) rainfall treatments receive 12 × 5 mm water applications; Large/infrequent (L) treatments receive 3 × 20 mm water applications from Jul-Sept. in addition to ambient precipitation.
[2]WENNDEx: Water treatments receive 4 × 5 mm + 1 × 10 mm + 1 × 20 mm water applications from Jan-March in addition to ambient precipitation.

Soil microsite and focal plant descriptions

Dryland fungi inhabit several microhabitat niches within the uppermost soil layers due to localized abundance of soil moisture and nutrient resources surrounding plant roots in the top 10 cm (Sokol et al., 2022; Thomey et al., 2011) and the presence of biological soil crusts (biocrusts) in the uppermost 0–2 cm. At the SNWR, biocrust communities are dominated by filamentous, nonheterocystous, bundle-forming cyanobacteria such as *Microcoleus vaginatus* (Vaucher) Gomont and members of the Coleofasciculaceae (Adelizzi et al., 2022; Fernandes et al., 2022), but can also include other micro- and macroscopic organisms like algae, cyanobacteria, fungi, bacteria, mosses and lichens. Prior studies of biocrust fungal diversity have found abundant Ascomycete fungi in the order Pleosporales within biocrust soils and associated with roots of perennial grasses (Green et al. 2008; Herrera et al. 2011), while arbuscular mycorrhizal fungi (AMF) have had low detection in perennial grass roots at this site (Herrera et al. 2010; Khidir et al. 2010; Porras-Alfaro et al. 2008; Green et al. 2008).

In addition to biocrust soils, we also sampled living roots of black grama (*Bouteloua eriopoda* (Torr.) Torr., a perennial C_4 grass species that comprises up to 80 – 90% of cover within nearly monospecific Chihuahuan Desert grasslands at SNWR (Collins et al. 2020; Muldavin et al. 2008; Peters and Yao 2012; Thomey et al. 2014). Individuals of black grama live up to 40 years and primarily reproduce vegetatively via stolons (clonal propagules), and as such their populations can be highly sensitive to changing climate patterns over time, especially when combined with other disturbances such as fire (Collins et al., 2020; Yanoff & Muldavin, 2008). Populations of black grama within SNWR were found to have high local genetic variation (Whitney et al., 2019) and exhibited negative growth responses to experimental drought and N fertilization treatments (Collins et al., 2010; Ladwig et al., 2012). Black grama populations

influence the establishment of other subdominant species in their habitat, and thus declines or changes to these communities may increase the vulnerability of Chihuahuan Desert grasslands to encroaching woody and/or non-native species, in turn affecting soil nutrient dynamics, resource competition, and carbon storage across multiple scales (Ladwig et al., 2021; Peters et al., 2006).

Biocrust soil sample collection and processing

On September 13-14th, 2019, we collected biocrust soils within each of the abovementioned control and treatment plots at all three experiments (Table 3.1). We determined a standardized method for biocrust soil collection using a removable 0.25 m^2 quadrat subdivided into a 10 × 10 grid, which was aligned with two existing nails inside each plot which marked the sampling area. We then collected 10 biocrust soil "cores" by pressing the open end (1 cm in diameter) of a sterile 2 mL microcentrifuge tube (Thermo Fisher Scientific, Waltham, MA, USA) down 2 cm into the soil surface at each intersection along a central transect within the quadrat grid. The entire quadrat frame was then flipped diagonally, and an additional 10 cores were collected using the same method (total area sampled per plot = 0.5 m^2). A new collection tube was used for each plot, and all soil cores (N = 20) were aggregated into one plastic Ziploc bag which was then sealed and placed in a portable cooler with dry ice for transport. Soils were then homogenized using a 2 mm sieve and temporarily stored at 2-4°C until further processing.

Soil ergosterol extraction and analysis

To quantify fungal biomass from control and N addition only plots (n = 10 for each experiment), we determined the ergosterol content of biocrust soils – note that arbuscular mycorrhizal fungi do not produce ergosterol (Olsson et al., 2003). We subset ~4 g of soil into a 15 mL centrifuge tube and then added 0.5 mL of 0.8% KOH in MeOH solution and mixed thoroughly by inverting each tube. Samples were then incubated in a dry block heater for 30

mins at 80°C (Wallander et al., 2001) and then placed in a tube rack to cool. Once cooled, we removed 1-2 mL of extraction solution using a 3 mL syringe with a 16 g needle attached, and then filtered the extracts through a 0.45 µm nitrocellulose membrane into a 1.5 mL glass HPLC vial. Ergosterol content of filtered extracts was determined using a high-performance liquid chromatograph (HPLC; Thermo Scientific Ultimate 3000, Waltham, MA, USA) with a C18 reversed phase column and standards of 10 mg L^{-1} and 1 mg L^{-1} for calibration. Ergosterol concentrations are provided on a dry mass basis (µg g^{-1} soil).

Soil FAME analysis

To quantify the presence and relative biomass of different microbial guilds from biocrust soils, we subset approximately ~5 g of homogenized biocrust soil from control and N addition only plots (n = 10 for each expt.) and analyzed fatty acid methyl ester (FAME) biomarkers to quantify fatty acids from the phospholipid, glycolipid, and neutral lipid fractions. Soils from each plot were lyophilized (freeze-dried) for 36 hours and sent to the DeForest Lab at Ohio State University for soil extraction and total FAME analysis. Briefly, lipids were extracted from soils using a solution of 5 mL MeOH and 2.5 mL $CHCl_3$ and then saponified using a solution of NaOH dissolved in MeOH and DI water. Samples were incubated at 95°C for 5 minutes, then cooled in a cold-water bath, vortexed, and incubated again for 25 minutes. A methylation reagent containing 6N HCl was added and samples were vortexed, incubated at 80°C for 10 minutes and then cooled. An extraction reagent containing a 1:1 ratio of hexane and MTBE was added and samples were centrifuged for phase separation. The bottom phase was removed, a NaOH base wash solution was added, and samples were centrifuged again for further phase separation. Approximately 0.5 ml of the upper phase was moved to a gas chromatography vial to evaporate the liquid with ultra-high purity N_2 (N-EVAP; Organomation Associates, Inc., Berlin, MA,

USA) at room temperature. Lastly, the FAMEs were suspended using 250 µl of the extraction reagent and sample FAME profiles were analyzed using a HP GC-FID gas chromatograph (HP 6890 series; Hewlett Packard, Palo Alto, CA, USA). Peaks were identified using a calibration standard (No. 1208, MIDI, Inc., Newark, DE, USA) in conjunction with the Sherlock System software (v. 6.2b, MIDI, Inc., Newark, DE, USA) to identify lipid profiles of different microbial functional groups (Zelles, 1999). In this process, 16 biomarkers were identified that are universal for all microbes (General), 18 biomarkers representing eukaryotic taxa (Eukaryote), 18 biomarkers for gram-positive bacteria, 35 biomarkers for gram-negative bacteria, 6 biomarkers for actinobacteria, and 3 biomarkers for fungi including arbuscular mycorrhizae (Joergensen & Wichern, 2008). Microbial biomass (µg C FAME per g soil) was estimated using external FAME standards (DeForest et al., 2012). For analysis, we separated data from individual functional groups into two broad categories – bacteria and fungi – and summed biomass from all bacteria (*Actinomycetes*, Gram-Negative, Gram-Positive, *Methanobacter* biomarkers) and all fungi (Fungi and AM Fungi biomarkers), respectively. General and Eukaryote biomarkers were not included in either bacteria or fungi groupings but were included in calculation of total FAME biomass. We then determined the proportions of total FAME derived from bacteria and fungi and calculated a ratio of bacterial:fungal biomass for each experiment × N treatment.

Plant root sample collection and processing

On September 13-14th, 2019, we also collected roots from one black grama individual per plot at all three experiments described above. Living roots were accessed using a soil knife to loosen soil up to ~10 cm deep around each plant to expose the fibrous root system. Ten active root segments (light color, flexible with visible root hairs) were gently excised by hand and placed inside a sterile 118 mL Nasco Whirl-Pak™ sampling bag (Thermo Fisher Scientific,

Waltham, MA, USA) which was then sealed and placed in a portable cooler with dry ice for transport. Soil was then replaced and loose soil was filled back in around each plant after collection. Gloves and soil knife were sterilized using bleach wipes in between each plot, and care was taken to minimize disturbance to surrounding plants and soils and to keep live grass individuals in-ground during sampling. Within 24 hours of field collection, roots were processed in the laboratory and rinsed in sterile deionized water to remove any soil particles. Clean, dried roots from each sample were then divided into two approximately equal subsamples for either microscopic assessment or DNA extraction. All laboratory tools (i.e., forceps) and surfaces were sterilized with bleach wipes between each sample.

Microscopic assessment of roots

For microscopic assessment of fungal root colonization, we cut individual roots into ~3 cm long segments using a sterile razor blade and placed 5-10 segments per individual into Simport™ M510 tissue cassettes which were submerged in 70% EtOH for temporary storage and transport. Roots were cleared in 500 mL of a 10% KOH solution at room temperature for 5 days, after which they were briefly soaked and rinsed with tap water to remove any residual solution. Samples were then submerged in 1000 mL of 0.1N HCl solution for 24 hours to acidify, then removed and soaked in a pre-heated 5% vinegar:ink staining solution containing 5% Parker Quink Blue ink (Parker, Nantes, France) for approximately 15 – 20 minutes (Vierheilig et al., 1998). Root cassettes were submerged in fresh DI water at room temperature for 2 days to further destain, and then stored in a 1:1 mix of glycerol and DI water at 4°C prior to microscopic assessment. We mounted stained roots onto clean microscope slides and quantified aseptate and septate hyphae and other fungal structures (e.g., vesicles and microsclerotia) at 100x magnification using the modified intersections method with approximately 100 fields of view per

slide (McGonigle et al., 1990). This method took into account only the presence/absence of features at each intersection.

DNA Extraction and Amplification

To extract DNA from biocrust soils, approximately 1.0 g of homogenized soil from each plot was used with a DNeasy PowerSoil® Kit (QIAGEN, Maryland, USA) following the manufacturer's protocols. The final soil DNA extracts (50 µl) were stored at -80°C prior to sequencing. For DNA extraction from roots, the remaining roots from each field-collected sample were cut into ~1 cm segments using a sterile scalpel, and approximately 20 segments were placed into a clean mortar. Approximately ~2 mL of liquid nitrogen was added to flash-freeze samples, which were then crushed with a pestle for ~5 mins until pieces were uniformly ground. All homogenized root tissue material was then transferred to a sterile 2 mL collection tube and DNA was extracted using the DNeasy® Plant Mini Kit (QIAGEN, Maryland, USA) following the manufacturer's protocol.

To identify the taxonomic assemblage of biocrust and root-associated fungi, sample DNA extracts were sent to the University of Arizona Genetics Core (UAGC; Tucson, AZ) for PCR amplification and sequencing. We targeted the Internal Transcribed Spacer (ITS2) region of the ribosomal RNA gene (Schoch et al., 2012) using the forward primer fITS7 (5'-GTGARTCATCGAATCTTTG-3'; Ihrmark et al., 2012) and reverse primer ITS4 (5'-TCCTCCGCTTATTGATATGC-3'; White et al., 1990). To generate amplicons, we amplified template DNA from all 118 samples plus a negative control (molecular grade water) using a Terra™ PCR Direct Kit (Takara Bio Inc., San Jose, CA, USA) following the manufacturer's protocol. Each PCR reaction contained the following: 2.5 µl template DNA (5 ng μl^{-1}), 5.0 µl 2X Terra PCR Direct Buffer containing Mg^{2+} and dNTPs, 0.02 µl each of fITS7 and ITS4 primers

(final concentration: 2 μM), 0.2 μl of Direct Polymerase, and 2.26 μl of sterile molecular grade water. PCR cycles included an initial denaturing at 98 °C for 5 m, followed by 34 cycles of denaturing at 98 °C for 30 s, annealing at 50 °C for 30 s, extension at 72 °C for 1 min, and a final extension at 72 °C for 5 m. Amplicons were purified using the MagBio HighPrep™ PCR Clean-up System (MagBio Genomics, Inc., Maryland, USA) following the manufacturer's protocol with a 0.8X ratio of reagent to sample. From there, a secondary Index PCR was performed on the purified amplicons (using 5 μl as template) to attach dual indices and Illumina sequencing adapters using the Nextera® XT Index Kit (Illumina, Inc., San Diego, CA, USA) following the manufacturer's protocol. Sample concentrations were quantified using a plate-based intercalating agent and pooled into one library at equal DNA amounts, which was then sequenced at the University of Arizona Genetics Core (UAGC; Tucson, AZ, USA) using a MiSeq Reagent Kit v3 (Illumina, Inc., San Diego, CA, USA) as 2 x 300PE with dual 8-bp index reads.

Bioinformatics

Sequence data generated from the high-throughput Illumina sequencing run were processed and analyzed following the mothur pipeline version 1.48.0 (Schloss et al., 2009). Raw sequence data were contiged resulting in a read library containing ~18 million sequences. These were then screened to remove any ambiguous bases and any sequences longer than 350 bp, and any homopolymers longer than 6 bases. This removed ~40% of total sequences (7.3 million sequences). Remaining sequences were trimmed to 250 bp length, which was the length of the shortest high-quality sequence, to facilitate clustering without alignment. Sequences were then pre-clustered to 2% difference, which grouped together similar sequences within 2 nucleotides of each other in order to reduce potential sequencing bias and computation time (Huse et al., 2010; Oliver et al., 2015). Sequences were then screened for chimeras, after which 67,815 putatively

chimeric sequences were removed (3.5% of total) and 1.86 million unique sequences remained. Sequences were classified using the Naive Bayesian Classifier (Wang et al. 2007) and the UNITE fungal ITS database v. 8.3 (Abarenkov et al. 2021) to create a consensus taxonomy for each unique sequence, and these were screened for unknown and non-fungal taxonomic lineages (no contaminant sequences detected). Sequences were then clustered into Operational Taxonomic Units (OTUs) at 97% sequence similarity using VSEARCH v. 2.17.1 (Rognes et al., 2016) and the distance-based greedy clustering method (DGC; Westcott & Schloss, 2015). OTUs were classified using the previous unique sequence assignments and the UNITE fungal ITS reference database described above (Abarenkov et al. 2021). Low-frequency OTUs with ≤ 10 sequences were removed to improve data integrity (Nguyen et al. 2015; Brown et al. 2015; Oliver et al. 2015), resulting in an initial OTU dataset of 3096 OTUs and 7.93 million sequences. Output files from mothur were imported into R version 4.2.2 (R Core Team 2022) for further processing and analysis. We rarefied all samples to an equal sampling depth of 9,484 sequences, which was the size of the sample with the second-lowest sequence yield, to avoid biases among experimental units resulting from differences in library size and sequence yield (Gihring et al. 2012; Cameron et al. 2021). Samples were rarefied without replacement to 9,484 sequences using the phyloseq package v. 1.42.0 (McMurdie & Holmes, 2013). This step removed 161 OTUs from the dataset which were no longer present in any sample after random subsampling and eliminated 1 sample (M1R) which had the lowest sequence yield overall (93 sequences). We excluded this experimental unit and the negative control (H_2O) from further downstream analyses. The final fungal OTU dataset consisted of 2935 OTUs and 1,109,628 total sequences from 117 samples (*n*samples = 60 biocrust; 57 root). We calculated Good's Coverage Index, or the ratio of local OTU singletons to the total number of sequences, in *mothur* using 1000

subsamples of 9484 sequences via the summary.single command, and index values were ≥ 0.99 for 117 samples following rarefaction. Additionally, rarefaction curves were saturating for both sample types (Fig. S3.1), indicating that our rarefied OTU data adequately captured the diversity of fungal groups in biocrusts and roots across all three experiments. We subset the rarefied OTU data by experiment site (MRME, NutNet and WENNDEx) for further analyses due to differences in experimental design (i.e., amounts and frequency of applied N and water treatments) and sample sizes (Table 3.1).

Analysis

Biocrust vs. root-associated fungal communities

All below analyses were performed in R version 4.2.2 (R Core Team 2022). To compare fungal community composition between biocrust soils and black grama roots in control (no treatment) plots from each experiment **(Q1)**, we identified the occurrence (presence/absence) of individual OTUs in biocrust and root samples and determined the proportional abundance of taxa found in both sample types (shared), or unique to either biocrust or root communities. We visualized this OTU overlap for each experiment using Venn diagrams via the ggvenn package v. 0.1.10 in R (Yan & Yan, 2023). To assess the similarity of biocrust and root communities, we calculated Bray-Curtis distances via the "vegdist" function in the vegan package (Oksanen et al., 2019) using subsets of the rarefied OTU data that included samples from C plots only for each experiment. We performed an Analysis of Similarity (ANOSIM) with 9999 permutations on each of the distance matrices using the "anosim" function in the vegan package (Oksanen et al., 2019). We also compared dispersion of biocrust and root samples, or the homogeneity of variance within and between each sample group, using a PERMDISP test via the "betadisper" function in the vegan package (Anderson, 2006; Oksanen et al., 2019). We then visualized

differences among sample types using nonmetric dimensional scaling (NMDS) ordinations of Bray-Curtis distances via the "metaMDS" function in the vegan package with 500 restarts (Oksanen et al., 2019).

Responses to N fertilization and changes in rainfall regime

To assess fungal community richness, diversity, and evenness in biocrusts and roots among experimental treatments, we determined taxon richness (S_{obs} or the number of observed OTUs), estimated richness (Chao1 Index or S_{chao1}), diversity (Shannon Diversity Index or H^l), and evenness (Pielou's Evenness Index or J) for each sample using the vegan package in R (Oksanen et al., 2019); see Table S3.4 for formulas). To test for significant differences in alpha diversity among sample types and N fertilization treatments **(Q2)**, or water addition/N + water addition treatments **(Q3)**, we fit linear mixed effects models via the lme4 package (Bates et al. 2015) using each diversity metric as a response variable and sample type, experimental treatment, and sample type × treatment as categorical fixed effects. Plot number was included as a random effect to account for statistical non-independence of biocrust and root samples collected from within the same treatment plot. The models for MRME also included experimental treatment nested within plot number as a random effect to account for the sampling of N addition subplots within each treatment plot. We assessed the significance of main effects and interactions using analysis of deviance Type II tests using the 'Anova' function in the car package version 3.0–10 (Fox et al., 2012), and performed post hoc pairwise comparisons of treatment means using the emmeans package version 1.6.1 (Lenth, 2021). *P* values were adjusted for multiplicity using the Tukey method for comparing a family of 3 estimates, and all pairwise comparisons of means used the Kenward-Roger degrees-of-freedom method and a 0.95 confidence level.

To detect compositional differences of biocrust and root fungal communities among control and treatment plots, we calculated Bray-Curtis distances using the rarefied OTU data subsets for each experiment as described above. To test whether fungal community structure (composition and relative abundance of taxa) significantly differed among control and experimental treatments (N addition, water addition, or water + N addition), we performed permutational multivariate analysis of variance (perMANOVA) with 9999 permutations on the respective Bray-Curtis distance matrices for biocrust and root samples via the "adonis2" function in the vegan package (Oksanen et al., 2019). N addition was included as a factor in models for all three experiments (Q2; control vs. N addition only), and MRME and WENNDEx models also included water addition (Q3; control vs. water addition only vs. N + water addition) and interactions between all levels of N × water addition treatments. For MRME, there were 5 levels of water and addition treatments: control (none), large/infrequent rainfall (L), small/frequent rainfall (S), large + N addition (LN) and small + N addition (SN). For WENNDEx, there were 3 levels of water addition treatments: control (none), water only (H_2O) and water + N addition (H_2O + N). Multiple pairwise comparisons of significant factors were performed using the "pairwise.adonis2" function (Martinez Arbizu 2020), and p-values were adjusted for multiple comparisons using the Benjamini-Hochberg correction method in the "p.adjust" function from the Rstats package v. 3.6.2 (R Core Team, 2022; Benjamini & Hochberg, 1995). We visualized the relationships between samples and responses of biocrust and root fungal communities to N and water addition treatments using nonmetric dimensional scaling (NMDS) ordinations as described above. We also compared dispersion within and between communities in control vs. treatment plots using a PERMDISP test as described above. We further assessed the trophic modes and functional guilds of fungal communities in biocrusts and roots using the FUNGuild

database (Nguyen et al., 2016) to classify OTUs with >80% confidence taxonomy at the genus level (N = 1740 OTUs).

The responses of soil fungal biomass, including soil ergosterol concentration, ratio of bacteria:fungi FAME biomass and proportion of fungi in total FAME biomass, were compared among control and N addition only treatments by fitting linear models to each variable with N treatment as a fixed effect for two of the experiments (NutNet and WENNDEx), and by fitting a linear mixed-effects model to each variable for MRME with N treatment as a fixed effect and plot number as a random effect to account for the sampling of N addition subplots nested within each control plot. We did not measure soil ergosterol concentration or quantify FAME biomass for biocrust samples in water addition or water + N addition treatments at MRME or WENNDEx.

To analyze the responses of fungal root colonization to experimental treatments, a linear mixed-effects model was fit to test for the main and interacting effects of experimental treatment (N addition only, water only, and water + N additions) on fungal colonization (% root length colonized) of *B. eriopoda* roots by two hyphal morphotypes (aseptate and septate hyphae) from each of 3 experiments (MRME, NutNet, WENNDEx). Sample ID was included as a random effect to account for the statistical non-independence of measuring both hyphal types from the same root sample, and the MRME model included experimental treatment nested within plot number as a random effect. We assessed the significance of main effects and interactions using Type II ANOVA tests and performed *post hoc* comparisons as described above.

RESULTS

Overall patterns in fungal community composition

Following sample rarefaction, our final fungal OTU matrix contained 2935 OTUs; the majority of which (75%) were from Ascomycota, which was the most dominant phylum overall representing ~80% or more of all reads in biocrust and root samples from all experiments/treatment plots (Table 3.2). The remaining OTUs were classified to Basidiomycota (9.7%), Glomeromycota (3%), Chytridiomycota (~1%), and Entomophthoromycota, Mucoromycota, and Rozellomycota (< 1% each). Around 11% of all OTUs were unclassified fungal taxa (*n* = 326 OTUs; Table 3.2). At the class level, OTUs were dominated by Dothideomycetes (43% of total), followed by Sordariomycetes (14%), Agaricomycetes (7%), Eurotiomycetes (5%), Glomeromycetes (3%), Pezizomycetes (2%), Tremellomycetes (2%), and 15 other fungal classes that made up 1% or less of all OTUs (Fig. 3.1). Taxa that were unclassified made up 20% of OTUs at the class level. Of the top 30 most common taxa, nearly half (43%) were from Order Pleosporales (Ascomycota), and Orders Agaricales and Geastrales (both Basidiomycota) made up 16% (Table 3.3). The few fungal taxa that occurred in the highest number of biocrust and root samples (*N* = 117 samples), were *Darksidea* (116 samples), *Aureobasidium subglaciale* (98 samples), *Acrophialophora* (92 samples), and *Curvularia buchloes* (81 samples; Table 3.3).

Table 3.2 Proportional distribution (%) of rarefied OTUs in each fungal phylum found in biocrust and root samples from each experiment site: MRME (M), NutNet (N), and WENNDEx (W). Total *N* OTUs = 2935 across all experiments/treatment plots.

	Biocrust			Roots		
Fungal Phylum	M	N	W	M	N	W
Ascomycota	81.8%	85.4%	84.1%	80.6%	81.1%	83.2%
Basidiomycota	5.3%	6.0%	7.5%	4.1%	7.6%	5.9%

Chytridiomycota	0.8%	0.8%	0.7%	0.0%	0.0%	0.0%
Entomophthoromycota	0.0%	0.0%	0.02%	0.0%	0.0%	0.0%
Glomeromycota	0.2%	0.0%	0.0%	11.0%	7.0%	7.3%
Mucoromycota	0.2%	0.2%	0.2%	0.1%	0.0%	0.2%
Rozellomycota	0.0%	0.0%	0.0%	0.03%	0.0%	0.0%
Unclassified Fungi	11.7%	7.6%	7.5%	4.3%	4.3%	3.4%

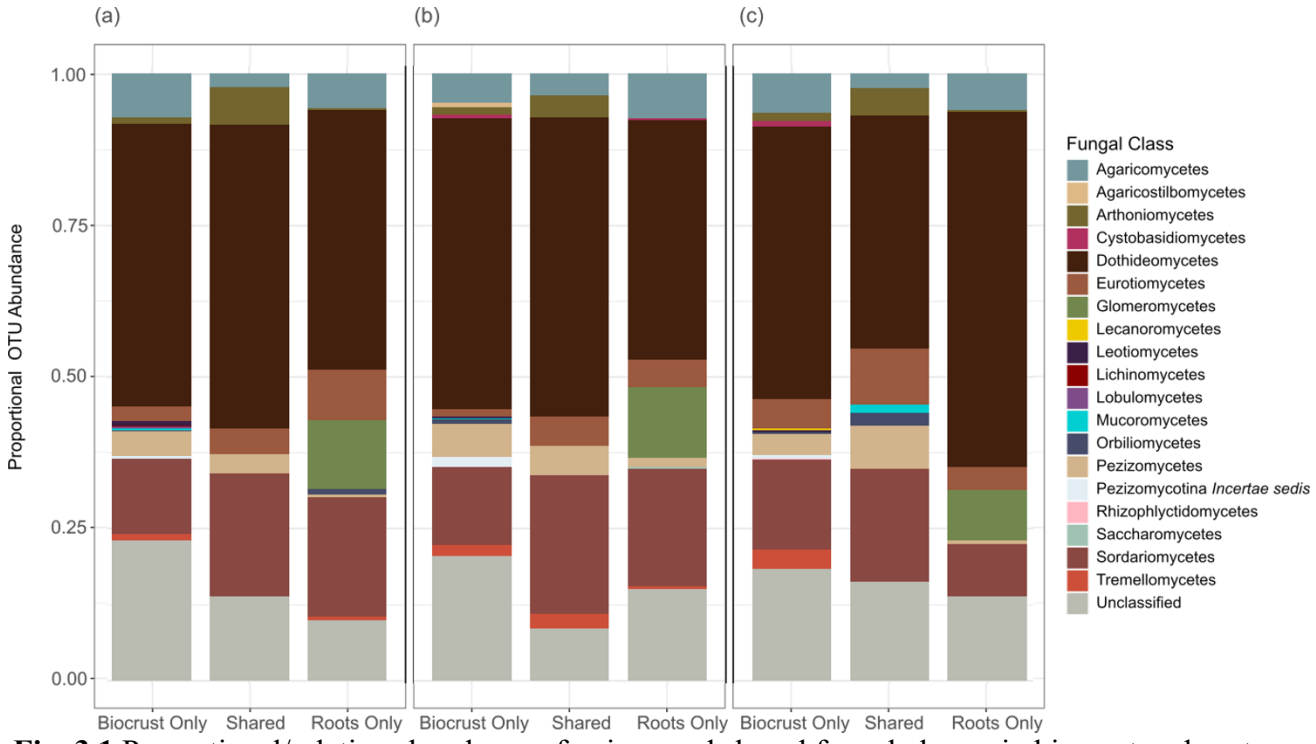

Fig. 3.1 Proportional/relative abundance of unique and shared fungal classes in biocrust and root communities from control (no treatment) plots from each of three experiments: (a) MRME, (b) NutNet, and (c) WENNDEx (n = 10 samples each).

Table 3.3 List of 30 most common taxa (top ~1% of sequences) across biocrust and root samples collected from all experiments. Samples with < 97% consensus taxonomy at the phylum level and < 80% confidence taxonomy at the genus level were filtered out prior to making FUNGuild assignments (*N* = 1740 OTUs).

OTU	*n*reads	Phylum	Class	Order	Taxon	B	R	*N*	FUNGuild Assignment[b]
1	68758	Ascomycota	Dothideomycetes	Pleosporales	*Laburnicola*	21	53	74	Endophyte Lichen Parasite Plant Pathogen Undefined Saprotroph
6	38670	Ascomycota	Dothideomycetes	Pleosporales	*Darksidea*	60	56	116	Endophyte
4	36099	Ascomycota	Dothideomycetes	Pleosporales	*Paraconiothyrium* sp.	6	30	36	Endophyte Lichen Parasite Plant Pathogen Undefined Saprotroph
3	31326	Ascomycota	Sordariomycetes	Xylariales	*Monosporascus ibericus*	11	28	39	Plant Pathogen Plant Saprotroph
7	27440	Ascomycota	Dothideomycetes	Dothideales	*Aureobasidium subglaciale*	58	40	98	*Animal Pathogen Endophyte Epiphyte Plant Pathogen Undefined Saprotroph
11	21335	Ascomycota	Sordariomycetes	Sordariales	*Acrophialophora* sp.	45	47	92	Plant Pathogen
10	20819	Ascomycota	Sordariomycetes	Sordariales	*Subramaniula thielavioides*	59	24	83	Undefined Saprotroph
8	20475	Ascomycota	Dothideomycetes	Pleosporales	*Chaetosphaeronema* sp.	60	6	66	Fungal Parasite

									Plant Pathogen Plant Saprotroph
14	20014	Ascomycota	Dothideomycetes	Pleosporales	*Alternaria* sp.	59	10	69	Endophyte Lichen Parasite Plant Pathogen Undefined Saprotroph
16	18221	Basidiomycota	Agaricomycetes	Agaricales	*Panaeolus* sp.	2	24	26	Dung Saprotroph Plant Saprotroph Soil Saprotroph
9	17283	Ascomycota	Eurotiomycetes	Mycocaliciales	*Mycocalicium victoriae*	54	13	67	*Lichenized
19	15516	Ascomycota	Sordariomycetes	Xylariales	*Monosporascus* sp.	7	29	36	Plant Pathogen Plant Saprotroph
20	11838	Ascomycota	Dothideomycetes	Pleosporales	*Preussia terricola*	49	15	64	Dung Saprotroph Plant Saprotroph
22	11554	Ascomycota	Sordariomycetes	Magnaporthales	*Budhanggurabania cynodonticola*	3	14	17	Plant Pathogen
18	10868	Ascomycota	Sordariomycetes	Xylariales	*Monosporascus* sp.	8	30	38	Plant Pathogen Plant Saprotroph
23	10784	Ascomycota	Dothideomycetes	Pleosporales	*Comoclathris* sp.	58	11	69	Endophyte Lichen Parasite Plant Pathogen Undefined Saprotroph
32	10739	Ascomycota	Dothideomycetes	Pleosporales	*Megacapitula* sp.	1	15	16	Undefined Saprotroph
21	10392	Basidiomycota	Agaricomycetes	Agaricales	*Conocybe deliquescens*	1	17	18	Dung Saprotroph Plant Saprotroph Soil Saprotroph
17	9297	Ascomycota	Dothideomycetes	Pleosporales	*Laburnicola* sp.	1	16	17	Endophyte Lichen Parasite Plant Pathogen Undefined Saprotroph
40	8763	Ascomycota	Sordariomycetes	Hypocreales	*Gibberella nygamai*	35	32	67	*Animal Pathogen Endophyte Fungal Parasite

									Lichen Parasite Plant Pathogen Wood Saprotroph
28	7870	Ascomycota	Dothideomycetes	Pleosporales	*Curvularia buchloes*	52	29	81	Endophyte Lichen Parasite Plant Pathogen Undefined Saprotroph
24	7774	Ascomycota	Dothideomycetes	Pleosporales	*Trematosphaeria* sp.	2	18	20	Undefined Saprotroph
37	6565	Ascomycota	Sordariomycetes	Hypocreales	*Fusarium algeriense*	33	34	67	*Animal Pathogen Endophyte Fungal Parasite Lichen Parasite Plant Pathogen Wood Saprotroph
25	6323	Basidiomycota	Agaricomycetes	Geastrales	*Geastrum* sp.	3	7	10	Undefined Saprotroph
62	6310	Ascomycota	Eurotiomycetes	Onygenales	*Uncinocarpus* sp.	9	32	41	Dung Saprotroph Soil Saprotroph
35	5924	Ascomycota	Dothideomycetes	Pleosporales	*Biappendiculispora* sp.	50	2	52	Plant Pathogen Undefined Saprotroph
58	5791	Ascomycota	Dothideomycetes	Pleosporales	*Darksidea alpha*	27	56	83	Endophyte
49	5784	Basidiomycota	Agaricomycetes	Agaricales	*Chlorophyllum arizonicum*	1	11	12	Undefined Saprotroph
39	5031	Ascomycota	Dothideomycetes	Pleosporales	*Neostagonospora* sp.	43	18	61	Fungal Parasite Plant Pathogen Plant Saprotroph
67	4794	Ascomycota	Sordariomycetes	Sordariales	*Cladorrhinum flexuosum*	40	2	42	Undefined Saprotroph

[a]**Sample Assignment**: number of occurrences of OTU in biocrust (B) and root (R) samples; N = total occurrences across all samples
[b]**FUNGuild Assignment**: An asterisk (*) denotes a confidence ranking of "Possible" (all other assignments are ranked "Probable" or "Highly Probable")

Biocrust vs. root-associated fungal communities

We compared the overall similarity of biocrust and root taxa in control (no treatment) plots and found that across all three experiments, biocrust samples had a greater number of unique taxa (911 unique OTUs) compared to roots (597 unique OTUs), and the two sample types shared ~12% of taxa across all experiments (n = 208 OTUs; Fig 3.2a). Within each experiment, biocrust samples tended to have a greater number of unique OTUs compared to roots, and MRME had the most similar number of unique OTUs in biocrusts and roots (Fig. 3.2b) while NutNet and WENNDEx both had a higher number of unique OTUs in biocrusts compared to roots (Fig. 3.2c-d). WENNDEx had the least amount of OTU overlap between biocrust and root samples (only 8% of OTUs shared) and the highest proportion of unique biocrust OTUs overall (Fig. 3.2d, Fig. 3.3a). Results from ANOSIM models indicated that the means of ranked dissimilarities differed significantly between biocrusts and roots for each experiment, and R values suggested greater dissimilarity between biocrusts and roots than within each sample type group (ANOSIM for MRME: R = 0.85, P = 0.008; for NutNet: R = 0.84, P = 0.008; for WENNDEx: R = 0.91, P = 0.009; Fig 3.4). Within-group dispersion (average distance from individual points to centroids of each group) also differed significantly among biocrusts and roots for each experiment (PERMDISP $P < 0.05$), indicating that differences within groups (particularly among root samples; Fig. 3.4) could potentially influence the significance of treatment effects among groups, and interpretation of any further significant results should also look at dispersion effects.

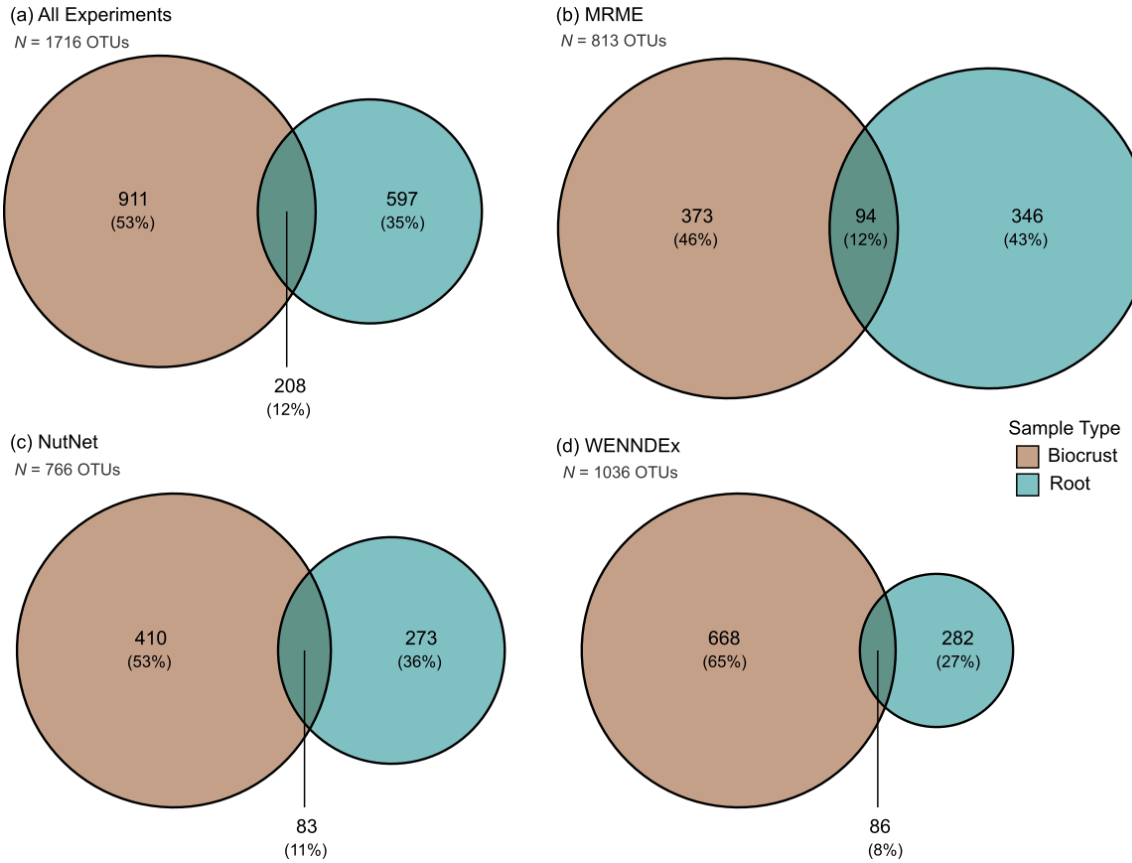

Fig 3.2 Fungal OTU overlap between biocrust and root communities in control (no treatment) plots from (a) all three experiments combined; (b) MRME only; (c) NutNet expt. only; (d) WENNDEx only. Values within each circle represent the number and proportion (%) of total OTUs that are unique (only found in one sample type) or shared between both sample types.

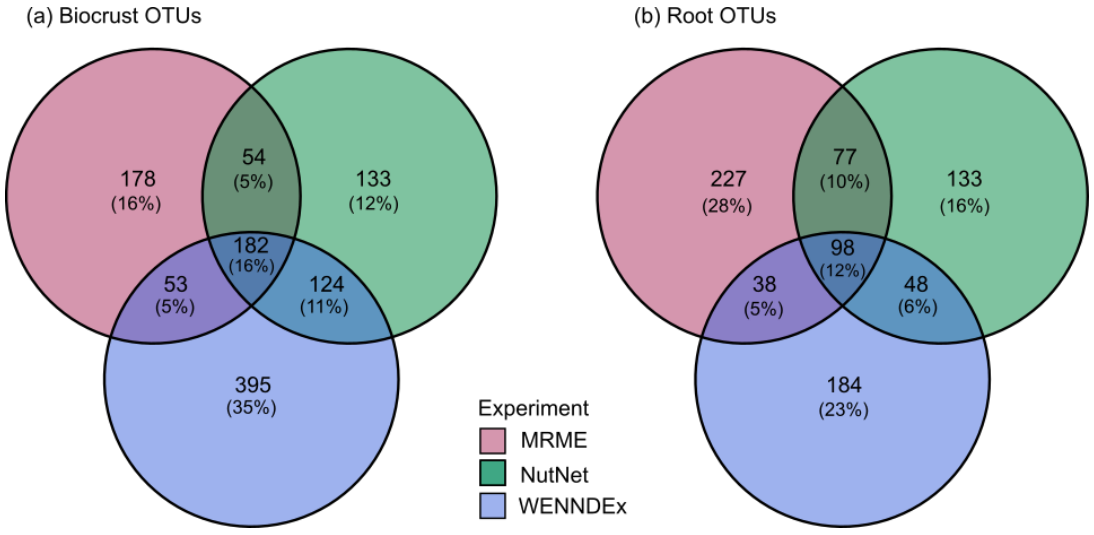

Fig. 3.3 Fungal OTU overlap among biocrust and root communities in control plots (no treatment) from 3 experiments. Values within each circle represent the number and proportion (%) of total OTUs that are unique to one experiment or shared among one or more experiments.

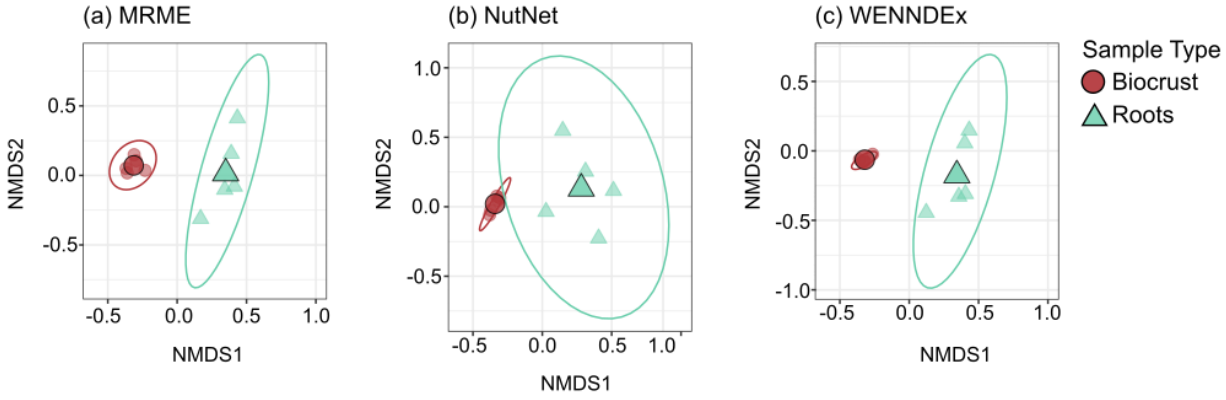

Fig. 3.4 NMDS ordinations of Bray-Curtis distances between biocrust and root samples from control plots only (no treatment) in each experiment: (a) MRME, (b) NutNet, (c) WENNDEx. Analysis of Similarity (ANOSIM) indicated significant differences (P = 0.01) between sample types for each experiment. Ellipses represent 95% confidence interval around centroid for each group. Note differences in axis scales. NMDS stress value = 0.131.

To better understand the potential functional roles of biocrust and root fungi, we determined the 30 most common taxa (*n*sequence reads > 5,000) found in control plots across experiments to one or more fungal functional guilds using the FUNGuild database (Table 3.3). The most frequent guild assignments were plant pathogens (22% of total), and undefined saprotrophs (17%) followed by endophytes (14%), lichen parasites (11%), plant saprotrophs (11%), and dung saprotrophs (7%). Making up 5% or less of the top 30 taxon guild assignments were fungal parasites, soil and wood saprotrophs, animal pathogens, lichenized, and ephiphytic fungi (Table 3.3). We also looked at trophic modes of unique and shared biocrust/root taxa (Fig S3.3), and those found only in biocrusts were largely saprotrophs (39% of total), followed by

pathotroph-saprotrophs (32%) and pathotroph-saprotroph-symbiotrophs (17%). Unique root taxa had a higher representation of symbiotrophs (33%) and pathotroph-saprotroph-symbiotrophs (38%), and fewer saprotrophs than biocrust taxa (14%). Shared taxa were mostly classified as pathotroph-saprotrophs (33%) and saprotrophs (31%).

Responses to N fertilization

Diversity Metrics

For each experiment, we tested the responses of observed and estimated richness (S_{obs} and Chao1), diversity (H^1), and evenness (J) to experimental N additions among biocrust and root samples. At MRME (Fig. 3.5), our model results indicated significant responses of observed OTU richness (S_{obs} main effect of treatment: $X^2 = 15.34$, $P = 0.009$), diversity (H^1 main effect of treatment: $X^2 = 53.98$, $P < 0.001$) and evenness (J main effect of treatment: $X^2 = 47.81$, $P < 0.001$) to experimental treatments (Table S3.1). Pairwise comparisons indicated that N addition alone did not drive significant changes in either observed or estimated richness for either sample type ($P > 0.1$; Fig. 3.5a-b), but did result in significant decreases for both sample types in diversity (pairwise comparisons of H^1 in C vs. N for biocrust: $t = 3.57$, $P = 0.015$; for roots: $t = 4.24$, $P = 0.002$) and in evenness (pairwise comparisons of J in C vs. N for biocrust: $t = 3.78$, $P = 0.009$; for roots: $t = 3.98$, $P = 0.004$) compared to controls (Fig. 3.5c-d). Results also indicated significant interactions between sample type × treatment for all four response variables ($P < 0.01$, Table S3.1). Among sample types, root samples had greater observed and estimated richness compared to biocrusts in control plots at MRME (pairwise comparisons of biocrust vs. roots for S_{obs}: $t = -2.02$, $P = 0.055$; for Chao1: $t = -2.15$, $P = 0.04$); however, there were no significant differences in diversity or evenness among biocrusts and roots in either C or N addition plots (Fig. 3.5).

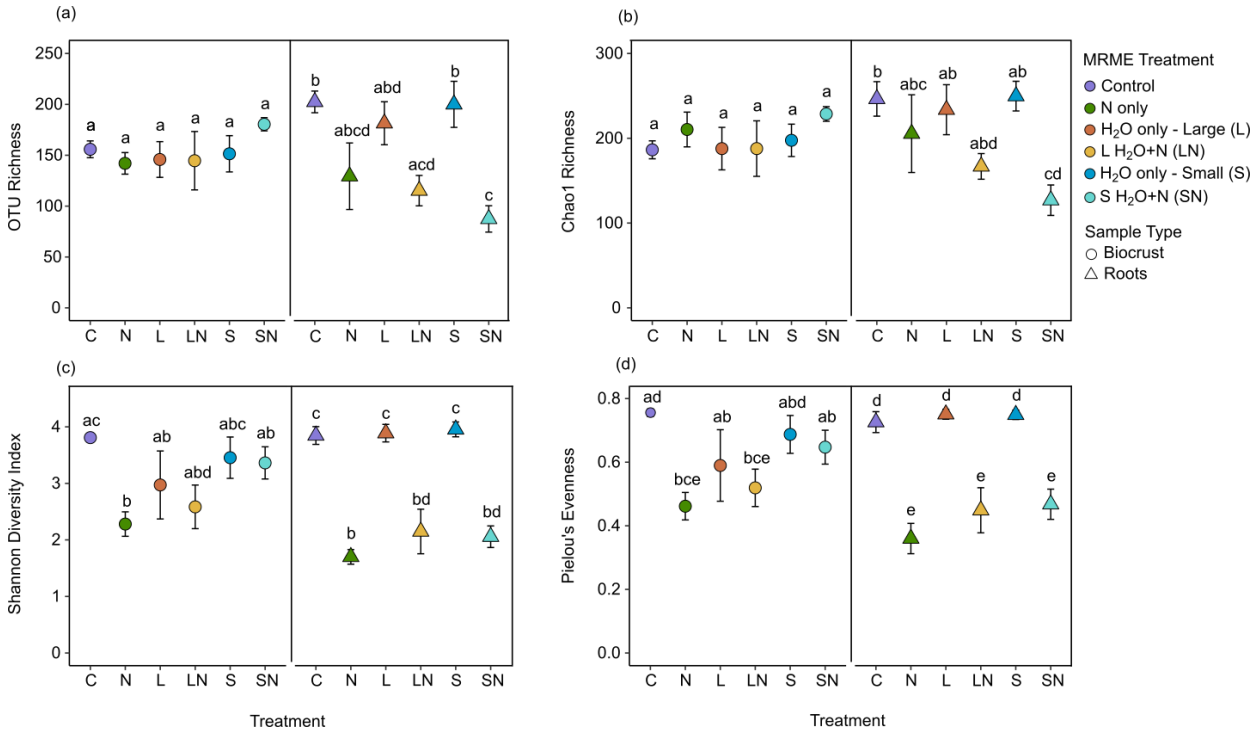

Fig 3.5 Alpha diversity metrics of fungal communities in biocrust and root samples from MRME across 6 levels of N and water addition treatments levels including: (a) Taxon (OTU) richness, (b) Chao Richness (c) Shannon Diversity Index and (d) Pielou's Evenness Index. Points represent mean ± standard error values, and lowercase letters above points indicate significant *post hoc* differences ($P < 0.05$) among treatments for each sample type and between sample types (biocrust vs. root) within each treatment level.

At the NutNet experiment (Fig. 3.6), observed and estimated richness and diversity of fungi in roots, but not biocrusts, showed significant declines (main effect of treatment for H^1: $X^2 = 4.39$, $P = 0.036$; Table S3.1) under N addition (pairwise comparisons of roots in C vs. N treatments for S_{obs}: $t = 2.159$, $P = 0.05$; Chao1: $t = 2.077$, $P = 0.05$; and H^1: $t = 2.55$, $P = 0.02$; Fig. 3.6). Evenness in root communities also decreased under N addition, and this trend was marginally significant ($P = 0.06$; Fig. 3.6). At NutNet, biocrust community richness, diversity and evenness were unchanged among C and N treatments, and biocrust fungi showed no significant directional responses to N addition treatments. Among sample types, biocrust communities had significantly higher richness, diversity, and evenness compared to roots across

both C and N treatments at NutNet (main effect of sample type for all 4 responses: $P < 0.001$; Table S3.1).

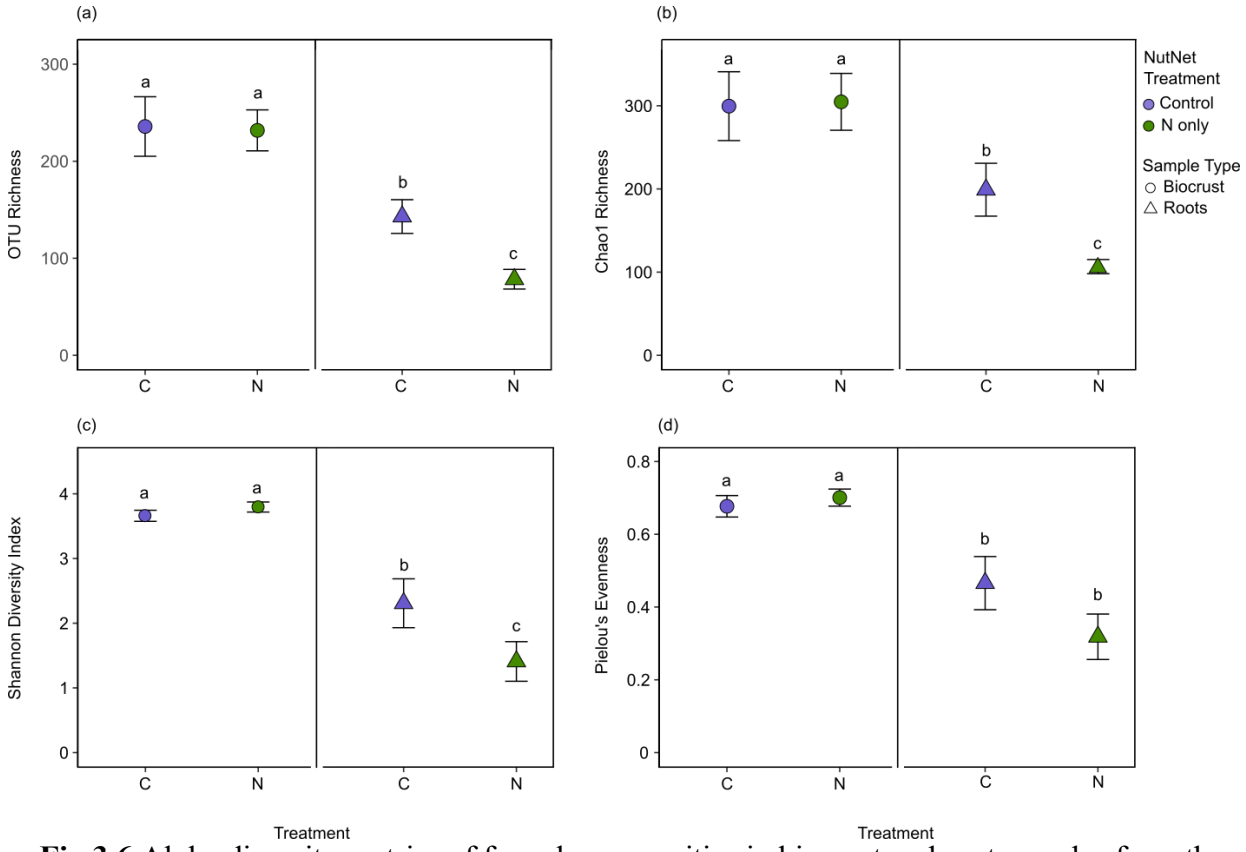

Fig 3.6 Alpha diversity metrics of fungal communities in biocrust and root samples from the NutNet experiment across 2 treatment levels (control vs. N addition) including: (a) Taxon (OTU) richness, (b) Chao Richness (c) Shannon Diversity Index and (d) Pielou's Evenness Index. Points represent mean ± standard error values, and lowercase letters above points indicate significant *post hoc* differences ($P < 0.05$) among treatments for each sample type and between sample types (biocrust vs. root) within each treatment level.

WENNDEx had the highest richness values overall, but unlike the other two experiments, there were no statistically significant differences apparent in any alpha diversity responses under N addition treatments for either biocrust or root samples. Root samples showed slight trends towards higher richness and diversity under N addition compared to C, but overall values were consistently similar among C and N treatments within each sample type grouping ($P > 0.3$; Fig.

3.7). Among sample types at WENNDEx (Fig. 3.7), similar to NutNet, biocrust communities had significantly higher richness, diversity, and evenness compared to roots across both C and N treatments (main effect of sample type for all 4 responses: $P < 0.001$; Table S3.1).

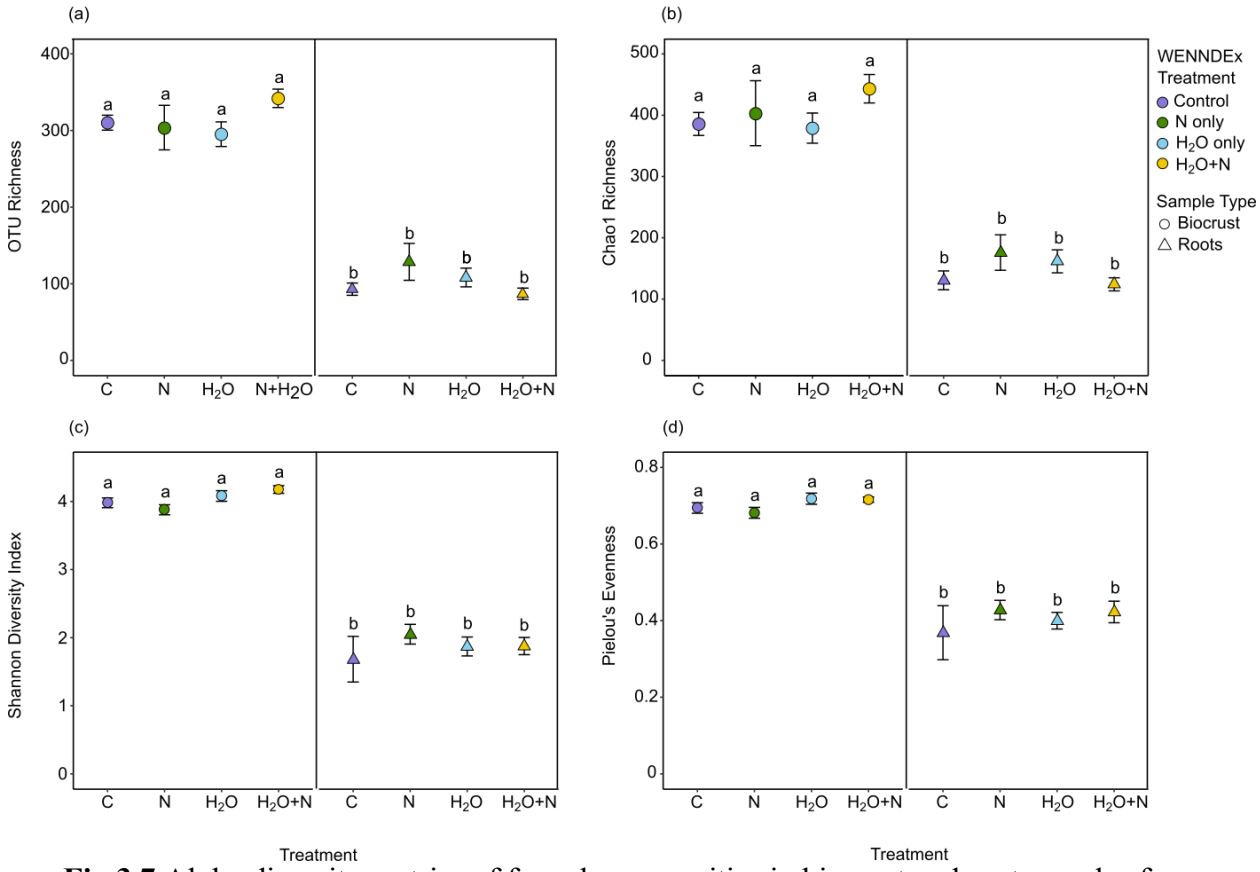

Fig 3.7 Alpha diversity metrics of fungal communities in biocrust and root samples from WENNDEx across 4 treatment levels (control, N only, water only, water + N addition) including: (a) Taxon (OTU) richness, (b) Chao Richness (c) Shannon Diversity Index and (d) Pielou's Evenness Index. Points represent mean ± standard error values, and lowercase letters above points indicate significant *post hoc* differences ($P < 0.05$) among treatments for each sample type and between sample types (biocrust vs. root) within each treatment level.

Community Similarity

At MRME, the similarity of fungal communities in biocrusts – but not roots – showed significant changes under N addition treatments (Fig. 3.8, top panel; N treatment main effect for

biocrust: pseudo-F = 1.75, P = 0.016; for roots: pseudo-F = 0.84, P = 0.694; Table 3.4). Dispersion tests for both biocrust and root samples were not significant among C and N treatments (P > 0.1) suggesting a valid treatment effect on the structure of biocrust communities under N addition. A similar trend was observed at NutNet (Fig. 3.8, middle panel), with biocrust community structure significantly changing under N addition (N treatment main effect for biocrust: pseudo-F = 2.73, P = 0.016), but no significant changes to community structure of roots (P = 0.7; Table 3.4). However, the dispersion test for biocrust (but not roots) was significant (PERMDISP P = 0.009), which indicates that within-group dispersion could also be influencing these results for biocrusts. At WENNDEx, neither biocrust nor root communities showed significant changes in structure under N addition (P > 0.2 for both; Table 3.4; Fig. 3.8, bottom panel), and dispersion was also not significant for either sample type in response to N additions.

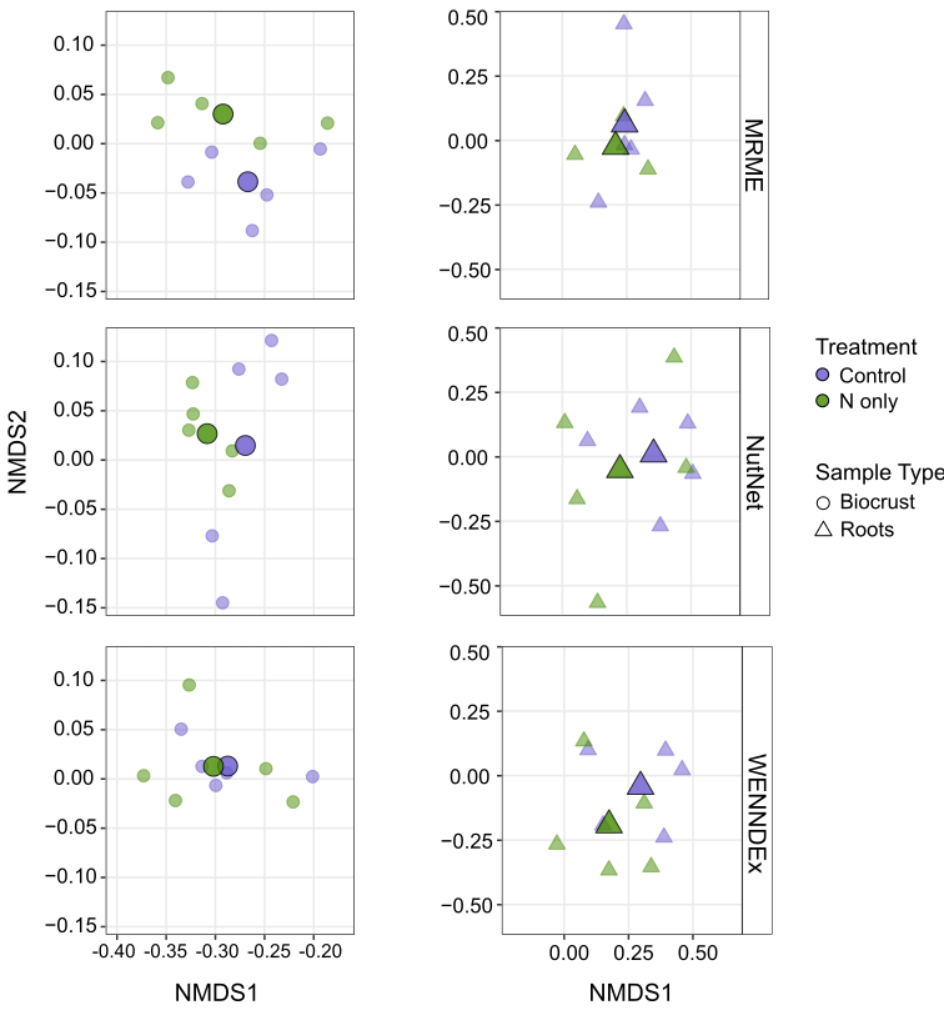

Fig. 3.8 NMDS ordinations of Bray-Curtis distances showing responses of biocrust (left) and root-associated (right) fungal communities to N addition treatments within each of 3 experiments (MRME, NutNet, and WENNDEx). Note difference in axis scales among sample types.

Table 3.4 Results from perMANOVA models using 9999 permutations to assess the response of biocrust and root-associated fungal community composition to experimental N and water treatments. The models for MRME and WENNDEx included the main and interacting effects of N addition only, water addition only, and water + N addition treatments, while the model for NutNet included the main effect of N addition treatment only. Significant values ($P < 0.05$) are bolded.

		Biocrust				**Roots**			
Expt.	**Factor**	R^2	Pseudo-*F*	df	*P*	R^2	Pseudo-*F*	df	*P*
MRME	N Treatment	0.180	1.751	1	**0.016**	0.122	0.837	1	0.694
	H_2O Treatment	0.203	1.277	4	**0.016**	0.160	0.902	4	0.694
	N:H_2O (All treats.)	0.218	1.339	5	**0.002**	0.185	0.954	5	0.600
NutNet	N Treatment	0.254	2.726	1	**0.016**	0.097	0.856	1	0.743
WENNDEx	N Treatment	0.129	1.185	1	0.202	0.081	0.707	1	0.809
	H_2O Treatment	0.192	1.424	2	**0.027**	0.154	1.093	2	0.303
	N:H_2O (All treats.)	0.189	1.240	3	0.067	0.155	0.981	3	0.498

Fungal Biomass

For soil fungal biomass measurements at MRME, mean soil ergosterol appeared to increase in response to N addition and total ergosterol content differed the most among treatments at MRME compared to the other two experiments (Fig. 3.9). Although this trend was not statistically significant (Table S3.2), N addition plots had 1.8x more total ergosterol (0.58 µg g^{-1} soil) compared to C plots (0.32 µg g^{-1} soil; Fig. 3.9), and the second-highest total ergosterol content measured overall. In contrast, C plots had the highest total FAME biomass (63.40 µg C FAME g^{-1} soil) measured overall, and the highest biomass ratio of bacteria:fungi (Table 3.5), although differences among C and N addition treatments were not statistically significant for this response (Table S3.2). The proportion of fungi out of total FAME biomass did not differ significantly in response to N addition and values were overall similar (~10%) for both C and N treatments (Table 3.5). Notably, MRME was the only experiment where bacterial FAME biomarkers for both Actinomycetes and Methanobacter were detected, the latter only found in C plots at MRME (data not shown).

At NutNet, mean soil ergosterol was slightly higher in C plots compared to N addition plots, but these trends were not statistically significant (Table S3.2). NutNet also had the overall highest total soil ergosterol content in control plots (0.64 µg g^{-1} soil; Fig. 3.9) compared to the other two experiments. The NutNet experiment also had relatively higher mean and total FAME biomass in control plots as well as slightly higher proportions of fungi compared to N addition plots (Table 3.5). AM fungal biomarkers were present in all C plots at this experiment. The ratios of bacterial:fungal biomass were similar among C and N plots, and there were overall no statistically significant responses to N treatments at NutNet (Table S3.2).

Soils from WENNDEx had similar mean ergosterol content overall (Fig. 3.9) and nearly the same total soil ergosterol content among C and N addition plots (0.49 and 0.50 μg g^{-1} soil, respectively). WENNDEx soils had the most similar mean and total FAME biomass and the lowest bacteria:fungi ratios among treatments compared to the other experiments (Table 3.5). There were no statistically significant differences in ergosterol content or FAME biomass among soils from C and N addition treatments at WENNDEx (Table S3.2).

Table 3.5 Mean ± standard error and total soil microbial biomass as determined by fatty acid methyl ester analysis (μg C FAME g^{-1} soil) and proportions of FAME biomass from bacterial (Actinomycetes, Gram Positive, Gram Negative, Methanobacter) and fungal (Fungi, AM Fungi) guilds. Note: additional quantification of General and Eukaryote FAME biomarkers (included in calculation of Total FAME biomass) were not included in analyses.

Experiment	Treatment	Mean FAME Biomass	Total FAME Biomass	Proportion of Bacteria	Proportion of Fungi	Ratio of Bacteria: Fungi
MRME	Control	12.68 ± 2.18	63.40	0.391	0.109	3.60
	N only	11.95 ± 2.24	59.76	0.303	0.104	2.92
NutNet	Control	11.80 ± 0.94	59.02	0.282	0.111	2.54
	N only	9.18 ± 2.30	45.92	0.270	0.105	2.57
WENNDEx	Control	9.31 ± 0.66	46.55	0.232	0.114	2.04
	N only	9.52 ± 1.50	47.62	0.209	0.102	2.04

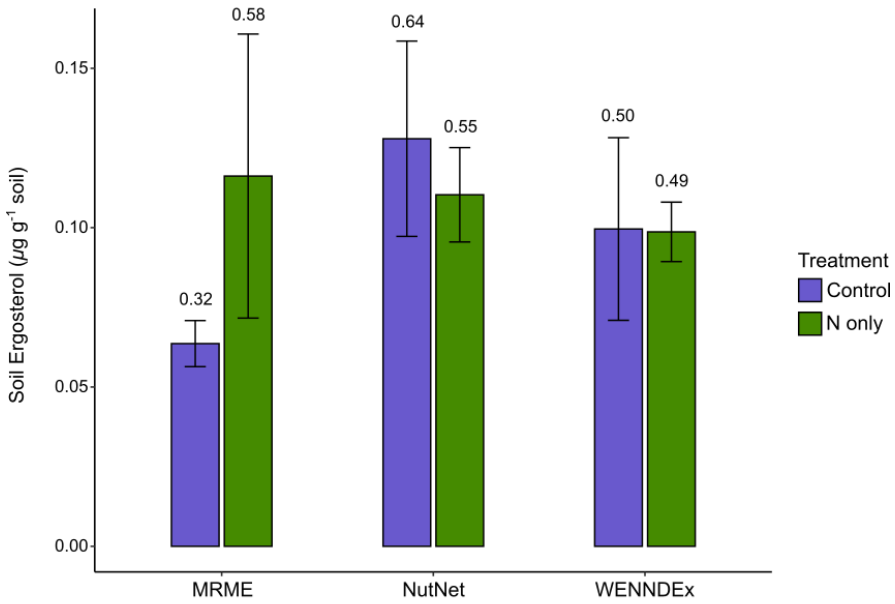

Fig. 3.9 Mean soil ergosterol concentrations ± standard error (μg g^{-1} soil) used as a proxy for fungal biomass in biocrust samples collected from control (no treatment) and N addition plots within each experiment (N = 30). Values at the top of each bar indicate the total amount of ergosterol summed across replicates (n = 5 for each experiment × treatment group).

Root Colonization

At MRME, fungal root colonization did not show significant changes in response to N addition alone (Fig. 3.10a), however, percent colonization by septate hyphae was significantly higher than aseptate hyphae (Hyphal type main effect: X^2 = 57.53, P < 0.001; Table S3.3), and on average the proportion of total views was ~2x higher for septate hyphae within roots of plants from C and N addition treatments (pairwise comparisons of aseptate:septate in C plots: t = -4.45, P < 0.001; in N addition: t = -2.56 , P = 0.01). The interaction between hyphal type and experimental treatment was also not statistically significant. At NutNet, there were no significant differences in root colonization among hyphal types or among C and N treatments (Table S3.3), although aseptate colonization was slightly higher in C plots for this experiment, trends were not significant (Fig. 3.10b). At WENNDEx, aseptate colonization was significantly lower under N addition compared to controls (Treatment main effect: X^2 = 12.37, P = 0.006), and septate hyphal

colonization was ~3.5x greater in N treatments for this experiment (pairwise comparisons of aseptate:septate in N addition only: $t = 3.58$, $P = 0.007$; Fig 3.10c). Septate and aseptate colonization did not differ significantly in control plots at WENNDEx.

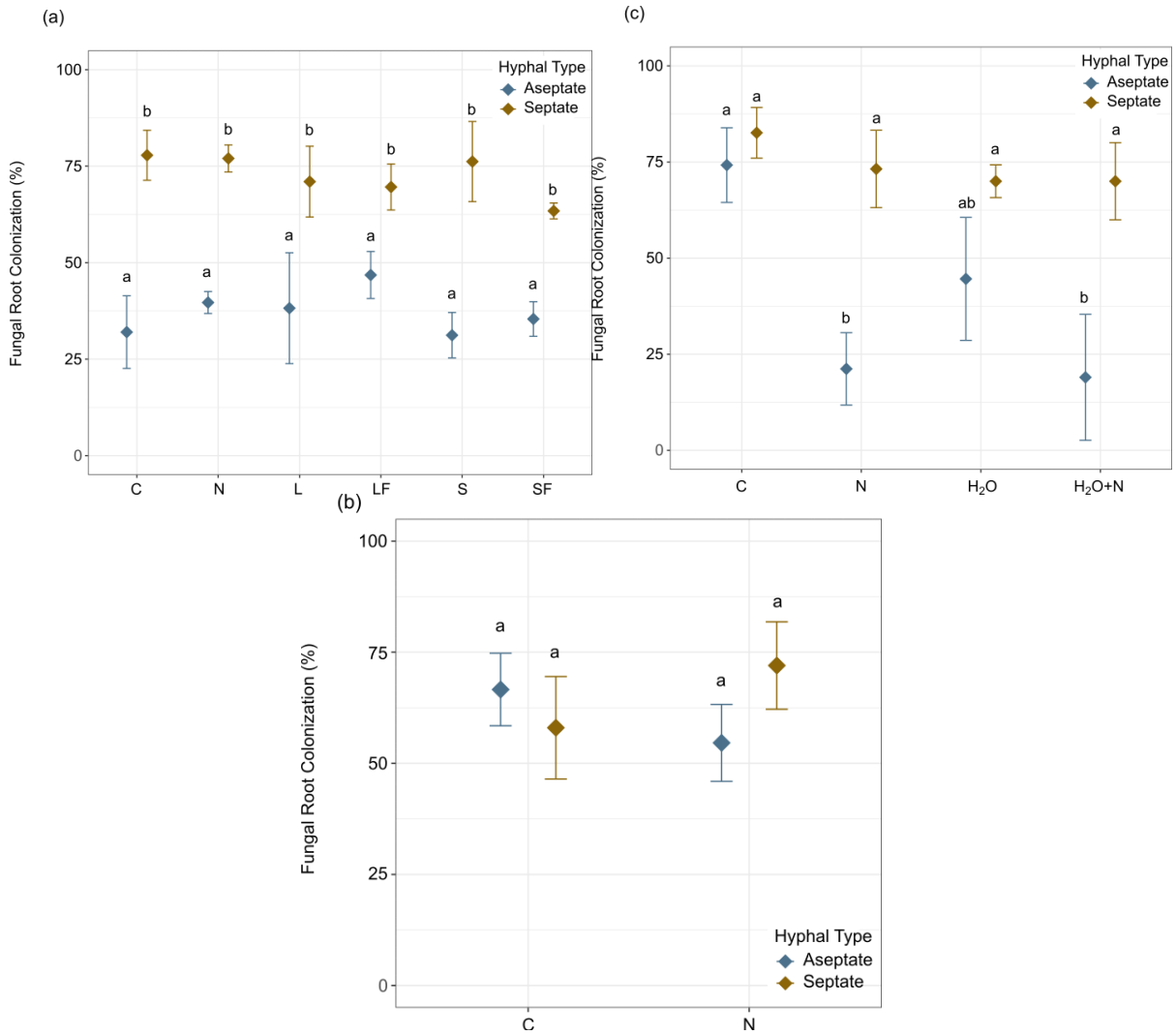

Fig. 3.10 Percent hyphal colonization of *B. eriopoda* roots by two fungal morphotypes (aseptate and septate) from control and N/water treatment plots within 3 experiments: (a) MRME, (b) NutNet, (c) WENNDEx. Points represent mean ± SE values and lowercase letters above points indicate significant *post hoc* differences ($P < 0.05$) among treatments for each hyphal type and between hyphal types (aseptate vs. septate pairwise comparisons) within each treatment level.

Responses to changes in rainfall regime and water × N additions

Diversity Metrics

At MRME, there were significant declines in richness, diversity, and evenness of root samples under experimental water treatments compared to controls (Table S3.1), and *post hoc* pairwise comparisons indicated that both large and small combined water + N additions (LN and SN) drove these trends, since decreases were apparent between control and water + N treatments (Fig. 3.5). Richness of biocrust communities was largely unaffected by either water addition treatment, although diversity and evenness showed a decreasing trend in C vs. large rainfall (L) vs. LN and C vs. small rainfall (S) vs. SN treatments (Fig. 3.5c-d), although only one of these decreases in evenness was statistically significant (pairwise comparison of J among C vs. LN treats for biocrust: $t = 3.04$, $P = 0.043$). Results also indicated significant interactions between sample type × treatment for all four response variables ($P < 0.01$, Table S3.1), and within treatments, richness, diversity and evenness of root samples tended to be higher than biocrust for L/S water additions only and tended to be lower than biocrusts in LN/SN water + N treatments (Fig. 3.5).

For WENNDEx, there were no significant effects of water additions on the responses of either biocrusts or roots among treatments (Fig. 3.7), but within each treatment category the two sample types differed significantly with biocrusts having significantly higher richness, diversity, and evenness compared to roots across water only and water + N addition treatments (main effect of sample type for all alpha diversity responses: $P < 0.001$; Table S3.1).

Community Similarity

In response to water addition only treatments at MRME, biocrust community composition showed significant divergence from untreated C plots (H_2O treatment main effect

for biocrust: pseudo-*F* = 1.27, *P* = 0.016) and also shifted in response to all water + N treatment combinations (Interacting effects of H_2O × N treatments for biocrust: pseudo-*F* = 1.34, *P* = 0.002), however, root communities did not show significant shifts in composition under any water treatment level or combination (Table 3.4; Fig. 3.11). Dispersion tests for both biocrust and root samples were not significant among C and water treatments.

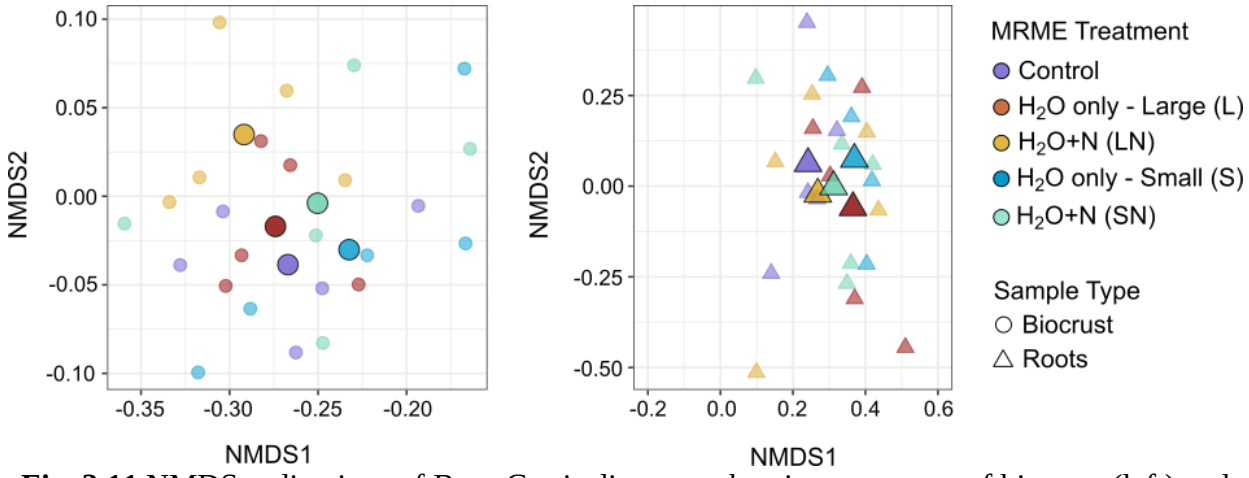

Fig. 3.11 NMDS ordinations of Bray-Curtis distances showing responses of biocrust (left) and root-associated (right) fungal communities in MRME to large (L) or small (S) water additions and L/S water additions + N addition treatments. Note difference in axis scales among sample types.

At WENNDEx, biocrust community composition shifted significantly compared to controls (H_2O treatment main effect for biocrust: pseudo-*F* = 1.42, *P* = 0.027; Table 3.4), and pairwise comparisons indicate that these differences were driven by communities in water + N treatments since water additions alone did not generate significant community shifts (pairwise comparisons of water treatments for biocrust: C vs. H_2O: pseudo-*F* = 0.70, *P* = 0.947; C vs. H_2O + N: pseudo-*F* = 1.92, *P* = 0.047; H_2O vs. H_2O + N: pseudo-*F* = 1.58, *P* = 0.047). Root communities at WENNDEx did not show significant shifts in response to either water or water + N treatments (Fig. 3.12). Dispersion tests were not significant among C and water treatments for either sample type.

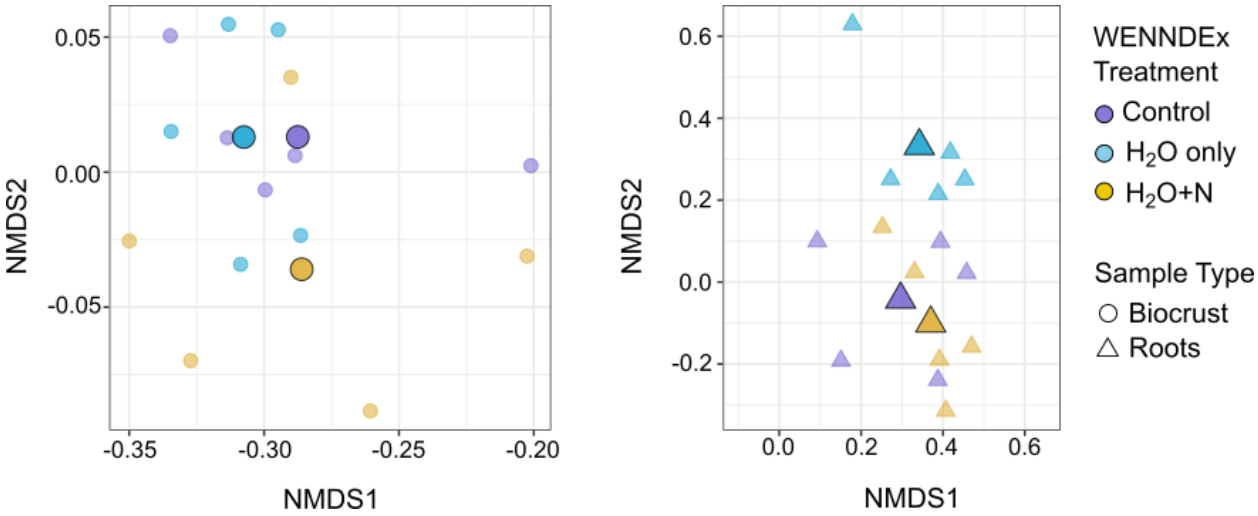

Fig. 3.12 NMDS ordinations of Bray-Curtis distances showing responses of biocrust (left) and root-associated (right) fungal communities in WENNDEx to water and water + N addition treatments. Note difference in axis scales among sample types.

Root Colonization

Fungal root colonization at MRME did not show significant changes in response to water additions alone nor to water + N additions for either rainfall treatment level (Treatment main effect: X^2 = 1.55, P = 0.907; Table S3.3; Fig. 3.10a), however, percent colonization by septate hyphae was significantly higher than aseptate hyphae across all treatments (Hyphal type main effect: X^2 = 57.53, P < 0.001; Table S3.3), and the proportion of total views was 1.5-2x higher for septate hyphae within roots of plants on average across C and water addition treatments (pairwise comparisons of aseptate:septate in L rainfall addition: t = -2.91, P = 0.008; in S rainfall addition: t = -3.99, P < 0.001; in LN: t = -2.02, P = 0.055 , in SN: t = -2.483, P = 0.021). At WENNDEx, root colonization by septate hyphae was similar across control and both water and water + N treatments (Fig. 3.10c). Colonization by aseptate hyphae was similar in roots from C and H_2O only treatments but significantly lower in roots from H_2O + N treatments compared to those from controls (pairwise comparisons of percent aseptate in C vs. H_2O + N: t = 3.51, P =

0.007). Between the two hyphal morphotypes, septate colonization was significantly higher (Hyphal type main effect: $X^2 = 19.23$, $P < 0.001$; Table S3.3), and tended to be ~1.5-2x greater than aseptate colonization in both water treatments (Fig. 3.10c). The proportion of septate hyphae in roots was notably ~3.7x higher than aseptate colonization in H_2O + N addition treatments at WENNDEx (pairwise comparisons of aseptate:septate in H_2O + N: $t = -3.08$, $P = 0.008$).

DISCUSSION

Overall patterns in fungal community composition

We found that across experiments and treatments, the majority (75%) of identifiable taxa belonged to Ascomycota, and at the class level, Dothideomycetes predominated in both biocrust and root samples with nearly half of the 30 most common taxa (based on sequence reads) belonging to the order Pleosporales, which made up ~38% of all OTUs ($n = 1106$) overall. These results are consistent with previous sequencing-based studies in New Mexico and Arizona, which found ~50-60% of fungi in biocrust and rhizosphere soils were classified to Pleosporales (Green et al., 2008, Porras-Alfaro et al., 2011, Bates et al., 2010). At a finer taxonomic resolution, some of the most common taxa across all experiments and treatments were found in an approximately equal number of biocrusts and root samples, and those included the genera *Darksidea*, *Aureobasidium, Gibberella*, *Fusarium,* and *Curvularia,* all of which were classified as fungal endophytes (among other functional classifications) through the FUNGuild database. The detection of *Darksidea* fungi in all 60 biocrust samples and nearly all (56) black grama root samples is notable as this was also the most abundant taxon in roots of blue grama at SNWR (Herrera et al., 2010, Porras-Alfaro et al., 2008), and *Darksidea* is thought to be one of the most

common DSE taxa in semiarid grasslands around the world (Knapp et al. 2012). The few common basidiomycete taxa represented were mostly from the order Agaricales, one of which (*Conocybe*) was also detected as a common taxon in a culture-based study of endophytes in blue grama roots (Khidir et al. 2010). Overall, our results from the most common taxa within biocrust soils and black grama roots support the results of previous comparative studies which used ITS sequencing to examine similarities between biocrusts and blue grama roots (Green et al., 2008; Porras-Alfaro et al., 2011). Ultimately, our data lend more robust support for the designation of these common taxa due to much higher sample sizes than previous work and provide insight into the potential similarities of fungi found in roots of both *Bouteloua* species at this site.

Biocrust vs. root-associated fungal communities

While the dominance of Ascomycete/Pleosporalean taxa was apparent in both biocrust and root communities, the overall community structure was relatively dissimilar among the two sample types. Biocrust and root samples each had higher proportions of unique taxa than they did shared, and OTU overlap ranged from 8-12% in untreated plots across the three experiments. Biocrusts had higher OTU richness, diversity, and evenness compared to roots in control plots at two experiments (NutNet and WENNDEx) and there were more uncommon taxa from phyla such as Chytridiomycota and Mucoromycota found in biocrust soils. These trends match a previous comparison at this site which found 3x greater fungal diversity in biocrust and rhizosphere soils compared to blue grama roots (Green et al., 2008), and overall biocrusts had ~1.5x higher OTU abundance compared to roots. Root communities showed greater within-group variability among samples but were still distinct from biocrusts in C plots at every experiment. There was also higher representation of arbuscular mycorrhizal fungi (AMF) in root communities, as would be expected, with Glomeromycota making up 7-11% of sequence reads

across root samples from three experiments and a very small proportion of reads (<1%) of biocrusts from just one experiment (MRME). This pattern was also apparent in the proportions of fungal trophic modes represented in unique taxa: 33% of root-specific taxa were classified as symbiotrophs, compared to just 3% of those unique to biocrusts and 11% of taxa shared by both biocrusts and roots. Our findings that Glomerales made up ~3% of total OTUs (n = 93), contrast with prior culture-based and sequencing studies from SNWR that found no representation of AMF in roots of blue grama (*Bouteloua gracilis*; Porras-Alfaro et al., 2008; 2011) or sand dropseed (*Sporobolus cryptandrus*; Herrera et al., 2010). We can conclude that AMF are in fact present in roots of black grama plants at this site, although likely at relatively lower abundance compared to mesic ecosystems with greater organic soil horizons (Taylor & Sinsabaugh, 2015).

Responses to N fertilization

At MRME, biocrust fungal communities showed declines in diversity and evenness in response to N addition alone (added at 5 g N m^{-2} y^{-1}), but observed and estimated OTU richness were not affected. The proportional abundance of certain rarer fungi may likely decline under N additions at this application rate, and the loss of these more sensitive taxa could lower the diversity index of a given sample (as measured by the Shannon Index) although the total species richness may remain unchanged. The loss of rare species under N fertilization may also impact overall microbial community composition, and we observed significant compositional differences in biocrust communities under N addition compared to samples from control plots at MRME.

In addition to losing potentially sensitive or specialized fungi, this shift in community structure could be due to a higher relative abundance and activity of taxa with broader growth tolerances and more flexible life-history strategies, similar to compositional changes observed in

soil bacterial communities under increased external N concentrations (Fierer et al. 2012). At NutNet, biocrust fungal community composition also differed significantly under N additions (10 g N m^{-2} y^{-1}) but did not show significant changes in any diversity response. Other studies have observed negative responses in biocrust fungal abundance under N fertilization due to soil acidification from N fertilization (Ochoa-Hueso et al., 2016), although acidification may not have as strong an impact in alkaline, carbonate-rich soils such those in our study (Stursova and Sinsabaugh 2008). Fungal biomass has also been shown to decrease more severely with greater duration and concentration of N fertilization (Treseder, 2008), and it is possible that in these experiments, N fertilization may have influenced the spatial distribution and accumulation of soil N resources over time, thus indirectly affecting the abundance and activity of soil fungi (Stursova et al. 2006; Ladwig et al. 2021; Ochoa-Hueso et al. 2020).

For root-associated fungi collected from both MRME and NutNet experiments, the overall community composition remained unchanged but there was a strong negative trend in richness, diversity, and evenness responses under N addition. Other N fertilization experiments have found decreased abundance of specialized fungal groups like arbuscular mycorrhizae under N fertilization at similar rates (Leff et al. 2015; Egerton-Warburton et al. 2007), and the responses of root-associated fungi are intimately tied with the responses of host plants. For example, dryland plants are generally N-limited and increase aboveground biomass production and cover under N fertilization (Xia and Wan 2008; Baldarelli et al. 2021), which can decrease the proportion of C allocated to roots and to rhizosphere microbes (Meng et al. 2022; Johnson et al. 2003; Corkidi et al. 2002). For some root-inhabiting fungi, reduced C from plant hosts could initiate a shift in trophic mode from facultative symbiosis to saprotrophy, thus allowing them to exploit organic matter substrates which may be more abundant following higher plant biomass

production and leaf litter inputs in response to N fertilization (Johnson et al. 2013; Aguilar-Trigueros et al. 2014). Finally, different plant hosts undoubtedly affect growth and coexistence of diverse root and rhizosphere fungi through variation in root traits, photosynthetic pathways, and seasonal biomass production (Sweeney et al. 2021; Ladwig et al. 2021), but since we sampled the same dominant species at only one time point, exploring the influence of plant responses on fungal community changes in N fertilized plots was beyond the scope of this study.

Prior studies at the WENNDEx observed that N fertilization treatments of 2 g N m^{-2} y^{-1} significantly increased plant available N and aboveground net primary production (Collins et al. 2010), however neither biocrust nor root communities showed significant changes in any diversity metrics or community structure under N addition treatments at this experiment. Biocrust soils also had similar biomass among C and N treatment plots, and the lowest ratio of bacteria:fungi according to FAME data. However, fungal root colonization by aseptate hyphae decreased significantly between C and N treatments, and WENNDEx was the only site where this response to N addition was observed. Aseptate hyphae are associated with more basal lineages of fungi, i.e., Glomeromycota and Mucoromycotina (Lanfranco et al. 2016; Stajich et al. 2009), and FAME data from WENNDEx soils show biomarkers for AM fungi in 8 out of 10 samples, the most out of the three experiments. While I did not specifically observe arbuscules in WENNDEx roots, I did find high amounts of conidial hyphae surrounding root sheaths and in cortical cells of black grama plants collected from this experiment. So it is possible that some AM fungi could have experienced biomass declines under higher soil N availability to plant hosts, although overall root community structure was unchanged.

Responses to changes in rainfall regime and water × N additions

For biocrust communities at MRME, there was little effect of either large or small water additions alone or in combination with N additions on diversity responses, however, biocrust fungal community structure showed significant shifts in response to all levels of water and water + N addition treatments. Compared to controls, biocrust community composition was more similar under large/infrequent (L) and small/frequent (S) rainfall additions and under the combined large + N (LN) or small + N (SN) treatments, but also did not shift among L and LN/SN nor S and LN/SN treatments, which indicates that biocrust communities may become more similar under increased precipitation variability in this habitat. This could potentially be driven by growth of few, dominant drought-intolerant community members once water limitations desist (Crowther et al. 2014). These patterns may also reflect changes to the relative abundance of fungi and the ratios of fungi:bacteria in soils under multiple environmental factors, both of which decreased under combined precipitation + N addition experiments in another grassland ecosystem (Yang et al. 2017).

Similarly, root fungal communities at MRME did not show strong diversity responses to water additions alone, but richness, diversity and evenness of root communities were negatively impacted by water + N additions at both levels compared to controls. In contrast to biocrusts, root-associated fungi at MRME had relatively stable community structure under all levels of water and water + N addition. These results indicate that community composition of roots could potentially be more stable in response to one or more changing environmental drivers, but the taxonomic diversity and abundance of root-associated fungi may decline if plant communities are similarly released from water and nutrient limitation during the growing season (She et al. 2018). Under these conditions, plants may no longer rely as heavily on root and rhizosphere

fungi to obtain soil water and nutrients, and plant-fungi feedbacks may be more strongly influenced by availability of other limiting nutrients such as phosphorus (Hoeksema et al., 2010). Fungal root colonization similarly did not show strong responses to water treatments at MRME, and there was a consistent pattern of higher septate > aseptate colonization across all experimental treatments.

At WENNDEx, diversity metrics of both biocrust and root communities were not significantly impacted among control, water, and water + N treatments; however, biocrusts had consistently higher richness, diversity, and evenness compared to roots across all treatments. Similar to the responses from MRME, biocrust community composition only showed significant changes under water + N treatments, but not water addition alone, compared to controls. In root communities at WENNDEx, composition was unchanged by either water or water + N additions, however root colonization by aseptate fungi showed the largest decreases under water + N additions compared to controls. This pattern was similar to the significant declines in aseptate colonization seen under N additions, which could suggest a negative feedback between N fertilization and growth of potentially mycorrhizal fungi, which has been demonstrated in drylands as well as other ecosystems (Hoeksema et al. 2010; Antoninka et al. 2011).

Overall, the responses observed in both experiments align with findings from another Chihuahuan Desert grassland study where there was no change to saprophytic fungal community structure (as measured by soil FAME levels) under high precipitation variability over the course of a 3-year experiment (Bell et al. 2009). It is possible that changes to soil moisture alone do not drive changes in biocrust or root fungal community diversity, but the indirect effects of water on increasing soil nutrient availability likely serves an important role in plant and microbial community responses (Schimel et al. 2007; Ramond et al. 2022). Multiple changing

environmental factors such as water and N deposition affect plant-soil interactions and may control seasonal feedbacks with important implications for ecosystem nutrient cycling and retention in drylands and other ecosystems (Jia et al. 2023; Parker and Schimel 2011). Overall, these patterns indicate that biocrust and root fungal communities in this experiment may show limited responses to water addition alone, especially applied early in the year (January-March) as is the case for WENNDEx.

Across experimental treatments, we observed greater compositional shifts in biocrust communities compared to root-associated fungi in response to N, water, and water + N additions, especially in the MRME experiment. Overall, the structure of root fungal communities was relatively unaffected among the various levels of experimental treatments, and these differences could be due to several factors. First, fungi in root microhabitats are better protected from environmental changes and may have narrower environmental tolerances compared to communities at the soil surface that experience fluctuations in external conditions (Crowther et al., 2014; Rudgers et al., 2022). Plants also cultivate specialized communities of obligate or facultative root symbionts including mycorrhizae and other non-pathogenic endophytes (Porras-Alfaro and Bayman 2011; Requena et al. 2007), and the assembly of these communities may be inherently more stable over time due to fungal transmission in plant propagules, such as clonal reproduction in grasses like black grama (Peters 2002) and/or production and germination of endophyte-containing seeds (Rodriguez et al. 2009). Another important factor driving these responses could be the relatively high number of unique taxa in biocrust soil communities compared to roots. Soil microhabitats contain many functional niches and thus may have a greater number of rare community members to potentially lose or change in response to environmental perturbations. Compared to root-associated fungal communities which may be

more functionally similar or uniform due to the constraints of living within plant tissues, changes to the abundances of these diverse soil taxa may drive more dramatic shifts in soil communities under altered conditions (Zhang et al. 2016).

CONCLUSIONS

Overall, we found evidence for the presence of distinct communities of fungal taxa in biocrust soils and black grama roots across the three experiments sampled. Although DSE taxa in Pleosporales accounted for nearly half of all OTUs, biocrusts had a relatively higher amount of unique OTUs compared to roots, and surface soil communities likely contain more diversity from unclassified fungal taxa at this site compared to root microsites. Under N fertilization treatments > 2 g m^{-2} y^{-1}, biocrust fungi showed significant shifts in community composition, but had fewer declines in richness, diversity, evenness, and biomass compared to roots. At MRME, biocrust fungal community structure significantly shifted in response to water and water + N additions while root community structure was less impacted by water addition treatments, but root fungi showed significant declines in richness, diversity and evenness under water + N additions. This indicates that the effects of multiple environmental drivers on the diversity, abundance and colonization of root-associated fungi may be stronger than singular changes alone. We observed that black grama root communities overall are lower in diversity and abundance compared to biocrust soils, but may exhibit more stable community composition under changing external conditions, even if declines in taxonomic diversity are evident. Overall, predicted changes to dryland ecosystems such as increases in precipitation variability and drought periods, and higher anthropogenic N inputs to soils may drive changes to the composition of biocrust soil fungal communities and could decrease root-associated fungal

diversity and abundance. Both feedbacks will have larger consequences for C and N cycling and retention and overall functioning of microbial and plant communities in these ecosystems.

Chapter 4: Fungal exclusion does not impede movement or plant uptake of biocrust soil nitrogen

ABSTRACT

In dryland ecosystems, diverse microbial communities are concentrated in the topmost layers of soil in plant interspaces due to the presence of biological soil crusts (biocrusts). It has been hypothesized that soil fungi that also colonize plant roots may facilitate the exchange of water and nutrients such as nitrogen (N) and carbon (C) between biocrusts and plants via a network of shared hyphae, effectively re-coupling cycles of nutrient release and uptake between these primary producers and minimizing ecosystem N losses. However, the number of direct tests of fungal nutrient exchange networks in drylands is limited. In this study, we attempted to isolate the role of fungi in nutrient translocation between biocrust soils and individual plants. We set up a series of experiments using two types of fungal exclusion mesh to impede potential connections between roots and hyphae, and used isotopic tracers to track nitrogen movement through soils and into aboveground plant tissues over time. We found that plant uptake of ^{15}N applied to biocrust soils was not inhibited by either vertical or horizontal mesh treatments or surface soil barriers, and excess N in leaves was higher after 3-10 days versus 1 day following application. Overall, our results illustrate that N transfer in these soils does not occur at rapid timescales and may be driven by soil diffusion of dissolved nutrients to plant root zones, rather than active fungal facilitation.

INTRODUCTION

The high spatial variability of soil nutrients affects plant growth and establishment, and plant cover in these ecosystems is generally discontinuous based on the availability of soil water

and essential nutrients such as nitrogen (Delgado-Baquerizo et al. 2013). In plant interspaces, the topmost 0-2 cm of soil is often colonized by diverse communities of photoautotrophic organisms known as biological soil crusts (biocrusts), which are estimated to cover approximately 12% of Earth's terrestrial surface (Rodríguez-Caballero et al. 2018) and serve important functions in biogeochemical cycling in dryland ecosystems around the world (Weber et al., 2022).

Biocrust constituents can include cyanobacteria, algae, fungi, bacteria, lichens, bryophytes and other organisms, and in North American deserts, these communities contain filamentous free-living and symbiotic cyanobacteria that can aggregate soil particles and fix atmospheric carbon (C) and nitrogen at the soil surface (Barger et al. 2016). Biocrusts can function as alternate primary producers to plants due to their widespread cover on the surface of undisturbed interspace soils (Belnap et al., 2016; Garcia-Pichel et al., 2013). In addition to mediating soil nutrient inputs via C and N fixation, biocrusts also capture nutrients from airborne dust and organic matter and can internally transfer and redistribute N within soils (Barger et al. 2016). Dryland microbes such as bacteria and fungi can rapidly mineralize N sources and control N transformation processes such as nitrification (Collins et al. 2008), and thus serve important roles in the movement and retention of soil nutrients in these otherwise nutrient-poor environments.

For dryland plants, primary production and carbon cycling processes are limited by the availability of both water and inorganic and organic N sources to roots (Hooper and Johnson 1999), and competitive interactions within and among plant species are driven by the distribution and supply of soil nutrients (Chesson et al. 2004). Furthermore, bioavailable sources of soil N can be depleted or lost to the atmosphere within 24 hours if plant root uptake is decoupled from microbial release following a precipitation event (Brown et al. 2022; Homyak et al. 2016; Austin

et al. 2004). In drylands with high ecosystem N losses, it has been proposed that soil fungi may facilitate the exchange of water, carbon, and nutrients between plants and biocrusts, effectively re-coupling these producers and retaining resources in the biotic pool (Collins et al. 2008; Rudgers et al. 2018). This connection, also known as the "fungal loop," operates parallel to—and may dominate over —the more familiar C and N cycling patterns in mesic systems, which are driven by litter input and subsequent mineralization of soil organic matter (SOM; Schimel and Bennett 2004).

There are several direct tests of nitrogen movement from biocrusts to plants, including key field experiments which used stable isotope ^{15}N tracers to successfully trace the movement of N solutions applied directly to biocrust soils into plant root and leaf tissues (reviewed by Rudgers et al. 2018). While these studies did not necessarily isolate fungi as the sole N movement vector, there are several lines of indirect evidence supporting the role of fungal networks in dryland nutrient movement. First, the dominance of fungi in dryland N_2O production indicates that fungi are key agents of N transformation in dryland soils (McLain and Martens 2006; Crenshaw et al. 2008; Chen et al. 2015). Second, fungi, particularly the Ascomycota that dominate dryland soils, can metabolize at lower water potentials than either plants or bacteria and may be physiologically active under dry conditions (Chowdhury et al., 2011; Stevenson et al., 2015). Third, networks of fungal hyphae can effectively increase water conductivity in dry soils by bridging gaps across soil pores (Allen 2007; Boddy 1999), and studies have shown that fungal hyphal networks can translocate water from plant roots even under drought conditions (Querejeta et al., 2003), so it is likely that fungi could facilitate movement of C and N among biocrusts and plants. Fourth, there is general taxonomic overlap among ascomycete fungi that colonize plant roots (DSE) and fungi found in surface soil biocrust communities (Bates et al.

2012; Green et al. 2008), and these shared taxa could potentially be functionally integrated and facilitate water and nutrient exchanges among biocrusts and roots.

In this study, we aim to test a key aspect of the fungal loop hypothesis by isolating the role of fungal hyphae in nutrient exchange and retention among biocrusts and plants. Our main questions are: **(1)** How rapidly does N translocation occur from biocrust surface soils to plant leaves, and are there common patterns of N uptake across study sites and plant species? We expect to see rapid plant uptake to leaves within ~24 h, based on a previous greenhouse experiment (Chapter 2) where N movement from roots to leaves of target species occurred on the scale of 12-48 h and a field study where significant uptake of ^{15}N was documented within 24 hours of application to biocrust soils < 1 m away (Green et al., 2008); and **(2)** Can ^{15}N movement through biocrusts be impeded by fungal exclusion mesh or other barriers placed in soils? If the fungal loop hypothesis is correct, we expect to see a decrease in N translocation in response to vertical and horizontal fungal-exclusion mesh treatments. This expectation is based on previous experiments with mycorrhizal fungi as well as one potted-plant study where the transfer of ^{15}N between biocrusts and plants was marginally reduced under different rainfall treatments by impeding fungal connections to roots using a similar mesh barrier (Dettweiler-Robinson et al. 2020).

METHODS

Site description

We compared two semiarid grassland sites in New Mexico; the Sevilleta National Wildlife Refuge (SEV; 34.338 N, -106.735 W, 1605 m) and the Jornada Experimental Range (JOR; 32.5879 N, -106.74200 W, 1360 m), both of which are part of the Long-Term Ecological

Research (LTER) network. These sites were chosen because they share features representative of diverse Northern Chihuahuan Desert ecosystems and have grass- and shrubland transition zones where soil nutrient dynamics, resource competition, and ecosystem functioning are actively shifting (J. Chen et al., 2015; Schaeffer et al., 2003). Both sites are characterized by broad temperature ranges, (~2-26 °C annually) and variable annual precipitation (200-300 mm) with the majority of rainfall occurring during the monsoon season (July to September), and some precipitation during the winter months (Notaro et al., 2010; Pennington & Collins, 2007).

Species descriptions

Black grama (*Bouteloua eriopoda*) is a long-lived, stoloniferous perennial C_4 grass with fibrous, finely divided roots concentrated in the upper 5 – 10 cm of soils (Burnett et al., 2012; Gibbens & Lenz, 2001; Kurc & Small, 2004). At JOR, black grama grasslands have experienced significant declines due to shrub encroachment driven by grazing, drought and other factors (Peters & Gibbens, 2006). At SEV, black grama accounts for up to 80 – 90% of cover within nearly monospecific Chihuahuan Desert grassland habitats and is considered a foundation grass species (Collins et al. 2020; Muldavin et al. 2008). Broom snakeweed (*Gutierrezia sarothrae*) is a woody, perennial C_3 subshrub with a taproot that can extend to 1–2 m below the soil surface that allows for rapid subsoil water uptake (Gibbens & Lenz, 2001; Wan et al., 1995). Within Chihuahuan Desert grasslands at SEV, snakeweed is a sub-dominant species that has shown marginal cover increases in response to N addition (Collins et al., 2010). Biocrusts at both study sites are cyanobacteria-dominated communities containing filamentous species of *Microcoleus*, which form bundled filaments that bind soil particles together in the surface layer (Fernandes et al., 2022). At SEV, biocrusts can also contain heterocystous, nitrogen-fixing cyanobacteria such as *Scytonema* and *Nostoc* spp. in addition to *Microcoleus* spp. (Fernandes et al., 2018).

Field plot set-up

In 2016 and early 2017, we set up 50 cm × 50 cm plots at both sites to surround a target plant individual with an adjacent, intact biocrust patch. The plots were split into two rectangles: we added aluminum flashing in a rectangle 50 cm × 25 cm to a depth of 8-10 cm to isolate the target plant on one end and biocrust patch on the other end (Fig. 4.1) and designated the adjacent 50 cm × 25 cm rectangle using pin flags instead of aluminum flashing on three sides (Fig. 4.2). These unconstrained plot halves were used to collect soil samples without disturbing the biocrusts inside the flashing where ^{15}N tracer addition occurred.

In 2017, we installed a "vertical" mesh component to a subset of plots (Fig. 4.1) to exclude connections between fungal hyphae and *B. eriopoda* plant roots. We placed hydrophilic mesh (GE Healthcare Life Science, Pittsburg, Pennsylvania) vertically at the center of each plot (approx. 25 cm wide x 10 cm deep) using two mesh types: coarse mesh (50 μm diameter pores), which allowed fungal hyphae (but not plant roots) to penetrate; and fine mesh (0.45 μm diameter pores) which and impeded both roots and fungal hyphae (Fig. 4.2a). Although we could not completely eliminate potential movement below 10 cm or around the edges of the mesh, this technique impeded the majority of the surface area between biocrusts and plants on opposite sides of each plot. Control plots were undisturbed without any mesh installed.

In 2018, we installed a 2 cm barrier to determine if transport was occurring in the uppermost biocrust soil layers or at deeper soil depths. We cut a 25 cm × 2 cm piece of aluminum flashing and placed it 10 cm from the base of target plants to separate the biocrust end from plants (Fig. 4.1). Controls were undisturbed with no 2 cm barrier. We replicated this with individuals of *G. sarothrae* in addition to *B. eriopoda* at both JOR and SEV sites during the monsoon season in 2018.

In 2019, we installed a "horizontal" mesh component using the same coarse and fine mesh as in 2017 to a subset of *B. eriopoda* plots to impede fungal-root connections in shallow soil layers. Top layers of soil (~0-2 cm) were watered to minimize crust breakage and disturbance, and then carefully lifted up away from the soil surface to place pieces of flat mesh directly underneath each biocrust patch (Fig. 4.1). Soils were then placed back over the mesh layer with minimal disturbance to the surface crust structure (Dettweiler-Robinson et al., 2020). Controls were undisturbed with no mesh barrier.

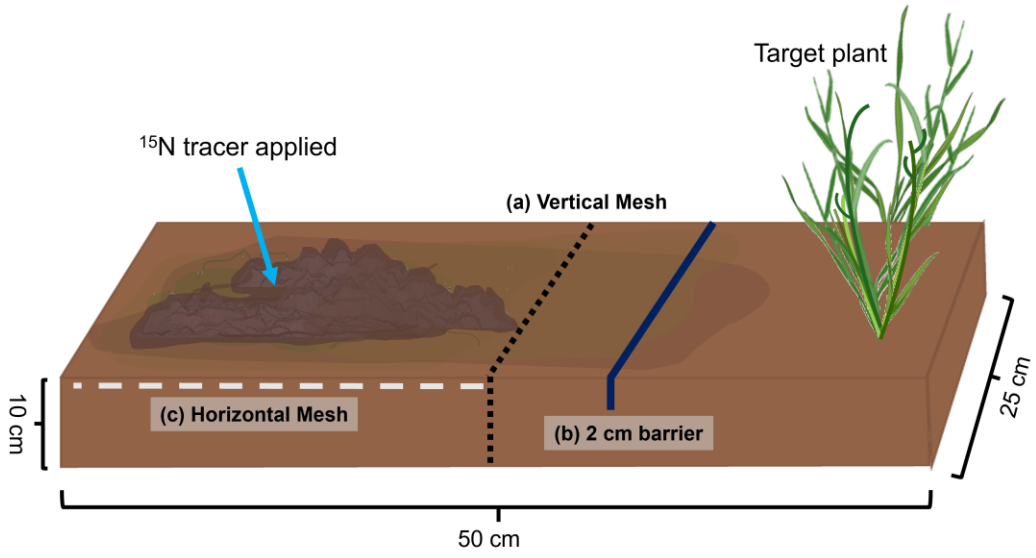

Fig 4.1 Field plot diagram showing plant and biocrust ends and three types of fungal exclusion treatment based on experiment year: (a) Vertical mesh in 2017; (b) 2 cm barrier in 2018; and (c) Horizontal mesh in 2019. Based on an illustration by K. Young.

Fig 4.2 Field plot set-up for individual plants and biocrust patches at JOR: (a) *B. eriopoda* with vertical mesh installed in center; and (b) *G. sarothrae* (no treatment)

^{15}N tracer application

All raceways were weeded for annual and non-target plants 1-2 weeks prior to tracer addition; we also measured target plant diameter at the base (*B. eriopoda*) or canopy (*G. sarothrae*) and perpendicular diameter in the field and built allometric equations for each species/site to estimate aboveground biomass without harvesting individuals at each site. Prior to tracer addition, plots were watered in the early morning for an equal length of time until the surface was visibly wet in order to ensure plant and microbial activity. We did not apply ^{15}N tracer to biocrusts until the soil surface in each plot was visibly dry (~1 h at Jornada, ~3 h at Sevilleta). In the 2017 experiment, we added 1.0 mL of 48 mmol L^{-1} potassium nitrate solution (98 at% $K^{15}NO_3$; Sigma-Aldrich, Inc., St. Louis MO, USA) directly to a 5 cm diameter patch of biocrust soil using a pipette (0.71 mg N per plot). In 2018 and 2019, we used a combined inorganic tracer $^{15}NH_4{}^{15}NO_3$ at significantly higher solution concentrations: 11.6 mg N per plot in 2018 and 12.6 mg N per plot in 2019, due in part to low ^{15}N recovery in 2017 plots. These

latter tracer concentrations were chosen to match the methods of a prior study in the same ecosystem (Green et al., 2008) where 12.5 mg (an amount the authors determined to be approximately 0.5% of the N stock of surrounding biocrust and grass foliage) of $Na^{15}NO3$ was added to biocrust patches 3 cm in diameter.

Sample collection and processing

To determine if the ^{15}N tracer was found in plant tissues, we collected 5-10 leaf samples from plots on day 0 (pre-tracer addition), day 1, day 3, day 7 or 10, and day 365 (1 year post application). Samples were dried for 3 days at 60 °C and then ground in 2 mL plastic bead beater tubes (Thermo Fisher Scientific, Waltham, MA, USA) using metallic beads for 2 × 30 s to fully homogenize all tissues. Approximately 4.5 mg of ground leaf material was then packed in aluminum capsules (CE Elantech, Lakewood, NJ) for isotopic ^{15}N analysis at the Center for Stable Isotopes (University of New Mexico) on an ECS 4010 Elemental Analyzer and a Delta V Isotope Ratio Mass Spectrometer (Thermo Fisher Scientific, Waltham, MA, USA).

Response Variables

Nitrogen isotope ratios were expressed in δ notation (‰) using atmospheric N_2 as the standard (Mariotti 1983). Leaf samples collected prior to tracer addition (day 0) were used to calculate natural abundance or background $\delta^{15}N$ values for each species (*B. eriopoda* and *G. sarothrae*) at each site (see Table 4.1). We used these average natural abundance values to estimate species-specific "enrichment cutoff" values by fitting a kernel density function to each set (one set per species × location; Warren and Silverman 1987) and selecting the 99th percentile as the cutoff value. We considered post-addition leaf samples with $\delta^{15}N$ values above the respective species cutoff value to be "enriched", and those with $\delta^{15}N$ values equal to or below the species cutoff as "unenriched". For our analyses, we used a subset of enriched leaf samples out

of the total collected (Table 4.2) and excluded day 0 samples (leaves collected prior to ^{15}N tracer addition) from analysis. For enriched samples only, we first determined the total mass of all N (M_{sample}) in leaves using the following equation:

$$M_{sample} = \%N_{plant} \times adw_{plant}$$

where $\%N_{plant}$ is the average %N across all leaf samples of the same plant, and adw_{plant} is the total aboveground dry weight (adw) of all leaf samples plus the final harvested biomass from the plant in milligrams. We then determined the proportion of ^{15}N measured in each leaf sample (F) using the following equation:

$$F = \frac{R}{(1 + R)}$$

where R = sample $\delta^{15}N$ value converted to atom %. We then calculated the total mass of ^{15}N in each post-addition sample ($M_{labeled}$) using the following equation (Robinson, 2001):

$$M_{labeled} = M_{sample} \times F$$

We did the same for all leaves collected at Time 0 to calculate the total mass of ^{15}N in each natural abundance sample ($M_{background}$). We then subtracted $M_{background}$ (mg) from $M_{labeled}$ (mg) to determine *excess N,* or the total mass of ^{15}N recovered in leaves in excess of natural abundance (mg and µg ^{15}N per g leaf dry biomass).

Table 4.1 Leaf natural abundance ± standard error and calculated enrichment cutoff δ15N values (permille, ‰) for two plant species (*B. eriopoda* and *G. sarothrae*) at two sites (JOR and SEV). Because both species were not used for mesh-based experiments at both sites every year, an "N/A" indicates that there were no experimental units for that year and and an "--" indicates that $\delta^{15}N$ natural abundance values were used from another season and/or year (duplicate values italicized). All values from monsoon season only.

		JOR		SEV	
Plant Species	Year	$\delta^{15}N$	Cutoff	$\delta^{15}N$	Cutoff
B. eriopoda	2017	0.99 ± 0.19	3.84	-0.85 ± 0.13	1.70

	2018	--	*3.84*	-0.06 ± 0.26	1.88
	2019	N/A	N/A	-2.16 ± 0.18	-1.23
G. sarothrae	2018	--	*2.98*	0.76 ± 0.41	2.98

Table 4.2 Sample sizes of "enriched" leaves for each species at JOR and SEV from three years of mesh experiments. Note that *G. sarothrae* was only used in 2018 and a mesh experiment was only done at SEV in 2019.

		Site		
Plant Species	Year	JOR	SEV	*N*
B. eriopoda	2017	16	20	36
	2018	0	5	5
	2019	N/A	24	24
G. sarothrae	2018	6	8	14
Total				79

Analysis

We performed all statistical analyses in R version 4.2.2 (R Core Team 2022). To answer Questions 1 and 2, a linear mixed-effects (lme) model was fit by maximum likelihood using the 'lmer' function in the *lme4* package version 1.1-27 (Bates et al., 2015) to compare excess N of plant species among experimental treatments and sites. Response data for each year were log-transformed in order to improve the normality of residuals. Because the experiment treatments and sample sizes differed, one model was fit for each year (2017, 2018, 2019). The full lme model for 2017 included mesh type (coarse, fine, or none), site, and day collected and their interactions as categorical fixed effects. For 2018, the linear model included mesh type (2 cm or none), day collected, plant species (*B. eriopoda* and *G. sarothrae*) and their interactions as fixed effects. Data from both sites were combined for 2018 due to limited sample sizes of enriched samples for each species. For 2019, since the experiment was only performed at one site (SEV) the model included mesh type and day collected and the interaction of mesh type:day as fixed

effects. The lme models also included plot ID as a random effect to account for repeated collection of leaves from the same plot over multiple days. All models met the assumption of normality of residuals (Shapiro-Wilk test $P > 0.05$). The significance of main effects and interactions was assessed via analysis of deviance Type II tests using the 'Anova' function in the *car* package version 3.0–10 (Fox et al., 2012). *Post hoc* pairwise comparisons of treatment means for main effects and interactions among for each year were performed in the *emmeans* package version 1.6.1 (Lenth, 2021). *P* values were adjusted for multiplicity using the Tukey method for varying family sizes, and all pairwise comparisons of means used the Kenward-Roger degrees-of-freedom method and a 0.95 confidence level.

RESULTS

Patterns in N uptake across time, study sites and plant species

We found that across all experiments, plant ^{15}N uptake was low, and we did not see significant movement of N into leaves after 24 hours (1 day) following tracer application to biocrusts < 50 cm away despite the fact that we confirmed active water uptake and photosynthesis in the target plants prior to tracer application. Across all treatments and years, average excess N values of *B. eriopoda* leaves collected 3 days following ^{15}N tracer application were 53.0 ± 8.7 µg ^{15}N per g leaf dry biomass; by 7 days they were 61.0 ± 7.0 µg ^{15}N per g leaf dry biomass; and by 10 days they were 76.2 ± 22.2 µg ^{15}N per g leaf dry biomass (enriched samples only). Leaf samples (n = 15) collected from living *B. eriopoda* plants one year following the 2017 monsoon season tracer application at SEV were considered N-enriched, and the average excess N across all treatments was 31.6 ± 21.5 µg ^{15}N per g leaf dry biomass (Fig. 4.3).

Among study sites, we had sufficient sample sizes to compare the two locations in 2017 and observed significant trends in excess N uptake (main effect of site: $X^2 = 6.36$, $P = 0.011$; Table 4.3) over time. After 10 days, leaves from *B. eriopoda* plants at JOR tended to have significantly greater excess N values compared to SEV (main effect of day collected: $X^2 = 12.48$, $P = 0.006$; Table 4.3); and on average, plants in control plots at JOR took up ~74x more N than those at SEV, and plants in coarse mesh plots took up ~45x more N at day 10 (Table S4.1). This trend was significant for control plots with no mesh added (pairwise comparison of no mesh at JOR vs. SEV at day 10: $t = 2.21$, $P = 0.034$) but not for coarse mesh plots (pairwise comparison of coarse mesh at JOR vs. SEV on day 10: $t = 1.20$, $P = 0.286$). At SEV, there was also a significant trend across days collected for control plots only, and leaves had significantly greater excess N after 365 days compared to 10 days (pairwise comparison of control plots at SEV on day 10 vs. day 365: $t = -2.37$, $P = 0.025$).

Table 4.3 Results from linear mixed effects ANOVA model for the 2017 experiment testing for main and interacting effects of vertical mesh type (coarse, fine, none), site (JOR vs. SEV) and day collected (3, 10, 365) on excess N (mg ^{15}N per g leaf dry biomass) of *B. eriopoda* plants. Significant values ($P < 0.05$, Type II Wald Chi-square tests) are bolded.

2017		Leaf Excess N	
Predictors	df	X^2	P
Mesh Type	2	1.32	0.516
Site	**1**	**6.36**	**0.012**
Day Collected	**3**	**12.48**	**0.006**
Mesh Type: Site	2	0.26	0.877
Mesh Type: Day Collected	3	0.26	0.967

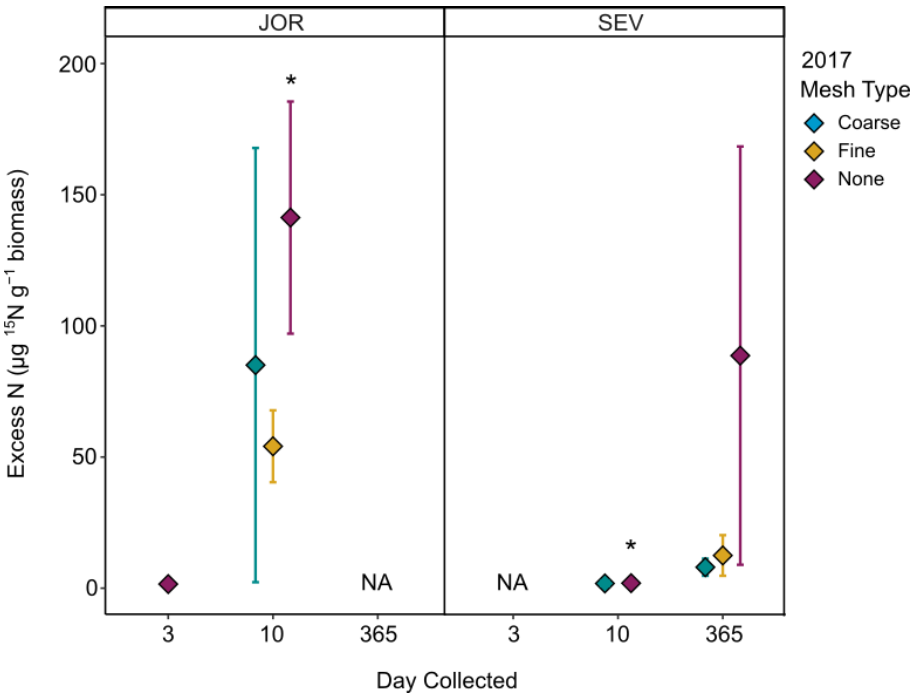

Fig. 4.3 Excess ^{15}N values in leaves from *B. eriopoda* individuals (N-enriched samples only) collected 3, 10, and 365 days following ^{15}N tracer application to biocrusts in the 2017 monsoon season mesh experiment plots (treatments: vertical coarse mesh, fine mesh, or no mesh) at both JOR and SEV sites. An "NA" indicates no enriched samples for that site/collection day, and significant pairwise comparisons ($P < 0.05$) are indicated by an asterisk.

Among plant species, in 2018 we combined data from both JOR and SEV to compare N uptake in *B. eriopoda* and *G. sarothrae* plants and found some notable differences among the two species, although this was not strongly statistically significant (main effect of plant species: F = 3.23, P 0.094; Table 4.4). After 3 days, *G. sarothrae* leaves had ~9x higher excess N than those of *B. eriopoda* in no mesh treatments and ~6x higher excess N in 2 cm mesh treatments (pairwise comparison of species averaged across treatments: t = -1.92, P = 0.076; Table S4.1). There was not sufficient data from enriched samples to compare differences among the two species after 365N days; and the excess N value for one *B. eriopoda* sample from 2018 (2 cm mesh) was 1.1 µg ^{15}N per g leaf dry biomass (Fig. 4.4).

Table 4.4 Results from linear ANOVA model for the 2018 experiment testing for main and interacting effects of mesh type (2 cm vs. none) and plant species (*B. eriopoda* vs. *G. sarothrae*) on excess N (mg ^{15}N per g leaf dry biomass); data was combined from two experiment sites to have adequate sampling sizes.

2018		Leaf Excess N	
Predictors	df	*F*	*P*
Mesh Type	1	0.94	0.349
Plant Species	1	3.23	0.094
Mesh Type:Species	1	0.48	0.500

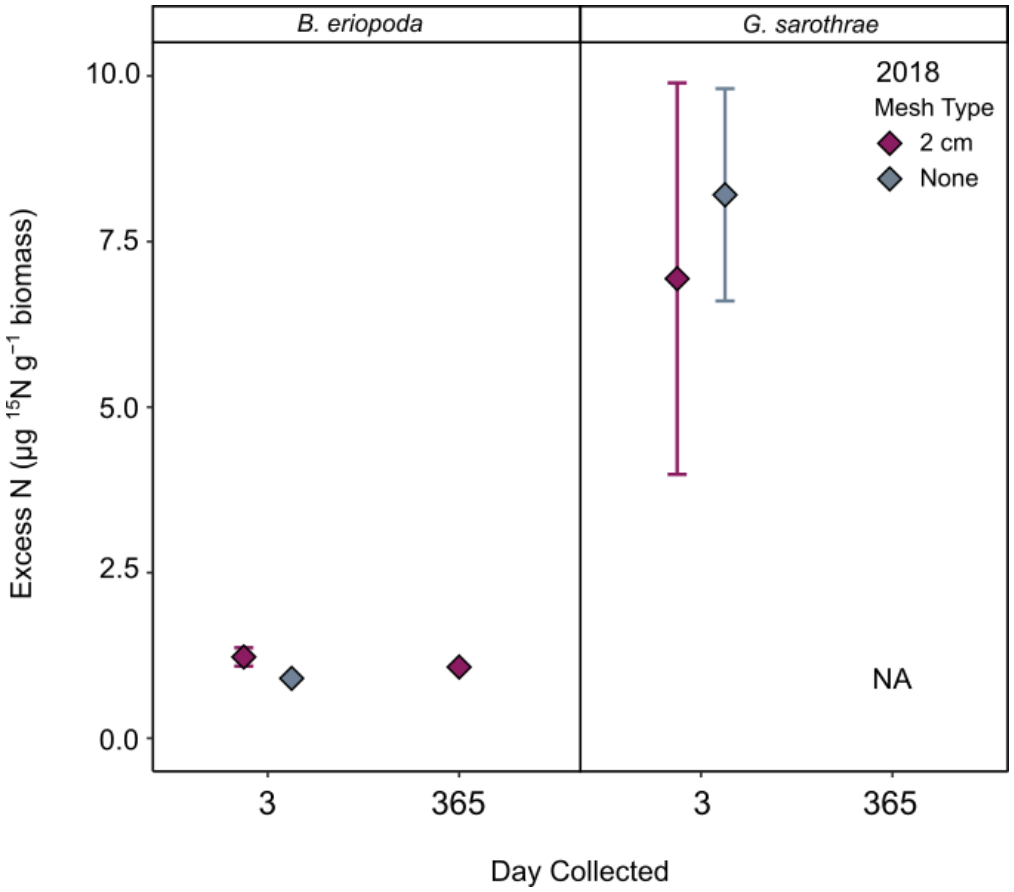

Fig. 4.4 Excess ^{15}N in leaves collected from *B. eriopoda* and *G. sarothrae* individuals (N-enriched samples only) collected 3 and 365 days following ^{15}N tracer application to biocrusts in the 2018 monsoon season mesh experiment plots (treatments: 2 cm barrier in biocrust layer vs. no barrier). Note that both JOR and SEV data were combined for this year due to low sample sizes of N-enriched plants for each plant species. An "NA" indicates no enriched samples for that species/collection day.

Effects of fungal exclusion mesh

In 2017, the amount of ^{15}N tracer that made it into leaves of *B. eriopoda* plants was not significantly different among the two types of vertical mesh treatments compared to control plots (main effect of mesh type: $X^2 = 1.32$, $P = 0.516$; Table 4.3). At JOR, after 10 days, there was a slightly higher amount of excess N in leaves from control plots compared to fine mesh, however this trend was not statistically significant, and excess in in leaves from coarse mesh plots was marginally significantly different from controls (pairwise comparison of coarse/no mesh at day 10: $t = -2.45$, $P = 0.053$, Fig. 4.3). At SEV, there was no difference observed among controls vs. coarse mesh treatments after 10 days following application (Fig. 4.3). One year following application, there tended to be higher leaf excess N on average in controls compared to coarse and fine mesh treatments at SEV, however this trend was not statistically significant based on *post hoc* testing (Fig. 4.3). $\delta^{15}N$ values of roots collected after 60 days at JOR also indicate that plants at this site may have also retained N in belowground tissues > 10 days following application (Fig. S4.1).

In the 2018 experiment, plants of each species showed similar N uptake among the two mesh treatments on average, and after 3 days there was no significant difference for either *B. eriopoda* or *G. sarothrae* in leaf excess N in plots with a 2 cm barrier vs. controls (main effect of mesh type: $F = 0.94$, $P = 0.349$; Table 4.4). However, the sample sizes for *B. eriopoda* were relatively low and this may obscure treatment responses for this species (Fig. 4.4).

In 2019, *B. eriopoda* plants with horizontal mesh placed underneath the surface soils did not show apparent differences in excess N uptake compared to controls after 3 or 7 days (main effect of mesh type: $X^2 = 3.74$; $P = 0.154$; Table 4.5), and both coarse and fine mesh treatments had similar amounts of mean excess N on average across both collection days, while plants in

control plots tended to take up less N than either of the two mesh treatments (means ± SE for coarse = 89.1 ± 16.9; fine = 70.6 ± 9.1; none = 45.4 ± 3.6 µg ^{15}N per g leaf dry biomass; Table S4.1), and while there appeared to be a similar pattern of higher uptake in plants in coarse mesh over fine mesh over control treatments among the two days collected, this trend was not statistically significant (Fig. 4.5).

Table 4.5. Results from linear mixed effects ANOVA model for the 2019 experiment testing for main and interacting effects of horizontal mesh type (coarse, fine, none) and day collected (3, 7) on excess N (mg ^{15}N per g leaf dry biomass) of *B. eriopoda* plants at one experiment site (SEV).

2019		Leaf Excess N	
Predictors	df	X^2	*P*
Mesh Type	2	3.74	0.154
Day Collected	1	0.71	0.399
Mesh Type:Day Collected	2	1.08	0.584

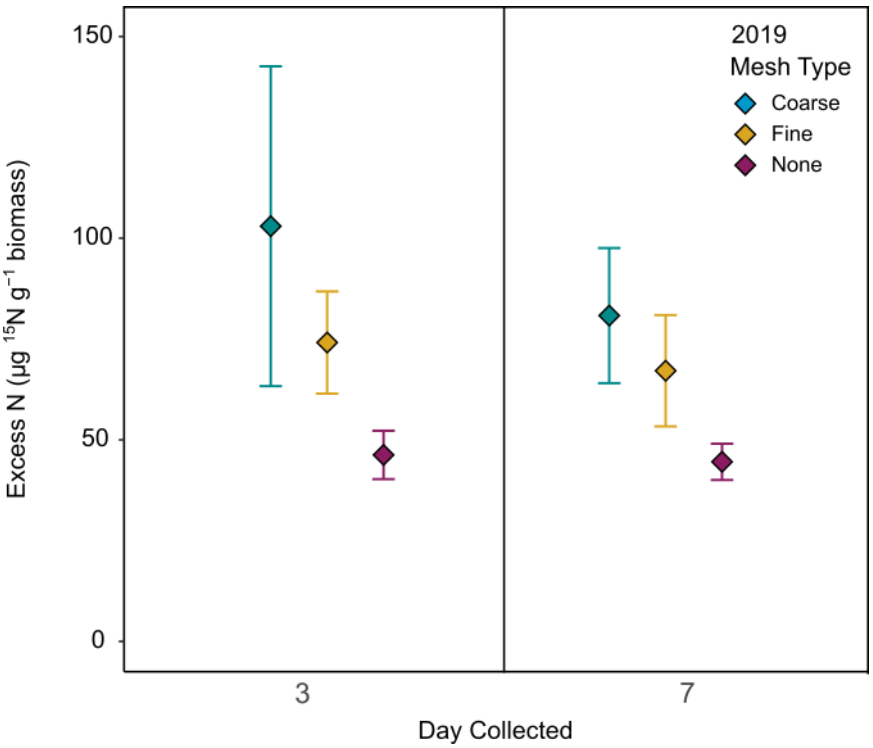

Fig. 4.5 Excess ^{15}N in leaves collected from *B. eriopoda* individuals (N-enriched samples only) collected 3 and 7 days following ^{15}N tracer application to biocrusts in the 2019 monsoon season mesh experiment plots (treatments: horizontal coarse mesh, fine mesh, or no mesh). Note that experiments were only conducted at SEV in 2019.

DISCUSSION

Overall, we did not find conclusive evidence that plant N uptake to leaves was impeded by physical fungal or root exclusion barriers in soils across three years of experimental manipulations. In general, movement of ^{15}N tracer into plants was very low across all three experiments and this was reflected in the low proportion of N-enriched leaf samples out of the total (22% of samples) collected during monsoon season experiments at each site (Table 4.2). After seeing such low rates of uptake in 2017, we tried to ameliorate this in the field by adding substantially more N tracer to plots in 2018-2019 experiments, but sample sizes for N-enriched leaves were relatively low across all three experiment years.

Patterns in N uptake across time, study sites and plant species

Previous dryland experiments have shown that ^{15}N from different forms of inorganic and amino acid-N forms (i.e., nitrate, ammonium, glycine, glutamate) can appear in leaves of perennial grass and woody shrub/subshrub species < 72 h following application of water and N to biocrust soils (Green et al., 2008; Hawkes, 2003; Zhuang et al., 2015); however, for some of these experiments there were not substantial increases in leaf $\delta^{15}N$ until 4-7 days following application (Adelizzi et al., 2022; Carvajal Janke & Coe, 2021). In our 2017 study, we saw significantly higher excess N in leaves after 10 days compared to 3 days following application, and maximum percent recovery was 45% and 18%, respectively. Soil microbes such as bacteria and fungi typically have high turnover rates and can rapidly respond to soil rewetting events on the scale of minutes to hours in drylands (Jackson et al., 1989; Krichels et al., 2022). We did not

find evidence of rapid (~24 h) N translocation through soils in our plots which may have indicated microbial activity was responsible for transferring N to plants. It is therefore possible that N was immobilized in microbial biomass before reaching plant roots, as evidenced by our relatively low number of N-enriched leaf samples, and that increased microbial activity due to water application could have inhibited, rather than facilitated, N movement to plants in our experimental plots (Chen et al., 2015; Schaeffer et al., 2003). These findings are supported by the results of two previous field-based experiments which similarly traced ^{15}N movement from cyanobacteria-dominated biocrusts to perennial grass species (Aanderud et al., 2018; Kwiecinski et al., 2020) and found significant ^{15}N enrichment in surface biocrust soils, but not in leaves of target plants.

For plants that did take up significant amounts of applied N, it is likely that physical soil processes were the main drivers of N movement to soil root zones (Querejeta et al. 2012). For example, we watered our study plots to a depth of ~2cm prior to tracer application, and although we allowed them to dry completely before N tracers were added, it is possible that there was enough soil moisture availability for diffusion and/or mass flow processes to facilitate root N uptake (BassiriRad et al. 1999; Cui and Caldwell 1997). Previous studies in semiarid grasslands have shown that even small rainfall events (~5 mm) can improve N diffusion to roots and activate new root growth and photosynthesis for some plant species, which further boosts the transpirational pull of water and nutrients into roots (Ivans et al. 2003; Thomey et al. 2011). Plants are known to capture and store nitrogen over longer periods of growth and activity than microbes (Hodge et al. 2000; Schimel and Bennett 2004), and N acquisition via these processes of soil diffusion and root uptake could have reasonably occurred at the relatively slower timescales (> 72 h) that we observed. Furthermore, we added ^{15}N-nitrate to soils, which is highly

soluble in water and has an effective soil diffusion coefficient of 0.28 cm^2 d^{-1} and can move a distance of 0.75 cm in 1 day through soils with a bulk density of 1.16 g cm^3 (Owen and Jones 2001), which also supports why we may have observed a relatively longer timescale of N movement into plants over the sampling period.

In 2018, we compared two plant species to see if N uptake responses were driven by differences in physiology and/or nutrient requirements of plants with different life history strategies – *B. eriopoda*, a C_4 grass and *G. sarothrae*, a C_3 subshrub. A previous comparison of N uptake between these species found that *B. eriopoda* tended to have higher N recovery, especially of $^{15}NO_3$, within 12 to 48 h of root application in a controlled greenhouse experiment (Chapter 2). In our study, we observed significantly higher excess N in *G. sarothrae* after 3 days compared to *B. eriopoda*, which could be explained by differences in growth strategy and belowground root architecture among the two species. Previous studies have reported that the size, density, and depth of root systems is an important driver of plant N acquisition, especially in patchy dryland soils where species may be competing for the same temporary soil N pools following a rainfall event (Hodge 2004; James et al. 2009). Woody shrubs and subshrub species like *G. sarothrae* have deeper taproot systems which allow them to access sub-surface soil water and take up N more rapidly than shallow-rooted grass species under limited soil moisture conditions (Wan et al. 1995; Gherardi et al. 2013). C_3 shrub species like *G. sarothrae* also have higher relative growth rates and can transpire year-round, which may allow them to respond more effectively to short-term nutrient availability compared to C_4 grasses like *B. eriopoda* (Yang et al. 2022; Kurc and Small 2004; Zhuang et al. 2020). Furthermore, our findings in a greenhouse study (Chapter 2) illustrated that *G. sarothrae* leaves were nearly all N-enriched as soon as 12 h following tracer application to roots, while *B. eriopoda* leaves more gradually

increased in enrichment from 12 to 48 h, which supports that this woody, taproot species may have greater uptake capacity under some circumstances.

Effects of fungal exclusion mesh

In our fungal exclusion mesh experiments from 2017 and 2019, we did not find evidence that either coarse or fine mesh treatment limits N movement through biocrust soils to plant roots. In a prior study with similar design set-up to our 2019 horizontal mesh experiment, the same mesh was used to impede fungal connections between surface biocrusts ~0.5 to 1 cm deep and grass root zones, and they similarly found significant plant N uptake to leaves within 72 h of ^{15}N tracer application (Dettweiler-Robinson et al. 2020). In other studies, mesh barriers have been used to prevent formation of hyphal connections between plant roots and to create root-free hyphal compartments (Teste et al. 2006; Tu et al. 2006). These methods have previously been successful in isolating the role of mycorrhizal fungi in experiments where isotopically-labelled ^{15}N and ^{13}C tracers were used to trace uptake of organic N from mycorrhizae to plants (Leigh et al. 2009) and to track carbon flux through mycorrhizal hyphae from plants into soils (Johnson et al. 2002). However, in our 2017 vertical mesh and 2019 horizontal mesh experiments, we did not find significant impediment of in N movement into leaves among the two mesh types compared to controls. It is likely that mesh openings of either size did not block physical movement of nutrients in soil solution (Teste et al. 2006). It is also likely that *B. eriopoda* plants could have potentially been able to access nutrient leachate below biocrust soils due to their relatively shallow root systems (Young et al. 2022). Roots of *Bouteloua* spp. are concentrated < 20 cm deep beneath the plant canopy, where they can access soil water and available nutrients following small, episodic rainfall events (Thomey et al. 2011; Burnett et al. 2012; Patrick et al.

2009). Individual *B. eriopoda* plants have also been observed growing a widespread network of lateral roots up to 40-80 cm away into plant interspaces (Gibbens and Lenz 2001).

In our 2018 experiment we saw similar N uptake in plants with a 2 cm soil barrier and those without one, and it is also possible that some of these shallow surface roots (< 10 cm) were able to access biocrust soil layers below the 2 cm metal barrier placed ~20 cm from the base of plants. Another factor that may have influenced these results could have been disturbance to biocrust organisms. For the mesh experiments, we allowed 4-5 months between installation and N tracer application for biocrusts to recover and for potential fungal connections to re-form, but for the 2018 experiment we placed the 2 cm barriers into plots < 1 month prior to N application. Previous studies found that physical disturbance to surface biocrusts can impact the structure and functioning of biocrust cyanobacteria (Steven et al. 2015) and can increase soil N availability and fungal abundance (Adelizzi et al. 2022). Although our experiment was not equivalent to the level of disturbance from soil compaction in these studies, it is possible that the installation of physical barriers disrupted soil processes and microbial communities enough to inhibit N retention in biocrust layers and thus more leaching to subsurface roots could have occurred.

CONCLUSIONS

Overall, we did not find strong support for the intermediary role of fungi in nutrient movement between biocrusts and plant roots in these systems, and our results ultimately did not support this potential line of evidence for the fungal loop hypothesis. We deployed three types of fungal exclusion mesh treatments across three experiment years and found greater excess N in plant leaves after 3-10 days, which also contrasts with the idea that rapid, microbially mediated nutrient translocation was occurring. It is likely that differences in N acquisition among grass

and subshrub species were due to physiological adaptations, however more data is needed to support these results since sample sizes were low for this growing season. In dryland ecosystems, non-mycorrhizal fungi likely serve key biogeochemical functions as decomposers and as members of soil food webs, but their hypothesized role in closing the "loop" of nutrient and water exchange between primary producers is less evident. Further exploration of fungal responses to different soil moisture thresholds and the amount and timing of nutrient availability could help better characterize the roles of dryland fungi in C and N cycling and retention in these ecosystems.

Chapter 5: Conclusions

SUMMARY OF FINDINGS

In this dissertation, I sought to investigate the roles of plants, fungi, and biocrusts as drivers of connectivity in soil nitrogen (N) cycling within a Northern Chihuahuan Desert grassland system. Understanding the interactions between soil microbes and plant roots in this ecosystem are important to regulating potential soil losses that can occur when microbial mineralization and N transformations are decoupled from plant uptake due to episodic moisture availability. Previous dryland experiments have suggested that belowground fungal networks could play a central role in exchanging plant-derived carbon (C) and biocrust-derived N among disconnected patches of primary producers, essentially recoupling dryland biogeochemical cycles separated in both space and time. Connecting and effectively "closing" the so-called "fungal loop" could increase soil nutrient retention in biotic pools and allow for greater N availability for growth and coexistence of communities in highly heterogeneous dryland environments. To investigate some of the mechanisms involved in the fungal loop, we performed three experiments focused on N cycling responses of plants, fungi, and biocrusts at two study sites, summarized below.

The research presented in Chapter 2 provides novel insights into rates and controls on short-term plant N uptake following a pulse of water and nutrients in a semiarid mixed grassland community. By tracing inorganic and organic N uptake in species with different life histories and nutrient requirements, our findings are consistent with scenarios in which N is a limiting resource, since all species took up each N form under non-water limiting conditions. Our experiment also fills in knowledge gaps about the potential for dryland plant partitioning of chemical N forms in these nutrient-limited habitats and we did not find evidence of this

phenomenon in our study system. I also summarized the results of 30 published N uptake experiments to gain a more complete picture of short-term N acquisition for dryland plant species, and to better understand the various methods by which researchers have quantified N uptake in both *in situ* and *ex situ* studies. I found that less than half of studies compared uptake of multiple inorganic and organic soil N forms. Our findings matched the results of these studies that similarly observed significantly higher uptake and recovery of inorganic soil N forms (NH_4^+ and NO_3^-) versus amino acid-N in 12 different dryland plant species regardless of habitat. The results of our study suggest that in this Chihuahuan Desert grassland, soil NO_3^- may be widely exploited following a precipitation pulse and inorganic N may comprise a greater proportion of plant N nutrition compared to amino acid-N. This study also identified the need for more systematic comparisons of soil inorganic and organic N pools in studies where ^{15}N tracers are applied to soils to better understand potential drivers (or limitations) on microbially-mediated N movement through soils. We hope our results will help guide other dryland researchers in choosing more uniform methods to evaluate the contribution of different chemical N forms (including diverse forms of soil organic N) to plant N nutrition in these habitats.

In Chapter 3, I present the results of a project in which we sampled biocrust soil and black grama root communities within three ongoing nitrogen and/or water addition experiments within the Sevilleta LTER and compared fungal responses to experimental manipulations. This work presents a more refined understanding of differences in fungal communities in dryland soil microsites where microbial activity is highly concentrated, and where fungal loop connections are predicted to occur. We found that biocrust- and root-associated fungi growing within a few meters of each other are similarly dominated by fungi in Ascomycota; however, at finer taxonomic levels, the abundance and structure of communities differs significantly and they

share < 15% of taxa. We used amplicon sequencing, soil fungal biomass comparisons, and direct observation of fungal root colonization to compare the structure, abundance and diversity of fungal communities under changes in nutrient and/or water availability. These comprehensive comparisons allowed us to gain a clearer understanding of the range of community responses environmental changes and supplement previous characterizations of fungal communities at this site, including those from a related, co-dominant grass species (blue grama). We found that biocrust and root-associated fungi had different sensitivities to levels of N addition - richness and diversity, but not structure of root fungal communities may be more impacted by changes in N inputs and could decline under predicted climate change scenarios, while biocrust soil communities may become more similar in composition under increased precipitation variability. Additionally, the abundance of saprotrophic fungal guilds in biocrust communities and of symbiotrophs in roots helps understand a key piece of the fungal loop hypothesis, the assumption that taxonomic similarity = functional similarity, and why it may not be supported in this ecosystem.

In Chapter 4, we directly tested the N exchange component of the fungal loop hypothesis by performing extensive field trials at two study sites over three years. We explicitly examined the roles of fungal hyphae in connecting spatially separated biocrust and plant patches by impeding fungal connections with three types of fungal exclusion mesh. We also tested the conditions under which plants may take up N from surface soil communities. Across our experiments, N translocation from soils to plant leaves was overall very low, and in trials where N movement occurred, we did not find significant obstruction due to mesh treatments. There was greater excess N in plant leaves after 3-10 days, which also contrasts with the idea that rapid, microbially-mediated nutrient translocation was occurring across biocrusted surface soils. At the

spatial scales we investigated, it was not evident that fungi were functioning as mediators of N transfer and uptake between biocrusts and plants. We think it is more likely that soil physical processes, including nutrient leaching and diffusion to roots (Young et al. 2022), were the primary drivers of N uptake in leaves under the conditions we tested.

Collectively, our results did not support that dryland nutrient cycling is mediated by shared networks of fungi facilitating resource exchanges among biocrusts and plant roots. While our greenhouse N uptake experiment conclusively demonstrated that once ^{15}N reaches the roots of plants, 24 hours would be a reasonable time frame to see differences in N form movement into leaves, we were ultimately not able to replicate the results of prior field-based experiments where ^{15}N tracers applied to biocrust soil patches were transferred to leaves of target plant species within 24 hours of application (Green et al. 2008; Zhuang et al. 2015). We also did not find strong support for the high functional similarity of fungi in biocrust soils and plant roots, and our results ultimately indicated that fungi in biocrust surface soils and within roots of dominant grass species are more distinct than alike, and will likely show diverging responses to environmental changes in N and water availability. This finding contrasts with previous comparisons of overlap between biocrust and rhizosphere fungi and illustrates the small-scale differences in microsites and plant feedbacks that may ultimately partition these fungal community members. Overall, we did not find strong support for the key role of fungi in nutrient movement between biocrusts and plant roots in these systems, and our results did not strongly support the direct and indirect evidence underlying the fungal loop hypothesis.

The Roles of Fungi in Dryland Ecosystems

In dryland ecosystems, the diverse physiological and chemical adaptations of fungi allow them to withstand extreme abiotic conditions, such as those experienced by biocrust microbes at the soil surface in plant interspaces. However, a clear understanding of the functional roles of dryland soil remains elusive due to relatively high proportions of unknown and/or unclassified taxa and the numerous capacities of fungi to shift functional traits and trophic modes in response to changing environmental conditions (Bui et al. 2020). Biocrust fungi are overwhelmingly classified as Dothidiomycetes (Ascomycota) in most studies to date, although Agaricomycetes (Basidiomycota) also appear as common biocrust constituents. These latter taxa include some of the most frequently encountered aboveground fungal fruiting bodies in sandy soils of mixed black grama grasslands and mesquite dunelands (*personal observation,* Fig. 5.1). Fungi in Asco- and Basidiomycota include highly diverse lineages, and many of these taxa probably exist as saprotrophs mineralizing soil organic matter and other organic substrates (Taylor and Sinsabaugh 2015). Saprotrophic fungi can serve key functions in biochemical weathering and translocation of inorganic nutrients from mineral interfaces (Bhattacharjee et al. 2022) and can liberate mineral-bound organic matter to be broken down by oxidative and other enzymes and become soluble for other microbes and plants (Jilling et al. 2018; Sinsabaugh 2010). Dryland fungi in the rhizospheres of grasses have been found to produce unique oxidative enzymes adapted to breaking down plant cellulose and other biomass constituents in hot, dry soils (Hudson et al., 2015), and there is a high likelihood that most dryland soil saprotrophs are concentrated in "hotspots" of nutrient availability and microbial activity (Darrouzet-Nardi and Bowman 2011), such as plant rhizospheres (Ochoa-Hueso et al. 2018). Some specialized saprotrophs are also

mycoparasitic or secondary lichen parasites and so inhabit the collective biomass of other microbes (Hawksworth 1982).

Fig. 5.1 An assortment of macrofungi (Agaricales) growing within or near cyanobacteria-dominated biocrusts at JOR

While undoubtedly many free-living dryland fungi form filamentous hyphal networks, their activity rates and biomass likely remain low during hot and dry conditions. Like the majority of desert organisms, soil fungi may favor energy conservation strategies and find localized soil microhabitats, such as those beneath plant canopies and surrounding plant roots, or form microcolonies and/or facultative lichen associations with algae or cyanobacterial cells as a survival strategy (Cantrell et al. 2011; Gostinčar et al. 2022). Compared to the more extreme UV radiation and heat conditions at the soil surface, even very small microhabitats can offer some

level of protection and enough energy to sustain activity and biomass levels (Kuzyakov and Blagodatskaya 2015). At the individual scale, some biocrust-inhabiting fungi likely reduce their metabolic activity prior to the arrival of monsoonal moisture pulses and may modify different aspects of their physiology for optimal drought tolerance (Fernandez and Koide 2013). Similar to soil cyanobacteria, fungi can also produce extracellular polymeric substances (EPS) to maintain internal moisture balance (Coleine et al. 2022). Hyphal growth may even respond fairly rapidly to increased soil moisture and carbon inputs during or after monsoon rainfall events. However, these rehydration growth responses may not necessitate the formation of (relatively) widespread, active hyphal nutrient transport networks through soils, especially in and around biocrusts where hyphae may not need to travel far to locate abundant carbon and nitrogen substrates like microbial necromass (Hu et al., 2020; Maier et al., 2016). Episodic precipitation events are usually followed by a fairly rapid soil dry down, and the combined stressors of high summer temperatures plus frequent cycles of soil drying/rewetting (Borken and Matzner 2009; Austin et al. 2004; Schimel 2018) may not favor high biomass accumulation for soil fungi.

Our results and those from other studies of dryland soil fungi have suggested that, in contrast to the responses of plant and bacterial communities, soil moisture alone may not be a strong determinant of community functioning and activity. This could mean that monsoon season is not the peak activity period for fungi, even though it may be a period of high productivity and biomass growth for many plants. It is possible that dryland fungi may to be most active during winter months, when temperatures are cooler and soil moisture and organic matter accumulation is high (Clark et al. 2009). In a cold desert ecosystem on the Colorado Plateau, biocrust soils were even found to be active beneath a layer of snow during the winter (Darrouzet-Nardi et al. 2015), which could provide a slower and more consistent moisture source for surface soil

microbes compared to the summer months. Winter conditions may favor more consistent fungal activity and biomass production in soils, as seen in some alpine microbial communities where fungi dominate winter nutrient cycling processes and are succeeded by active bacterial populations in summer months (Schadt et al. 2003). These activity patterns may also hold true for root-associated fungi, including AMF and endophytes growing in roots of woody C_3 plants. Compared to warm-season C_4 grasses which are dormant for most of the year, some deeper-rooted shrubs can be photosynthetically active for longer periods throughout the entire year, potentially releasing higher and more frequent levels of labile C to root and rhizosphere microbes including fungi (Ladwig et al. 2021). Additionally, productivity of some cool-season C_3 species in the Chihuahuan Desert was found to be highest early in the year following winter moisture inputs (Muldavin et al. 2008), which may similarly facilitate growth and activity of heat-intolerant fungal taxa. One experiment tracing ^{15}N movement through fungal networks in Sonoran Desert shrublands found significant N transport from moss-dominated crusts into leaves of *Larrea tridenta* plants (and to other spatially separate biocrust patches) after 6 days following a rainfall event (Carvajal & Coe, 2021). It is possible that testing the fungal loop in shrub-dominated habitats outside of hot summer months could provide new insights into the activity and nutrient cycling of biocrust and root-associated fungi in the Chihuahuan Desert as well. For example, another study that measured FAME profiles of soil microbes in a mixed sotol (*Dasylirion*) grassland in the Chihuahuan Desert (near Big Bend Ntl. Park) found that the ratio of bacteria:fungi was consistently high throughout the year, but soil fungi generally exhibited higher carbon substrate activity in winter compared to summer months (Bell et al. 2009). Further exploration of fungal responses to different temperature thresholds (or combined temperature

and moisture thresholds) could ultimately aid in better understanding the functional roles of fungi in C and N cycling and nutrient retention in dryland ecosystems.

CHALLENGES AND CONSIDERATIONS

Overall, my dissertation and the larger fungal loop project attempted to understand several aspects of short- and long-term plant N uptake and retention in this ecosystem. From 2017 to 2019, Fungal Loop project members set up an extensive field experiment across three study sites (Sevilleta LTER, Jornada LTER, Moab, UT – 2018 only), and installed > 600 experimental plots to examine ^{15}N addition across different seasons (Spring/Monsoon). We had a multitude of experiments within this larger study to test the effects of N form (inorganic – nitrate vs. organic – glutamic acid), N concentration (including a concentration gradient and a "crust death test" where we quantified minimum N toxicity thresholds that would harm biocrust organisms), and sampling for tracer outside of constrained plots. We also tested the effects of constrained plots - most of our plots had a 50 cm × 25 cm × 10 cm rectangle of aluminum flashing around each individual plant and biocrust patch versus open plot design, and deployed three different types of fungal exclusion treatments – fine mesh (0.45 µm), coarse mesh (50 µm) and a 2 cm piece of aluminum flashing to determine if transport was occurring in the biocrust or at deeper soil depths (2018 experiment only). We also collected small amounts of surface biocrust soil at each time point when leaves were collected following ^{15}N application (e.g., 1, 3, 7, 10 days post-application), and sampled full destructive harvests of soils and plants from ~1/3 of plots after 10 days and 3 months following application in the 2017 experiment. We also sampled adjacent soils outside of plots at each time point and measured gravimetric and volumetric water content, soil ergosterol and chlorophyll *a* concentrations, available soil nutrients (NH_4^+, NO_3^- and dissolved organic carbon), microbial biomass (via chloroform

fumigation), soil inorganic carbon (via loss-on-ignition) fungal root colonization, and hyphal extractions from soils. We also attempted to assess soil fungal activity by placing bags (made from fungal exclusion mesh) of ^{13}C-labeled leaf litter belowground and monitoring decomposition activity over several months in 2019. Despite all our efforts, a relatively low proportion of plants in our experimental plots took up a significant amount of ^{15}N tracer to aboveground leaves. We additionally tested the timing of root to leaf uptake in a greenhouse experiment using 225 field-collected plants to verify that any N reaching the roots of target plants in our field plots would be transported within the plant to leaves within 12-48 hours (Chapter 2), but this remained a major challenge to interpreting any treatment effects in this experiment and forming verifiable explanations for the patterns of soil N movement we did detect. In considering a future experiment, I think installing soil collars around target individuals but having more space between plant individuals, could be more effective than the rectangular soil surface plots we used to constrain tracer movement. If we grew seedling individuals ourselves, that could also ensure we were not disturbing the biocrusts during different times of the year, but that type of field experiment could take substantially more time. I think choosing relatively shallow-rooted *Bouteloua* bunchgrasses also made it difficult to constrain an individual plant with an individual biocrust patch without potentially damaging the natural spread of lateral roots. Ultimately, there are many considerations for why N did not always travel laterally across the soil surface (or at all), and in other cases it may have diffused vertically to plant root zones. However, the fact that the label was able to move past our 2-cm solid flashing in some cases does suggest that the surface soil hyphal networks are not the main mechanism of movement.

FUTURE DIRECTIONS

After extensively reviewing the background literature on dryland N uptake experiments, it is apparent that most field tracer experiments do not follow a standard set of methods for watering plots, applying N solutions at similar concentrations, collecting samples, and more. From my research, I also learned that in these grassland habitats, the root systems of grasses, shrubs, and other plant species all intermix within the top 10 cm where nutrients and water are most concentrated. Although surely we were not the first to understand or discover this, it still came as somewhat of a surprise when an undergraduate project showed that > 90% of all surface soil samples at any distance from the plant—and even in shallow depths that are part of the biocrust—contained live plant roots (Fig. 5.2). Previous evidence showed that plant roots were more prevalent in exploring the entire volume of the soil than we had expected during the project design phase. There are some soil spaces where larger, woody roots create a pathway to water and nutrients which smaller, fibrous roots follow, and there are several potentially interesting questions to test among the microbial communities associated with these species, especially for those with N-fixing rhizobia (i.e., legumes) and those without. I think the potential for understanding competitive or facilitative interactions among rhizosphere communities, and between fungi found within roots vs. those found in rhizosphere and surface soils could yield new insights into some of the smaller-scale (hyphal scale) dynamics that may also influence nutrient cycling at these sites.

Fig. 5.2 Plant roots observed growing in biocrust soil layers (upper ~2 cm) at JOR

Furthermore, I would be interested in explicitly testing the activity levels of culturable fungi under different soil moisture and temperature thresholds by performing a xerotolerance assay and comparing taxa with the highest growth capacity under increased abiotic stress (Ndinga-Muniania et al. 2021). Definitively addressing this piece of indirect evidence for a fungal loop in this system, if Ascomycota fungi "can metabolize at lower water potentials than either plants or bacteria" and explicitly testing whether or not they "may be physiologically active under dry conditions" would build on the sequencing and fungal biomass data I collected and perhaps yield exciting results about the adaptations of Chihuahuan Desert fungi.

CONCLUSIONS

In this dissertation, I examined different drivers of N cycling processes among dryland plant and soil communities in order to improve our understanding of the roles of biodiverse soil and plant-associated fungi in dryland biogeochemical cycles. These experiments tested, and ultimately did not show support for, several lines of direct and indirect evidence underlying the

fungal loop hypothesis. In this system, it is unlikely that nutrient cycling is mediated by shared, connected networks of fungi among biocrusts and plants at the seasonal and spatial scales we measured. Instead, the processes of microbial nutrient release and plant uptake in dryland soils could be driven by physical soil processes (e.g., diffusion and leaching to root zones) and plant root activity once soil moisture limitations are lifted during the growing season. These findings still leave the door open to investigations of rhizosphere dynamics, root distribution and foraging responses that may influence the timing and magnitude of N uptake in these systems. More comprehensive studies combining multiple measurements of fungal activity and biomass, especially under varying temperature and moisture conditions, may be necessary to discern finer-scale community differences and to make more accurate predictions about the roles and responses of soil and root fungi to environmental changes in this system. This dissertation altogether adds to the growing body of knowledge about the taxonomic and functional diversity of fungi in dryland ecosystems and provides further insight into the forms and functions of some of the most diverse and adaptive organisms on Earth.

References

Aanderud, Z. T., & Bledsoe, C. S. (2009). Preferences for ^{15}N-ammonium, ^{15}N -nitrate, and ^{15}N -glycine differ among dominant exotic and subordinate native grasses from a California oak woodland. *Environmental and Experimental Botany*, *65*(2), 205–209.

Aanderud, Z. T., Smart, T. B., Wu, N., Taylor, A. S., Zhang, Y., & Belnap, J. (2018). Fungal loop transfer of nitrogen depends on biocrust constituents and nitrogen form. *Biogeosciences* , *15*(12), 3831–3840.

Abarenkov, Kessy; Zirk, Allan; Piirmann, Timo; Pöhönen, Raivo; Ivanov, Filipp; Nilsson, R. Henrik; Kõljalg, Urmas (2021): UNITE mothur release for Fungi. Version 10.05.2021. UNITE Community. https://doi.org/10.15156/BIO/1265786

Abed, R. M. M., Tamm, A., Hassenrück, C., Al-Rawahi, A. N., Rodríguez-Caballero, E., Fiedler, S., Maier, S., & Weber, B. (2019). Habitat-dependent composition of bacterial and fungal communities in biological soil crusts from Oman. *Scientific Reports*, *9*(1), 6468.

Adelizzi, R., O'Brien, E. A., Hoellrich, M., Rudgers, J. A., Mann, M., Fernandes, V. M. C., Darrouzet-Nardi, A., & Stricker, E. (2022). Disturbance to biocrusts decreased cyanobacteria, N-fixer abundance, and grass leaf N but increased fungal abundance. *Ecology*, *103*(4), e3656.

Aguilar-Trigueros, C. A., Powell, J. R., Anderson, I. C., Antonovics, J., & Rillig, M. C. (2014). Ecological understanding of root-infecting fungi using trait-based approaches. *Trends in Plant Science*, *19*(7), 432–438.

Allen, M.F. et al. (1989). Influence of clipping and soil water status on vesicular-arbuscular mycorrhizae of two semiarid tussock grasses. *Biol and Fert. Of Soils* 8(4), 285-289.

Allen, M. F. (2007). Mycorrhizal fungi: Highways for water and nutrients in arid soils. *Vadose Zone Journal: VZJ*, *6*(2), 291–297.

Allen, M. F. (2009). Bidirectional water flows through the soil–fungal–plant mycorrhizal continuum. In *New Phytologist* (Vol. 182, Issue 2, pp. 290–293). https://doi.org/10.1111/j.1469-8137.2009.02815.x

Allen, M. F. (2011). Linking water and nutrients through the vadose zone: a fungal interface between the soil and plant systems. In *Journal of Arid Land* (Vol. 3, Issue 3, pp. 155–163). https://doi.org/10.3724/sp.j.1227.2011.00155

Anderson, M. J. (2006). Distance-based tests for homogeneity of multivariate dispersions. *Biometrics*, *62*(1), 245–253.

Antoninka, A., Reich, P. B., & Johnson, N. C. (2011). Seven years of carbon dioxide enrichment, nitrogen fertilization and plant diversity influence arbuscular mycorrhizal fungi in a grassland ecosystem. *The New Phytologist*, *192*(1), 200–214.

Ashton, I. W., Miller, A. E., Bowman, W. D., & Suding, K. N. (2008). Nitrogen preferences and plant-soil feedbacks as influenced by neighbors in the alpine tundra. *Oecologia*, *156*(3), 625–636.

Ashton, I. W., Miller, A. E., Bowman, W. D., & Suding, K. N. (2010). Niche complementarity due to plasticity in resource use: plant partitioning of chemical N forms. *Ecology*, *91*(11), 3252–3260.

Augustine, D. J., & McNaughton, S. J. (2004). Temporal asynchrony in soil nutrient dynamics and plant production in a semiarid ecosystem. *Ecosystems* , *7*(8), 829–840.

Austin, A. T. (2011). Has water limited our imagination for aridland biogeochemistry? *Trends in Ecology & Evolution*, *26*(5), 229–235.

Austin, A. T., Yahdjian, L., Stark, J. M., Belnap, J., Porporato, A., Norton, U., Ravetta, D. A., & Schaeffer, S. M. (2004). Water pulses and biogeochemical cycles in arid and semiarid ecosystems. *Oecologia*, *141*(2), 221–235.

Báez, S., Fargione, J., Moore, D. I., Collins, S. L., & Gosz, J. R. (2007). Atmospheric nitrogen deposition in the northern Chihuahuan desert: Temporal trends and potential consequences. *Journal of Arid Environments*, *68*(4), 640–651.

Baldarelli, L. M., Throop, H. L., Collins, S. L., & Ward, D. (2021). Nutrient additions have direct and indirect effects on biocrust biomass in a long-term Chihuahuan Desert grassland experiment. *Journal of Arid Environments*, *184*, 104317.

Bardgett, R. D., Streeter, T. C., & Bol, R. (2003). Soil microbes compete effectively with plants for organic-nitrogen inputs to temperate grasslands. *Ecology*, *84*(5), 1277–1287.

Barger, N. N., Weber, B., Garcia-Pichel, F., Zaady, E., & Belnap, J. (2016). Patterns and Controls on Nitrogen Cycling of Biological Soil Crusts. In B. Weber, B. Büdel, & J. Belnap (Eds.), *Biological Soil Crusts: An Organizing Principle in Drylands* (pp. 257–285). Springer International Publishing.

Baron, N. C., & Rigobelo, E. C. (2022). Endophytic fungi: a tool for plant growth promotion and sustainable agriculture. *Mycology*, *13*(1), 39–55.

Barrow, J. R. (2003). Atypical morphology of dark septate fungal root endophytes of Bouteloua in arid southwestern USA rangelands. *Mycorrhiza*, *13*(5), 239–247.

BassiriRad, H., & Caldwell, M. M. (1992). Temporal changes in root growth and ^{15}N uptake and water relations of two tussock grass species recovering from water stress. *Physiologia Plantarum*, *86*(4), 525–531.

BassiriRad, H., Reynolds, J. F., Virginia, R. A., & Brunelle, M. H. (1997). Growth and root NO_3 and PO_4 uptake capacity of three desert species in response to atmospheric CO_2 enrichment. *Australian Journal of Plant Physiology*, *24*, 354–358.

BassiriRad, H., Tremmel, D. C., Virginia, R. A., Reynolds, J. F., de Soyza, A. G., & Brunell, M. H. (1999). Short-term patterns in water and nitrogen acquisition by two desert shrubs following a simulated summer rain. *Plant Ecology*, *145*, 27–36.

Bates, D., Mächler, M., Bolker, B., & Walker, S. (2015). Fitting Linear Mixed-Effects Models Using lme4. *Journal of Statistical Software*, *67*, 1–48.

Bates, S. T., Garcia-Pichel, F., & Nash, T. H., III. (2010). Fungal components of biological soil crusts: insights from culture-dependent and culture-independent studies. *Bibliotheca Lichenologica*, *105*, 197–210.

Bates, S. T., Nash, T. H., 3rd, & Garcia-Pichel, F. (2012). Patterns of diversity for fungal assemblages of biological soil crusts from the southwestern United States. *Mycologia*, *104*(2), 353–361.

Bates, S. T., Nash, T. H., Sweat, K. G., & Garcia-Pichel, F. (2010). Fungal communities of lichen-dominated biological soil crusts: Diversity, relative microbial biomass, and their relationship to disturbance and crust cover. *Journal of Arid Environments*, *74*(10), 1192–1199.

Baur, L., S. Collins, E. Muldavin, J.A. Rudgers, and W.T. Pockman. (2021a). Effects of Multiple Resource Additions on Community and Ecosystem Processes: NutNet NPP Quadrat Sampling at the Sevilleta National Wildlife Refuge, New Mexico ver 176384. Environmental Data Initiative. https://doi.org/10.6073/pasta/a5683384cff200de7e0f6b651c60d8d6

Baur, L., S. Collins, E. Muldavin, J.A. Rudgers, and W.T. Pockman. (2021b). Warming-El Nino-Nitrogen Deposition Experiment (WENNDEx): Net Primary Production Quadrat Data at the Sevilleta National Wildlife Refuge, New Mexico ver 234295. Environmental Data Initiative. https://doi.org/10.6073/pasta/b4c81c7073460ad91a5f0a77f6009ddc

Bell, C. W., Acosta-Martinez, V., McIntyre, N. E., Cox, S., Tissue, D. T., & Zak, J. C. (2009). Linking microbial community structure and function to seasonal differences in soil moisture and temperature in a Chihuahuan desert grassland. *Microbial Ecology*, *58*(4), 827–842.

Belnap, J., Weber, B., & Büdel, B. (2016). Biological Soil Crusts as an Organizing Principle in Drylands. In B. Weber, B. Büdel, & J. Belnap (Eds.), *Biological Soil Crusts: An Organizing Principle in Drylands* (pp. 3–13). Springer International Publishing.

Benjamini, Y., & Hochberg, Y. (1995). Controlling the false discovery rate: A practical and powerful approach to multiple testing. *Journal of the Royal Statistical Society*, *57*(1), 289–300.

Bhattacharjee, A., Qafoku, O., Richardson, J. A., Anderson, L. N., Schwarz, K., Bramer, L. M., Lomas, G. X., Orton, D. J., Zhu, Z., Engelhard, M. H., Bowden, M. E., Nelson, W. C., Jumpponen, A., Jansson, J. K., Hofmockel, K. S., & Anderton, C. R. (2022). A mineral-doped micromodel platform demonstrates fungal bridging of carbon hot spots and hyphal transport of mineral-derived nutrients. *MSystems*, *7*(6), e0091322.

Boddy, L. (1999). Saprotrophic cord-forming fungi: meeting the challenge of heterogeneous environments. *Mycologia*, *91*(1), 13–32.

Booth, M. S., Caldwell, M. M., & Stark, J. M. (2003). Overlapping resource use in three Great Basin species: implications for community invasibility and vegetation dynamics. In

Journal of Ecology (Vol. 91, Issue 1, pp. 36–48). https://doi.org/10.1046/j.1365-2745.2003.00739.x

Borken, W., & Matzner, E. (2009). Reappraisal of drying and wetting effects on C and N mineralization and fluxes in soils. *Global Change Biology*, *15*(4), 808–824.

Boudsocq, S., Niboyet, A., Lata, J. C., Raynaud, X., Loeuille, N., Mathieu, J., Blouin, M., Abbadie, L., & Barot, S. (2012). Plant preference for ammonium versus nitrate: A neglected determinant of ecosystem functioning? *The American Naturalist*, *180*(1), 60–69.

Breheny, P., & Burchett, W. (2017). Visualization of regression models using visreg. *The R Journal*, *9*(2), 56.

Britto, D. T., & Kronzucker, H. J. (2002). NH_4^+ toxicity in higher plants: a critical review. *Journal of Plant Physiology*, *159*, 567–584.

Brown, R. F., Sala, O. E., Sinsabaugh, R. L., & Collins, S. L. (2022). Temporal effects of monsoon rainfall pulses on plant available nitrogen in a Chihuahuan Desert Grassland. *Journal of Geophysical Research. Biogeosciences*, *127*(6). https://doi.org/10.1029/2022jg006938

Brown, S. P., Veach, A. M., Rigdon-Huss, A. R., Grond, K., Lickteig, S. K., Lothamer, K., Oliver, A. K., & Jumpponen, A. (2015). Scraping the bottom of the barrel: are rare high throughput sequences artifacts? *Fungal Ecology*, *13*, 221–225.

Bueno, A., Greenfield, L., Pritsch, K., Schmidt, S., & Simon, J. (2019). Responses to competition for nitrogen between subtropical native tree seedlings and exotic grasses are species-specific and mediated by soil N availability. *Tree Physiology*, *39*(3), 404–416.

Bueno de Mesquita, C. P., Sartwell, S. A., Ordemann, E. V., Porazinska, D. L., Farrer, E. C., King, A. J., Spasojevic, M. J., Smith, J. G., Suding, K. N., & Schmidt, S. K. (2018). Patterns of root colonization by arbuscular mycorrhizal fungi and dark septate endophytes across a mostly-unvegetated, high-elevation landscape. *Fungal Ecology*, *36*, 63–74.

Bui, A., Orr, D., Lepori-Bui, M., Konicek, K., Young, H. S., & Moeller, H. V. (2020). Soil fungal community composition and functional similarity shift across distinct climatic conditions. *FEMS Microbiology Ecology*, *96*(12). https://doi.org/10.1093/femsec/fiaa193

Burnett, S. A., Hattey, J. A., Johnson, J. E., Swann, A. L., Moore, D. I., & Collins, S. L. (2012). Effects of fire on belowground biomass in Chihuahuan Desert grassland. *Ecosphere* , *3*(11), 1–13.

Caldwell, M. M., Manwaring, J. H., & Durham, S. L. (1991). The microscale distribution of neighbouring plant roots in fertile soil microsites. *Functional Ecology*, *5*(6), 765–772.

Camargo-Ricalde, S. L., Montaño, N. M., Montaño-Arias, S. A., De la Rosa-Mera, C. J., & Chimal-Sánchez, E. (2021). Biocrusts inside and outside of *Mimosa luisana* resource islands as reservoirs of arbuscular mycorrhizal fungi in a Mexican semiarid ecosystem. *Scientia Fungorum*, *51*, e1370.

Cameron, E. S., Schmidt, P. J., Tremblay, B. J.-M., Emelko, M. B., & Müller, K. M. (2021). Enhancing diversity analysis by repeatedly rarefying next generation sequencing data describing microbial communities. *Scientific Reports*, *11*(1), 22302.

Cantrell, S. A., Dianese, J. C., Fell, J., Gunde-Cimerman, N., & Zalar, P. (2011). Unusual fungal niches. *Mycologia*, *103*(6), 1161–1174.

Carvajal Janke, N., & Coe, K. K. (2021). Evidence for a fungal loop in shrublands. *The Journal of Ecology*, *109*(4), 1842–1857.

Casper, B. B., & Jackson, R. B. (1997). Plant competition underground. *Annual Review of Ecology and Systematics*, *28*(1), 545–570.

Chalk, P., & Smith, C. (2021). On inorganic N uptake by vascular plants: Can ^{15}N tracer techniques resolve the NH_4^+ versus NO_3^- "preference" conundrum? *European Journal of Soil Science*, *72*(4), 1762–1779.

Chen, H., Mothapo, N. V., & Shi, W. (2015). Soil moisture and pH control relative contributions of fungi and bacteria to N_2O production. *Microbial Ecology*, *69*(1), 180–191.

Chen, J., Carrillo, Y., Pendall, E., Dijkstra, F. A., Dave Evans, R., Morgan, J. A., & Williams, D. G. (2015). Soil microbes compete strongly with plants for soil inorganic and amino acid nitrogen in a semiarid grassland exposed to elevated CO_2 and warming. *Ecosystems* , *18*(5), 867–880.

Chesson, P., Gebauer, R. L. E., Schwinning, S., Huntly, N., Wiegand, K., Ernest, M. S. K., Sher, A., Novoplansky, A., & Weltzin, J. F. (2004). Resource pulses, species interactions, and diversity maintenance in arid and semi-arid environments. *Oecologia*, *141*(2), 236–253.

Chowdhury, N., Marschner, P., & Burns, R. (2011). Response of microbial activity and community structure to decreasing soil osmotic and matric potential. *Plant and Soil*, *344*(1), 241–254.

Clark, J. S., Campbell, J. H., Grizzle, H., Acosta-Martìnez, V., & Zak, J. C. (2009). Soil microbial community response to drought and precipitation variability in the Chihuahuan Desert. *Microbial Ecology*, *57*(2), 248–260.

Coleine, C., Stajich, J. E., & Selbmann, L. (2022). Fungi are key players in extreme ecosystems. *Trends in Ecology & Evolution*, *37*(6), 517–528.

Coleman, M.D. et al. (1989). Pure culture response of ectomycorrhizal fungi to imposed water stress. *Canadian Journal of Botany* 67(1), 29-39.

Collins, S. 2023. Monsoon Rainfall Manipulation Experiment (MRME) Meteorology Data from a Chihuahuan Desert Grassland at the Sevilleta National Wildlife Refuge, New Mexico ver 8. Environmental Data Initiative. https://doi.org/10.6073/pasta/f3a14210adeaa762b2e78d1191d5e02b

Collins, S. L., Chung, Y. A., Baur, L. E., Hallmark, A., Ohlert, T. J., & Rudgers, J. A. (2020). Press–pulse interactions and long-term community dynamics in a Chihuahuan Desert grassland. *Journal of Vegetation Science: Official Organ of the International Association for Vegetation Science*, *31*(5), 722–732.

Collins, S. L., Fargione, J. E., Crenshaw, C. L., Nonaka, E., Elliott, J. R., Xia, Y., & Pockman, W. T. (2010). Rapid plant community responses during the summer monsoon to nighttime warming in a northern Chihuahuan Desert grassland. *Journal of Arid Environments*, *74*(5), 611–617.

Collins, S. L., Sinsabaugh, R. L., Crenshaw, C., Green, L., Porras-Alfaro, A., Stursova, M., & Zeglin, L. H. (2008). Pulse dynamics and microbial processes in aridland ecosystems. *The Journal of Ecology*, *96*(3), 413–420.

Corkidi, Rowland, Johnson, & Allen. (2002). Nitrogen fertilization alters the functioning of arbuscular mycorrhizas at two semiarid grasslands. *Plant and Soil*, *240*, 299–310.

Cramer, A. J., & Miller, M. (2005). Root nitrogen acquisition and assimilation. *Plant and Soil*, *274*(1), 1–36.

Crenshaw, C. L., Lauber, C., Sinsabaugh, R. L., & Stavely, L. K. (2008). Fungal control of nitrous oxide production in semiarid grassland. *Biogeochemistry*, *87*(1), 17–27.

Crowther, T. W., Maynard, D. S., Crowther, T. R., Peccia, J., Smith, J. R., & Bradford, M. A. (2014). Untangling the fungal niche: the trait-based approach. *Frontiers in Microbiology*, *5*, 579.

Cui, M., & Caldwell, M. M. (1997). A large ephemeral release of nitrogen upon wetting of dry soil and corresponding root responses in the field. *Plant and Soil*, *191*, 291–299.

Currie, W. S. (2008). Modeling the dynamics of stable-isotope ratios for ecosystem biogeochemistry. In *Stable Isotopes in Ecology and Environmental Science* (pp. 450–479). Blackwell Publishing Ltd.

Dadachova, E., & Casadevall, A. (2008). Ionizing radiation: how fungi cope, adapt, and exploit with the help of melanin. *Current Opinion in Microbiology*, *11*(6), 525–531.

Daly, A. B., Jilling, A., Bowles, T. M., Buchkowski, R. W., Frey, S. D., Kallenbach, C. M., Keiluweit, M., Mooshammer, M., Schimel, J. P., & Grandy, A. S. (2021). A holistic framework integrating plant-microbe-mineral regulation of soil bioavailable nitrogen. *Biogeochemistry*, *154*(2), 211–229.

Darrouzet-Nardi, A., & Bowman, W. D. (2011). Hot spots of inorganic nitrogen availability in an alpine-subalpine ecosystem, Colorado Front Range. *Ecosystems*, *14*(5), 848–863.

Darrouzet-Nardi, A., Reed, S. C., Grote, E. E., & Belnap, J. (2015). Observations of net soil exchange of CO_2 in a dryland show experimental warming increases carbon losses in biocrust soils. *Biogeochemistry*, *126*(3), 363–378.

DeFalco, L. A., Fernandez, G. C. J., & Nowak, R. S. (2007). Variation in the establishment of a non-native annual grass influences competitive interactions with Mojave Desert perennials. *Biological Invasions*, *9*, 293–307.

Delgado-Baquerizo, M., Maestre, F. T., Gallardo, A., Quero, J. L., Ochoa, V., García-Gómez, M., Escolar, C., García-Palacios, P., Berdugo, M., Valencia, E., Gozalo, B., Noumi, Z., Derak, M., & Wallenstein, M. D. (2013). Aridity modulates N availability in arid and semiarid Mediterranean grasslands. *PloS One*, *8*(4), e59807.

Dettweiler-Robinson, E., Sinsabaugh, R. L., & Rudgers, J. A. (2020). Fungal connections between plants and biocrusts facilitate plants but have little effect on biocrusts. *The Journal of Ecology*, *108*(3), 894–907.

Dighton, J. (2016). Fungi in Ecosystem Processes (2nd ed.). CRC Press. https://doi.org/10.1201/9781315371528

Dijkstra, F. A., Augustine, D. J., Brewer, P., & von Fischer, J. C. (2012). Nitrogen cycling and water pulses in semiarid grasslands: are microbial and plant processes temporally asynchronous? *Oecologia*, *170*, 799–808.

Dijkstra, F. A., Morgan, J. A., Blumenthal, D., & Follett, R. F. (2010). Water limitation and plant inter-specific competition reduce rhizosphere-induced C decomposition and plant N uptake. *Soil Biology & Biochemistry*, *42*(7), 1073–1082.

Dix, N.J. (1984). Minimum water potentials for growth of some litter-decomposing agarics and other basidiomycetes. *Trans. British Myco. Soc.* 83(1), 152-153.

Egerton-Warburton, L. M., & Johnson, N. C. (2007). Mycorrhizal community dynamics following nitrogen fertilization: a cross-site test in five grasslands. *Ecological*. https://esajournals.onlinelibrary.wiley.com/doi/abs/10.1890/06-1772.1

Elbert, W., Weber, B., Burrows, S., Steinkamp, J., Büdel, B., Andreae, M. O., & Pöschl, U. (2012). Contribution of cryptogamic covers to the global cycles of carbon and nitrogen. *Nature Geoscience*, *5*(7), 459–462.

Engels, C., & Marschner, H. (1995). Plant uptake and utilization of nitrogen. *Nitrogen Fertilization in the Environment*, 41–81.

Farrell, M., Hill, P. W., Farrar, J., DeLuca, T. H., Roberts, P., Kielland, K., Dahlgren, R., Murphy, D. V., Hobbs, P. J., Bardgett, R. D., & Jones, D. L. (2013). Oligopeptides represent a preferred source of organic N uptake: a global phenomenon? *Ecosystems* , *16*(1), 133–145.

Farzadfar, S., Knight, J. D., & Congreves, K. A. (2021). Soil organic nitrogen: an overlooked but potentially significant contribution to crop nutrition. *Plant and Soil*, *462*(1–2), 7–23.

Fernandes, V. M. C., Machado de Lima, N. M., Roush, D., Rudgers, J., Collins, S. L., & Garcia-Pichel, F. (2018). Exposure to predicted precipitation patterns decreases population size and alters community structure of cyanobacteria in biological soil crusts from the Chihuahuan Desert. *Environmental Microbiology*, *20*(1), 259–269.

Fernandes, V. M. C., Rudgers, J. A., Collins, S. L., & Garcia-Pichel, F. (2022). Rainfall pulse regime drives biomass and community composition in biological soil crusts. *Ecology*, *103*(9), e3744.

Fernandez, C. W., & Koide, R. T. (2013). The function of melanin in the ectomycorrhizal fungus Cenococcum geophilum under water stress. *Fungal Ecology*, *6*(6), 479–486.

Fierer, N. et al. (2003). Influence of drying-rewetting frequency on soil bacterial community structure. *Microbial Ecology*, 45, 63-71.

Fierer, N., Lauber, C. L., Ramirez, K. S., Zaneveld, J., Bradford, M. A., & Knight, R. (2012). Comparative metagenomic, phylogenetic and physiological analyses of soil microbial communities across nitrogen gradients. *The ISME Journal*, *6*(5), 1007–1017.

Fierer, N., Leff, J. W., Adams, B. J., Nielsen, U. N., Bates, S. T., Lauber, C. L., Owens, S., Gilbert, J. A., Wall, D. H., & Caporaso, J. G. (2012). Cross-biome metagenomic analyses of soil microbial communities and their functional attributes. *Proceedings of the National Academy of Sciences of the United States of America*, *109*(52), 21390–21395.

Forde, B. G., & Walch-Liu, P. (2009). Nitrate and glutamate as environmental cues for behavioural responses in plant roots. *Plant, Cell & Environment*, *32*(6), 682–693.

Fox, J., Weisberg, S., Adler, D., Bates, D., Baud-Bovy, G., Ellison, S., Firth, D., Friendly, M., Gorjanc, G., Graves, S., & Others. (2012). Package 'car.' *Vienna: R Foundation for Statistical Computing*, *16*. https://cran.uni-muenster.de/web/packages/car/car.pdf

Freckman, D. W. (1986). The ecology of dehydration in soil organisms. In: A.C. Leopold (ed.) *Membranes, metabolism and dry organisms.* Ithaca, NY: Cornell University Press, pp. 157-168.

Garcia-Pichel, F., Loza, V., Marusenko, Y., Mateo, P., & Potrafka, R. M. (2013). Temperature drives the continental-scale distribution of key microbes in topsoil communities. *Science*, *340*(6140), 1574–1577.

Gebauer, R. L. E., & Ehleringer, J. R. (2000). Water and nitrogen uptake patterns following moisture pulses in a cold desert community. *Ecology*, *81*(5), 1415–1424.

Gebauer, R. L. E., Schwinning, S., & Ehleringer, J. R. (2002). Interspecific competition and resource pulse utilization in a cold desert community. *Ecology*, *83*(9), 2602–2616.

Gherardi, L. A., Sala, O. E., & Yahdjian, L. (2013). Preference for different inorganic nitrogen forms among plant functional types and species of the Patagonian steppe. *Oecologia*, *173*(3), 1075–1081.

Gibbens, R. P., & Lenz, J. M. (2001). Root systems of some Chihuahuan Desert plants. *Journal of Arid Environments*, *49*(2), 221–263.

Gihring, T. M., Green, S. J., & Schadt, C. W. (2012). Massively parallel rRNA gene sequencing exacerbates the potential for biased community diversity comparisons due to variable library sizes. *Environmental Microbiology*, *14*(2), 285–290.

Glass, A. D. M. (2003). Nitrogen use efficiency of crop plants: physiological constraints upon nitrogen absorption. *Critical Reviews in Plant Sciences*, *22*(5), 453–470.

Gostinčar, C., Muggia, L., & Grube, M. (2012). Polyextremotolerant black fungi: oligotrophism, adaptive potential, and a link to lichen symbioses. *Frontiers in Microbiology*, *3*, 390.

Gostinčar, C., Zalar, P., & Gunde-Cimerman, N. (2022). No need for speed: slow development of fungi in extreme environments. *Fungal Biology Reviews*, *39*, 1–14.

Govindarajulu, M., Pfeffer, P. E., Jin, H., Abubaker, J., Douds, D. D., Allen, J. W., Bücking, H., Lammers, P. J., & Shachar-Hill, Y. (2005). Nitrogen transfer in the arbuscular mycorrhizal symbiosis. *Nature*, *435*(7043), 819–823.

Green, L. E., Porras-Alfaro, A., & Sinsabaugh, R. L. (2008). Translocation of nitrogen and carbon integrates biotic crust and grass production in desert grassland. *The Journal of Ecology*, *96*(5), 1076–1085.

Griffin, D. M. (1977). Water potential and wood-decay fungi. *Annual Review of Phytopathology* 15, 319–329.

Griffin, D.M. (1981). Water and microbial stress. *Advances in Microbial Ecology* 5, 91-136

Hamm, P. S., Mueller, R. C., Kuske, C. R., & Porras-Alfaro, A. (2020). Keratinophilic fungi: Specialized fungal communities in a desert ecosystem identified using cultured-based and Illumina sequencing approaches. *Microbiological Research*, *239*, 126530.

Hansen, F. A., James, D. K., Anderson, J. P., Meredith, C. S., Dominguez, A. J., Pombubpa, N., Stajich, J. E., Romero-Olivares, A. L., Salley, S. W., & Pietrasiak, N. (2023). Landscape characteristics shape surface soil microbiomes in the Chihuahuan Desert. *Frontiers in Microbiology*, *14*, 1135800.

Hartig, F. (2022). *DHARMa: Residual Diagnostics for Hierarchical (Multi-Level/Mixed) 910 Regression Models. R package version 0.4. 5*.

Hartley, A., Barger, N., Belnap, J., & Okin, G. S. (2007). Dryland Ecosystems. In P. Marschner & Z. Rengel (Eds.), *Nutrient Cycling in Terrestrial Ecosystems* (pp. 271–307). Springer Berlin Heidelberg.

Havrilla, C., Leslie, A. D., Di Biase, J. L., & Barger, N. N. (2020). Biocrusts are associated with increased plant biomass and nutrition at seedling stage independently of root-associated fungal colonization. *Plant and Soil*, *446*(1), 331–342.

Hawkes, C. V. (2003). Nitrogen cycling mediated by biological soil crusts and arbuscular mycorrhizal fungi. *Ecology*, *84*(6), 1553–1562.

Hawksworth, D. L. (1982). Secondary fungi in lichen symbioses: parasites, saprophytes and parasymbionts. *The Journal of the Hattori Botanical Laboratory*, *52*, 357-366.

Hawksworth, David L., & Lücking, R. (2017). Fungal Diversity Revisited: 2.2 to 3.8 Million Species. *Microbiology Spectrum*, *5*(4). https://doi.org/10.1128/microbiolspec.FUNK-0052-2016

Hernández-Hernández, R. M., Roldán, A., Caravaca, F., Rodriguez-Caballero, G., Torres, M. P., Maestre, F. T., & Alguacil, M. M. (2017). Arbuscular mycorrhizal fungal assemblages in biological crusts from a Neotropical savanna are not related to the dominant perennial Trachypogon. *The Science of the Total Environment*, *575*, 1203–1210.

Herrera, J., Khidir, H. H., Eudy, D. M., Porras-Alfaro, A., Natvig, D. O., & Sinsabaugh, R. L. (2010). Shifting fungal endophyte communities colonize Bouteloua gracilis: effect of host tissue and geographical distribution. *Mycologia*, *102*(5), 1012–1026.

Herrera, J., Poudel, R., Nebel, K. A., & Collins, S. L. (2011). Precipitation increases the abundance of some groups of root-associated fungal endophytes in a semiarid grassland. *Ecosphere* , *2*(4), art50.

Hill, P. W., Farrar, J., Roberts, P., Farrell, M., Grant, H., Newsham, K. K., Hopkins, D. W., Bardgett, R. D., & Jones, D. L. (2011). Vascular plant success in a warming Antarctic may be due to efficient nitrogen acquisition. *Nature Climate Change*, *1*(1), 50–53.

Hill, P. W., & Jones, D. L. (2019). Plant-microbe competition: does injection of isotopes of C and N into the rhizosphere effectively characterise plant use of soil N? *The New Phytologist*, *221*(2), 796–806.

Hodge, A., Robinson, D., & Fitter, A. (2000). Are microorganisms more effective than plants at competing for nitrogen? *Trends in Plant Science*, *5*(7), 304–308.

Hodge, A., Stewart, J., Robinson, D., Griffiths, B. S., & Fitter, A. H. (2000). Competition between roots and soil micro-organisms for nutrients from nitrogen-rich patches of varying complexity. *The Journal of Ecology*, *88*(1), 150–164.

Hodge, Angela. (2004). The plastic plant: root responses to heterogeneous supplies of nutrients. *The New Phytologist*, *162*(1), 9–24.

Hoeksema, J. D., Chaudhary, V. B., & Gehring, C. A. (2010). A meta-analysis of context-dependency in plant response to inoculation with mycorrhizal fungi. *Ecology*. https://onlinelibrary.wiley.com/doi/abs/10.1111/j.1461-0248.2009.01430.x

Homyak, P. M., Blankinship, J. C., Marchus, K., Lucero, D. M., Sickman, J. O., & Schimel, J. P. (2016). Aridity and plant uptake interact to make dryland soils hotspots for nitric oxide (NO) emissions. *Proceedings of the National Academy of Sciences of the United States of America*, *113*(19), E2608-16.

Hong, J., Ma, X., Zhang, X., & Wang, X. (2017). Nitrogen uptake pattern of herbaceous plants: coping strategies in altered neighbor species. *Biology and Fertility of Soils*, *53*(7), 729–735.

Hooper, D. U., & Johnson, L. (1999). Nitrogen limitation in dryland ecosystems: Responses to geographical and temporal variation in precipitation. *Biogeochemistry*, *46*(1–3), 247–293.

Hou, E., Rudgers, J. A., Collins, S. L., Litvak, M. E., White, C. S., Moore, D. I., & Luo, Y. (2021). Sensitivity of soil organic matter to climate and fire in a desert grassland. *Biogeochemistry*, *156*(1), 59–74.

Hu, Y., Zheng, Q., Noll, L., Zhang, S., & Wanek, W. (2020). Direct measurement of the in situ decomposition of microbial-derived soil organic matter. *Soil Biology & Biochemistry*, *141*, 107660.

Hudson, C. M., Kirton, E., Hutchinson, M. I., Redfern, J. L., Simmons, B., Ackerman, E., Singh, S., Williams, K. P., Natvig, D. O., & Powell, A. J. (2015). Lignin-modifying processes in the rhizosphere of arid land grasses. *Environmental Microbiology*, *17*(12), 4965–4978.

Huse, S. M., Welch, D. M., Morrison, H. G., & Sogin, M. L. (2010). Ironing out the wrinkles in the rare biosphere through improved OTU clustering. *Environmental Microbiology*, *12*(7), 1889–1898.

Huygens, D., Díaz, S., Urcelay, C., & Boeckx, P. (2016). Microbial recycling of dissolved organic matter confines plant nitrogen uptake to inorganic forms in a semi-arid ecosystem. *Soil Biology & Biochemistry*, *101*, 142–151.

Ihrmark, K., Bödeker, I. T. M., Cruz-Martinez, K., Friberg, H., Kubartova, A., Schenck, J., Strid, Y., Stenlid, J., Brandström-Durling, M., Clemmensen, K. E., & Lindahl, B. D. (2012). New primers to amplify the fungal ITS2 region--evaluation by 454-sequencing of artificial and natural communities. *FEMS Microbiology Ecology*, *82*(3), 666–677.

Ivans, C. Y., Leffler, A. J., Spaulding, U., Stark, J. M., Ryel, R. J., & Caldwell, M. M. (2003). Root responses and nitrogen acquisition by Artemisia tridentata and Agropyron desertorum following small summer rainfall events. *Oecologia*, *134*(3), 317–324.

Jackson, L. E., Schimel, J. P., & Firestone, M. K. (1989). Short-term partitioning of ammonium and nitrate between plants and microbes in an annual grassland. *Soil Biology & Biochemistry*, *21*(3), 409–415.

James, J. J., Davies, K. W., Sheley, R. L., & Aanderud, Z. T. (2008). Linking nitrogen partitioning and species abundance to invasion resistance in the Great Basin. *Oecologia*, *156*(3), 637–648.

James, J. J., Mangold, J. M., Sheley, R. L., & Svejcar, T. (2009). Root plasticity of native and invasive Great Basin species in response to soil nitrogen heterogeneity. *Plant Ecology*, *202*(2), 211–220.

James, J. J., & Richards, J. H. (2006). Plant nitrogen capture in pulse-driven systems: interactions between root responses and soil processes. *The Journal of Ecology*, *94*(4), 765–777.

James, J. J., & Richards, J. H. (2007). Influence of temporal heterogeneity in nitrogen supply on competitive interactions in a desert shrub community. *Oecologia*, *152*(4), 721–727.

Jasper, D. et al. (1989). Hyphae of a vesicular-arbuscular mycorrhizal fungus maintain infectivity in dry soil except when soil is disturbed. *New Phytologist* 112, 101-107.

Jia, Y., Van Der Heijden, M., Valzano-Held, A. Y., Jocher, M., & Walder, F. (2023). Mycorrhizal fungi mitigate nitrogen losses of an experimental grassland by facilitating plant uptake and soil microbial immobilization. *Pedosphere*. https://doi.org/10.1016/j.pedsph.2023.05.001

Jilling, A., Keiluweit, M., Contosta, A. R., Frey, S., Schimel, J., Schnecker, J., Smith, R. G., Tiemann, L., & Grandy, A. S. (2018). Minerals in the rhizosphere: overlooked mediators of soil nitrogen availability to plants and microbes. *Biogeochemistry*, *139*(2), 103–122.

Jin, V. L., & Evans, R. D. (2010). Elevated CO_2 increases plant uptake of organic and inorganic N in the desert shrub Larrea tridentata. *Oecologia*, *163*(1), 257–266.

Joergensen, R. G., & Wichern, F. (2008). Quantitative assessment of the fungal contribution to microbial tissue in soil. *Soil Biology & Biochemistry*, *40*(12), 2977–2991.

Johnson, D., Leake, J. R., Ostle, N., Ineson, P., & Read, D. J. (2002). In situ $^{13}CO_2$ pulse-labelling of upland grassland demonstrates a rapid pathway of carbon flux from arbuscular mycorrhizal mycelia to the soil. *The New Phytologist*, *153*(2), 327–334.

Johnson, Nancy C., Angelard, C., Sanders, I. R., & Kiers, E. T. (2013). Predicting community and ecosystem outcomes of mycorrhizal responses to global change. *Ecology Letters*, *16 Suppl 1*, 140–153.

Johnson, Nancy Collins, Rowland, D. L., Corkidi, L., Egerton-Warburton, L. M., & Allen, E. B. (2003). Nitrogen enrichment alters mycorrhizal allocation at five Mesic to semiarid grasslands. *Ecology*, *84*(7), 1895–1908.

Johnson, Nancy Collins, Wilson, G. W. T., Bowker, M. A., Wilson, J. A., & Miller, R. M. (2010). Resource limitation is a driver of local adaptation in mycorrhizal symbioses. *Proceedings of the National Academy of Sciences of the United States of America*, *107*(5), 2093–2098.

Jones, D. L., Healey, J. R., Willett, V. B., Farrar, J. F., & Hodge, A. (2005). Dissolved organic nitrogen uptake by plants—an important N uptake pathway? *Soil Biology & Biochemistry*, *37*(3), 413–423.

Jones, D. L., Kielland, K., Sinclair, F. L., Dahlgren, R. A., Newsham, K. K., Farrar, J. F., & Murphy, D. V. (2009). Soil organic nitrogen mineralization across a global latitudinal gradient. In *Global Biogeochemical Cycles* (Vol. 23, Issue 1). https://doi.org/10.1029/2008gb003250

Jumpponen, A., Herrera, J., Porras-Alfaro, A., & & Rudgers, J. A. (2017). Biogeography of Root-Associated Fungal Endophytes. In L. Tedersoo (Ed.), *Biogeography of Mycorrhizal Symbiosis* (pp. 195–222). Springer.

Jumpponen, A., Högberg, P., Huss-Danell, K., & Mulder, C. P. H. (2002). Interspecific and spatial differences in nitrogen uptake in monocultures and two-species mixtures in north European grasslands. *Functional Ecology*, *16*(4), 454–461.

Jumpponen, Ari, & Trappe, J. M. (1998). Dark septate endophytes: a review of facultative biotrophic root-colonizing fungi. *The New Phytologist*, *140*(2), 295–310.

Jumpponen, Ari, Trowbridge, J., Mandyam, K., & Johnson, L. (2005). Nitrogen enrichment causes minimal changes in arbuscular mycorrhizal colonization but shifts community composition—evidence from rDNA data. *Biology and Fertility of Soils*, *41*(4), 217–224.

Kahmen, A., Renker, C., Unsicker, S. B., & Buchmann, N. (2006). Niche complementarity for nitrogen: an explanation for the biodiversity and ecosystem functioning relationship? *Ecology*, *87*(5), 1244–1255.

Kazarina, A., Sarkar, S., Thapa, S., Heeren, L., Kamke, A., Ward, K., Hartung, E., Ran, Q., Galliart, M., Jumpponen, A., Johnson, L., & Lee, S. T. M. (2023). Home-field advantage affects the local adaptive interaction between Andropogon gerardii ecotypes and root-associated bacterial communities. *Microbiology Spectrum*, *11*(5), e0020823.

Khidir, H. H., Eudy, D. M., Porras-Alfaro, A., Herrera, J., Natvig, D. O., & Sinsabaugh, R. L. (2010). A general suite of fungal endophytes dominate the roots of two dominant grasses in a semiarid grassland. *Journal of Arid Environments*, *74*(1), 35–42.

Kieft, T. L., White, C. S., Loftin, S. R., Aguilar, R., & Craig, J. A. (1998). Temporal dynamics in soil carbon and nitrogen resources at a grassland–shrubland ecotone. *Ecology*. https://doi.org/10.1890/0012-9658(1998)079[0671:TDISCA]2.0.CO;2

Kivlin, S. N., Emery, S. M., & Rudgers, J. A. (2013). Fungal symbionts alter plant responses to global change. *American Journal of Botany*, *100*(7), 1445–1457.

Knapp, D. G., Németh, J. B., Barry, K., Hainaut, M., Henrissat, B., Johnson, J., Kuo, A., Lim, J. H. P., Lipzen, A., Nolan, M., Ohm, R. A., Tamás, L., Grigoriev, I. V., Spatafora, J. W., Nagy, L. G., & Kovács, G. M. (2018). Comparative genomics provides insights into the

lifestyle and reveals functional heterogeneity of dark septate endophytic fungi. *Scientific Reports*, *8*(1), 6321.

Knapp, D. G., Pintye, A., & Kovács, G. M. (2012). The dark side is not fastidious--dark septate endophytic fungi of native and invasive plants of semiarid sandy areas. *PloS One*, *7*(2), e32570.

Knops, J. M. H., Bradley, K. L., & Wedin, D. A. (2002). Mechanisms of plant species impacts on ecosystem nitrogen cycling. *Ecology Letters*, *5*(3), 454–466.

Kraiser, T., Gras, D. E., Gutiérrez, A. G., González, B., & Gutiérrez, R. A. (2011). A holistic view of nitrogen acquisition in plants. *Journal of Experimental Botany*, *62*(4), 1455–1466.

Krichels, A. H., Homyak, P. M., Aronson, E. L., Sickman, J. O., Botthoff, J., Shulman, H., Piper, S., Andrews, H. M., & Jenerette, G. D. (2022). Rapid nitrate reduction produces pulsed NO and N_2O emissions following wetting of dryland soils. *Biogeochemistry*, *158*(2), 233–250.

Kurc, S. A., & Small, E. E. (2004). Dynamics of evapotranspiration in semiarid grassland and shrubland ecosystems during the summer monsoon season, central New Mexico. *Water Resources Research*, *40*(9). https://doi.org/10.1029/2004wr003068

Kuster, T. M., Wilkinson, A., Hill, P. W., Jones, D. L., & Bardgett, R. D. (2016). Warming alters competition for organic and inorganic nitrogen between co-existing grassland plant species. *Plant and Soil*, *406*(1), 117–129.

Kuypers, M. M. M., Marchant, H. K., & Kartal, B. (2018). The microbial nitrogen-cycling network. *Nature Reviews. Microbiology*, *16*(5), 263–276.

Kuzyakov, Y., & Blagodatskaya, E. (2015). Microbial hotspots and hot moments in soil: Concept & review. *Soil Biology & Biochemistry*, *83*, 184–199.

Kwiecinski, J. V., Stricker, E., Sinsabaugh, R. L., & Collins, S. L. (2020). Rainfall pulses increased short-term biocrust chlorophyll but not fungal abundance or N availability in a long-term dryland rainfall manipulation experiment. *Soil Biology & Biochemistry*, *142*, 107693.

Ladwig, L. M., Bell-Dereske, L. P., Bell, K. C., Collins, S. L., Natvig, D. O., & Taylor, D. L. (2021). Soil fungal composition changes with shrub encroachment in the northern Chihuahuan Desert. *Fungal Ecology*, *53*, 101096.

Ladwig, L. M., Collins, S. L., Swann, A. L., Xia, Y., Allen, M. F., & Allen, E. B. (2012). Above- and belowground responses to nitrogen addition in a Chihuahuan Desert grassland. *Oecologia*, *169*(1), 177–185.

Ladwig, L. M., Sinsabaugh, R. L., Collins, S. L., & Thomey, M. L. (2015). Soil enzyme responses to varying rainfall regimes in Chihuahuan Desert soils. *Ecosphere* , *6*(3), art40.

Lagueux, D., Jumpponen, A., Porras-Alfaro, A., Herrera, J., Chung, Y. A., Baur, L. E., Smith, M. D., Knapp, A. K., Collins, S. L., & Rudgers, J. A. (2021). Experimental drought re-ordered assemblages of root-associated fungi across North American grasslands. *The Journal of Ecology*, *109*(2), 776–792.

Lajtha, K., & Schlesinger, W. H. (1986). Plant response to variations in nitrogen availability in a desert shrubland community. *Biogeochemistry*, *2*(1), 29–37.

Lanfranco, L., Bonfante, P., & Genre, A. (2016). The Mutualistic Interaction between Plants and Arbuscular Mycorrhizal Fungi. *Microbiology Spectrum*, *4*(6). https://doi.org/10.1128/microbiolspec.FUNK-0012-2016

Lauenroth, W. K., Sala, O. E., Milchunas, D. G., & Lathrop, R. W. (1987). Root dynamics of Bouteloua gracilis during short-term recovery from drought. *Functional Ecology*, *1*(2), 117–124.

Lee, C. A., & Lauenroth, W. K. (1994). Spatial distributions of grass and shrub root systems in the shortgrass steppe. *The American Midland Naturalist*, *132*(1), 117–123.

Leff, J. W., Jones, S. E., Prober, S. M., Barberán, A., Borer, E. T., Firn, J. L., Harpole, W. S., Hobbie, S. E., Hofmockel, K. S., Knops, J. M. H., McCulley, R. L., La Pierre, K., Risch, A. C., Seabloom, E. W., Schütz, M., Steenbock, C., Stevens, C. J., & Fierer, N. (2015). Consistent responses of soil microbial communities to elevated nutrient inputs in grasslands across the globe. *Proceedings of the National Academy of Sciences of the United States of America*, *112*(35), 10967–10972.

Leigh, J., Hodge, A., & Fitter, A. H. (2009). Arbuscular mycorrhizal fungi can transfer substantial amounts of nitrogen to their host plant from organic material. *The New Phytologist*, *181*(1), 199–207.

Leitner, S., Homyak, P. M., Blankinship, J. C., Eberwein, J., Jenerette, G. D., Zechmeister-Boltenstern, S., & Schimel, J. P. (2017). Linking NO and N2O emission pulses with the mobilization of mineral and organic N upon rewetting dry soils. *Soil Biology & Biochemistry*, *115*, 461–466.

Lenth, R. V. (2021). *emmeans: Estimated Marginal Means, Aka Least-Squares Means. R Package v 1.5. 5-1 (2021)*.

Li, Xia, He, X., Hou, L., Ren, Y., Wang, S., & Su, F. (2018). Dark septate endophytes isolated from a xerophyte plant promote the growth of Ammopiptanthus mongolicus under drought condition. *Scientific Reports*, *8*(1), 7896.

Li, Xiuyuan, Rennenberg, H., & Simon, J. (2016). Seasonal variation in N uptake strategies in the understorey of a beech-dominated N-limited forest ecosystem depends on N source and species. *Tree Physiology*, *36*(5), 589–600.

Lipson, D., & Näsholm, T. (2001). The unexpected versatility of plants: organic nitrogen use and availability in terrestrial ecosystems. *Oecologia*, *128*(3), 305–316.

Mack, K. M. L., & Rudgers, J. A. (2008). Balancing multiple mutualists: asymmetric interactions among plants, arbuscular mycorrhizal fungi, and fungal endophytes. *Oikos* , *117*(2), 310–320.

Maier, S., Muggia, L., Kuske, C. R., & Grube, M. (2016). Bacteria and Non-lichenized Fungi Within Biological Soil Crusts. In B. Weber, B. Büdel, & J. Belnap (Eds.), *Biological Soil Crusts: An Organizing Principle in Drylands* (pp. 81–100). Springer International Publishing.

Magan, N. and Lynch, J.M. (1986). Water potential, growth and cellulolysis of fungi involved in decomposition of cereal residues. *Journ. Of Gen. Microbiol.* 132, 1181-1187.

Mandyam, K., & Jumpponen, A. (2005). Seeking the elusive function of the root-colonising dark septate endophytic fungi. *Studies in Mycology*, *53*(1), 173–189.

Manzoni, S., Schimel, J. P., & Porporato, A. (2012). Responses of soil microbial communities to water stress: results from a meta-analysis. *Ecology*, *93*(4), 930–938.

Mariotti, A. (1983). Atmospheric nitrogen is a reliable standard for natural ^{15}N abundance measurements. *Nature*, *303*, 685–687.

Martinez Arbizu, P. (2020). pairwiseAdonis: Pairwise multilevel comparison using adonis. R package version 0.4

Marusenko, Y., Huber, D. P., & Hall, S. J. (2013). Fungi mediate nitrous oxide production but not ammonia oxidation in aridland soils of the southwestern US. *Soil Biology & Biochemistry*, *63*, 24–36.

Maurer, G. E., Hallmark, A. J., Brown, R. F., & Sala, O. E. (2020). Sensitivity of primary production to precipitation across the United States. *Ecology*. https://onlinelibrary.wiley.com/doi/abs/10.1111/ele.13455

McGonigle, T. P., Miller, M. H., Evans, D. G., Fairchild, G. L., & Swan, J. A. (1990). A new method which gives an objective measure of colonization of roots by vesicular-arbuscular mycorrhizal fungi. *The New Phytologist*, *115*(3), 495–501.

McHugh, T. A., Morrissey, E. M., Mueller, R. C., Gallegos-Graves, L. V., Kuske, C. R., & Reed, S. C. (2017). Bacterial, fungal, and plant communities exhibit no biomass or compositional response to two years of simulated nitrogen deposition in a semiarid grassland. *Environmental Microbiology*, *19*(4), 1600–1611.

McKane, R. B., Johnson, L. C., Shaver, G. R., Nadelhoffer, K. J., Rastetter, E. B., Fry, B., Giblin, A. E., Kielland, K., Kwiatkowski, B. L., Laundre, J. A., & Murray, G. (2002). Resource-based niches provide a basis for plant species diversity and dominance in arctic tundra. *Nature*, *415*, 68–71.

McLain, J. E. T., & Martens, D. A. (2006). N2O production by heterotrophic N transformations in a semiarid soil. *Applied Soil Ecology: A Section of Agriculture, Ecosystems & Environment*, *32*(2), 253–263.

McMurdie, P. J., & Holmes, S. (2013). phyloseq: an R package for reproducible interactive analysis and graphics of microbiome census data. *PloS One*, *8*(4), e61217.

Meng, B., Li, J., Yao, Y., Nippert, J. B., Williams, D. G., Chai, H., Collins, S. L., & Sun, W. (2022). Soil N enrichment mediates carbon allocation through respiration in a dominant grass during drought. *Functional Ecology*, *36*(5), 1204–1215.

Miller, A. E., & Bowman, W. D. (2002). Variation in nitrogen-15 natural abundance and nitrogen uptake traits among co-occurring alpine species: do species partition by nitrogen form? *Oecologia*, *130*(4), 609–616.

Miller, A. E., & Bowman, W. D. (2003). Alpine plants show species-level differences in the uptake of organic and inorganic nitrogen. *Plant and Soil*, *250*, 283–292.

Miller, A. E., Bowman, W. D., & Suding, K. N. (2007). Plant uptake of inorganic and organic nitrogen: neighbor identity matters. *Ecology*, *88*(7), 1832–1840.

Miller, A. J., Fan, X., Shen, Q., & Smith, S. J. (2007). Amino acids and nitrate as signals for the regulation of nitrogen acquisition. *Journal of Experimental Botany*, *59*(1), 111–119.

Moe, L. A. (2013). Amino acids in the rhizosphere: from plants to microbes. *American Journal of Botany*, *100*(9), 1692–1705.

Moreau, D., Bardgett, R. D., Finlay, R. D., Jones, D. L., & Philippot, L. (2019). A plant perspective on nitrogen cycling in the rhizosphere. *Functional Ecology*, *33*(4), 540–552.

Mueller, R. C., Belnap, J., & Kuske, C. R. (2015). Soil bacterial and fungal community responses to nitrogen addition across soil depth and microhabitat in an arid shrubland. *Frontiers in Microbiology*, *6*, 891.

Muldavin, E. H. (2002). Some floristic characteristics of the northern Chihuahuan Desert: A search for its northern boundary. *Taxon*, *51*(3), 453.

Muldavin, E. H., Moore, D. I., Collins, S. L., Wetherill, K. R., & Lightfoot, D. C. (2008). Aboveground net primary production dynamics in a northern Chihuahuan Desert ecosystem. *Oecologia*, *155*(1), 123–132.

Näsholm, T., Huss-Danell, K., & Högberg, P. (2000). Uptake of organic nitrogen in the field by four agriculturally important plant species. *Ecology*, *81*(4), 1155–1161.

Näsholm, T., Kielland, K., & Ganeteg, U. (2009). Uptake of organic nitrogen by plants. *The New Phytologist*, *182*(1), 31–48.

Näsholm, T., & Persson, J. (2001). Plant acquisition of organic nitrogen in boreal forests. *Physiologia Plantarum*, *111*(4), 419–426.

Ndinga-Muniania, C., Mueller, R. C., Kuske, C. R., & Porras-Alfaro, A. (2021). Seasonal variation and potential roles of dark septate fungi in an arid grassland. *Mycologia*, *113*(6), 1181–1198.

Newsham, K. K. (2011). A meta-analysis of plant responses to dark septate root endophytes. *The New Phytologist*, *190*(3), 783–793.

Nguyen, N. H., Smith, D., Peay, K., & Kennedy, P. (2015). Parsing ecological signal from noise in next generation amplicon sequencing. *The New Phytologist*, *205*(4), 1389–1393.

Nguyen, N. H., Song, Z., Bates, S. T., Branco, S., Tedersoo, L., Menke, J., Schilling, J. S., & Kennedy, P. G. (2016). FUNGuild: An open annotation tool for parsing fungal community datasets by ecological guild. *Fungal Ecology*, *20*, 241–248.

Nielsen, U. N., & Ball, B. A. (2015). Impacts of altered precipitation regimes on soil communities and biogeochemistry in arid and semi-arid ecosystems. *Global Change Biology*, *21*(4), 1407–1421.

Notaro, M., Liu, Z., Gallimore, R. G., Williams, J. W., Gutzler, D. S., & Collins, S. (2010). Complex seasonal cycle of ecohydrology in the Southwest United States. *Journal of Geophysical Research: Biogeosciences*, *115*(G4). https://doi.org/10.1029/2010JG001382

Ochoa-Hueso, R., Delgado-Baquerizo, M., Gallardo, A., Bowker, M. A., & Maestre, F. T. (2016). Climatic conditions, soil fertility and atmospheric nitrogen deposition largely determine the structure and functioning of microbial communities in biocrust-dominated Mediterranean drylands. *Plant and Soil*, *399*, 271-282.

Ochoa-Hueso, Raúl, Borer, E. T., Seabloom, E. W., Hobbie, S. E., Risch, A. C., Collins, S. L., Alberti, J., Bahamonde, H. A., Brown, C. S., Caldeira, M. C., Daleo, P., Dickman, C. R., Ebeling, A., Eisenhauer, N., Esch, E. H., Eskelinen, A., Fernández, V., Güsewell, S., Gutierrez-Larruga, B., … Zamin, T. (2020). Microbial processing of plant remains is co-limited by multiple nutrients in global grasslands. *Global Change Biology*, *26*(8), 4572–4582.

Ogle, K., & Reynolds, J. F. (2004). Plant responses to precipitation in desert ecosystems: integrating functional types, pulses, thresholds, and delays. *Oecologia*, *141*(2), 282–294.

Oksanen, J., Blanchet, F. G., Friendly, M., Kindt, R., Legendre, P., McGlinn, D., Minchin, P. R., O'hara, R. B., Simpson, G. L., Solymos, P., & Others. (2019). Package 'vegan.' *Community Ecology Package, Version*, *2*(9). https://cran.r-hub.io/web/packages/vegan/vegan.pdf

Oliver, A. K., Callaham, M. A., & Jumpponen, A. (2015). Soil fungal communities respond compositionally to recurring frequent prescribed burning in a managed southeastern US forest ecosystem. *Forest Ecology and Management*, *345*, 1–9.

Olsson, P. A., Larsson, L., Bago, B., Wallander, H., & Van Aarle, I. M. (2003). Ergosterol and fatty acids for biomass estimation of mycorrhizal fungi. *The New Phytologist*, *159*(1), 7–10.

Omari, H., Pietrasiak, N., Ferrenberg, S., & Nishiguchi, M. K. (2022). A spatiotemporal framework reveals contrasting factors shape biocrust microbial and microfaunal communities in the Chihuahuan Desert. *Geoderma*, *405*, 115409.

Osborne, B. B., Roybal, C. M., Reibold, R., Collier, C. D., Geiger, E., Phillips, M. L., Weintraub, M. N., & Reed, S. C. (2022). Biogeochemical and ecosystem properties in three adjacent semi-arid grasslands are resistant to nitrogen deposition but sensitive to edaphic variability. *The Journal of Ecology*, *110*(7), 1615–1631.

Ouyang, S., Tian, Y., Liu, Q., Zhang, L., Wang, R., & Xu, X. (2016). Nitrogen competition between three dominant plant species and microbes in a temperate grassland. *Plant and Soil*, *408*(1), 121–132.

Owen, A. G., & Jones, D. L. (2001). Competition for amino acids between wheat roots and rhizosphere microorganisms and the role of amino acids in plant N acquisition. *Soil Biology & Biochemistry*, *33*(4), 651–657.

Parker, S. S., & Schimel, J. P. (2011). Soil nitrogen availability and transformations differ between the summer and the growing season in a California grassland. *Applied Soil Ecology: A Section of Agriculture, Ecosystems & Environment*, *48*(2), 185–192.

Patrick, L. D., Ogle, K., Bell, C. W., Zak, J., & Tissue, D. (2009). Physiological responses of two contrasting desert plant species to precipitation variability are differentially regulated by soil moisture and nitrogen dynamics. *Global Change Biology*, *15*(5), 1214–1229.

Pennington, D. D., & Collins, S. L. (2007). Response of an aridland ecosystem to interannual climate variability and prolonged drought. *Landscape Ecology*, *22*(6), 897–910.

Peters, D. P. C. (2002). Plant species dominance at a grassland–shrubland ecotone: an individual-based gap dynamics model of herbaceous and woody species. *Ecological Modelling*, *152*(1), 5–32.

Peters, D. P. C., & Gibbens, R. P. (2006). Plant communities in the Jornada Basin: the dynamic landscape. *Structure and Function of a Chihuahuan Desert Ecosystem: The Jornada Basin Long-Term Ecological Research Site*, 211–231.

Peters, D. P. C., Jin, Y., & & Gosz, J. R. (2006). Woody plant invasion at a semi-arid/arid transition zone: importance of ecosystem type to colonization and patch expansion. *Journal of Vegetation Science*, *17*, 389–396.

Peters, D. P. C., & Yao, J. (2012). Long-term experimental loss of foundation species: consequences for dynamics at ecotones across heterogeneous landscapes. *Ecosphere*, *3*(3), 1–23.

Petersen, S. L., Roundy, B. A., & Bryant, R. M. (2004). Revegetation methods for high-elevation roadsides at Bryce Canyon National Park, Utah. *Restoration Ecology*, *12*(2), 248–257.

Phillips, M. L., Winkler, D. E., Reibold, R. H., Osborne, B. B., & Reed, S. C. (2021). Muted responses to chronic experimental nitrogen deposition on the Colorado Plateau. *Oecologia*, *195*(2), 513–524.

Pointing, S. B., & Belnap, J. (2012). Microbial colonization and controls in dryland systems. *Nature Reviews. Microbiology*, *10*(8), 551–562.

Pombubpa, N., Pietrasiak, N., De Ley, P., & Stajich, J. E. (2020). Insights into dryland biocrust microbiome: geography, soil depth and crust type affect biocrust microbial communities

and networks in Mojave Desert, USA. *FEMS Microbiology Ecology*, *96*(9). https://doi.org/10.1093/femsec/fiaa125

Porras-Alfaro, A., & Bayman, P. (2011). Hidden fungi, emergent properties: endophytes and microbiomes. *Annual Review of Phytopathology*, *49*, 291–315.

Porras-Alfaro, A., Herrera, J., Natvig, D. O., Lipinski, K., & Sinsabaugh, R. L. (2011). Diversity and distribution of soil fungal communities in a semiarid grassland. *Mycologia*, *103*(1), 10–21.

Porras-Alfaro, A., Herrera, J., Sinsabaugh, R. L., Odenbach, K. J., Lowrey, T., & Natvig, D. O. (2008). Novel root fungal consortium associated with a dominant desert grass. *Applied and Environmental Microbiology*, *74*(9), 2805–2813.

Querejeta, J. I., Egerton-Warburton, L. M., & Allen, M. F. (2003). Direct nocturnal water transfer from oaks to their mycorrhizal symbionts during severe soil drying. *Oecologia*, *134*(1), 55–64.

Querejeta, J. I., Egerton-Warburton, L. M., Prieto, I., Vargas, R., & Allen, M. F. (2012). Changes in soil hyphal abundance and viability can alter the patterns of hydraulic redistribution by plant roots. *Plant and Soil*, *355*(1–2), 63–73.

R Core Team (2022). R: A language and environment for statistical computing. R Foundation for Statistical Computing, Vienna, Austria. https://www.R-project.org/.

Ramond, J.-B., Jordaan, K., Díez, B., Heinzelmann, S. M., & Cowan, D. A. (2022). Microbial biogeochemical cycling of nitrogen in arid ecosystems. *Microbiology and Molecular Biology Reviews: MMBR*, *86*(2), e0010921.

Ratliff, L.F. et al. (1983). Field-measured limits of soil water availability as related to laboratory-measured properties. *Soil Sci. Soc. Am. Journ.* 47, 764-769

Reichmann, L. G., Sala, O. E., & Peters, D. P. C. (2013). Precipitation legacies in desert grassland primary production occur through previous-year tiller density. *Ecology*, *94*(2), 435–443.

Requena, N., Serrano, E., Ocón, A., & Breuninger, M. (2007). Plant signals and fungal perception during arbuscular mycorrhiza establishment. *Phytochemistry*, *68*(1), 33–40.

Reynolds, H. L., Packer, A., Bever, J. D., & Clay, K. (2003). Grassroots ecology: Plant–microbe–soil interactions as drivers of plant community structure and dynamics. *Ecology*, *84*(9), 2281–2291.

Reynolds, T. D., & Fraley, L. (1989). Root profiles of some native and exotic plant species in Southeastern Idaho. *Environmental and Experimental Botany*, *29*(2), 241–248.

Robinson, D. (2001). $\delta^{15}N$ as an integrator of the nitrogen cycle. *Trends Ecol. Evol.*, *16*(3), 153–162.

Rodriguez, R. J., White, J. F., Jr, Arnold, A. E., & Redman, R. S. (2009). Fungal endophytes: diversity and functional roles. *The New Phytologist*, *182*(2), 314–330.

Rodriguez-Caballero, E., Belnap, J., Büdel, B., Crutzen, P. J., Andreae, M. O., Pöschl, U., & Weber, B. (2018). Dryland photoautotrophic soil surface communities endangered by global change. *Nature Geoscience*, *11*(3), 185–189.

Rodríguez-Caballero, E., Castro, A. J., Chamizo, S., Quintas-Soriano, C., Garcia-Llorente, M., Cantón, Y., & Weber, B. (2018). Ecosystem services provided by biocrusts: From ecosystem functions to social values. *Journal of Arid Environments*, *159*, 45–53.

Rognes, T., Flouri, T., Nichols, B., Quince, C., & Mahé, F. (2016). VSEARCH: a versatile open source tool for metagenomics. *PeerJ*, *4*, e2584.

Romero, F., Argüello, A., de Bruin, S., & van der Heijden, M. G. A. (2023). The plant–mycorrhizal fungi collaboration gradient depends on plant functional group. *Functional Ecology*. https://doi.org/10.1111/1365-2435.14395

Romero-Jiménez, M.-J., Rudgers, J. A., Jumpponen, A., Herrera, J., Hutchinson, M., Kuske, C., Dunbar, J., Knapp, D. G., Kovács, G. M., & Porras-Alfaro, A. (2022). *Darksidea phi*, sp. nov., a dark septate root-associated fungus in foundation grasses in North American Great Plains. *Mycologia*, *114*(2), 254–269.

Rothstein, D. E. (2014). In-situ root uptake and soil transformations of glycine, glutamine and ammonium in two temperate deciduous forests of contrasting N availability. *Soil Biology & Biochemistry*, *75*, 233–236. https://doi.org/10.1016/j.soilbio.2014.04.004

Rudgers, J. A., Dettweiler-Robinson, E., Belnap, J., Green, L. E., Sinsabaugh, R. L., Young, K. E., Cort, C. E., & Darrouzet-Nardi, A. (2018). Are fungal networks key to dryland primary production? *American Journal of Botany*, *105*(11), 1783–1787.

Rudgers, J. A., Fox, S., Porras-Alfaro, A., Herrera, J., Reazin, C., Kent, D. R., Souza, L., Chung, Y. A., & Jumpponen, A. (2022). Biogeography of root-associated fungi in foundation grasses of North American plains. *Journal of Biogeography*, *49*(1), 22–37.

Sala, O. E., & Lauenroth, W. K. (1982). Small rainfall events: An ecological role in semiarid regions. *Oecologia*, *53*(3), 301–304.

Savage, M.J. et al. (1996). Lower limit of soil water availability. *Agronomy Journal* 88(4), 644-651.

Schadt, C. W., Martin, A. P., Lipson, D. A., & Schmidt, S. K. (2003). Seasonal dynamics of previously unknown fungal lineages in tundra soils. *Science*, *301*(5638), 1359–1361.

Schaeffer, S. M., Billings, S. A., & Evans, R. D. (2003). Responses of soil nitrogen dynamics in a Mojave Desert ecosystem to manipulations in soil carbon and nitrogen availability. *Oecologia*, *134*(4), 547–553.

Schiller, P., Heilmeier, H., & Hartung, W. (1998). Uptake of amino acids by the aquatic resurrection plant Chamaegigas intrepidus and its implication for N nutrition. *Oecologia*, *117*(1–2), 63–69.

Schimel, J., Balser, T. C., & Wallenstein, M. (2007). Microbial stress-response physiology and its implications for ecosystem function. *Ecology*, *88*(6), 1386–1394.

Schimel, J. P. (2018). Life in dry soils: Effects of drought on soil microbial communities and processes. *Annual Review of Ecology, Evolution, and Systematics*, *49*(1), 409–432.

Schimel, J. P., & Bennett, J. (2004). Nitrogen mineralization: Challenges of a changing paradigm. *Ecology*, *85*(3), 591–602.

Schimel, J. P., & Chapin, F. S., III. (1996). Tundra plant uptake of amino acid and NH_4^+ nitrogen in situ: Plants complete well for amino acid N. *Ecology*, *77*(7), 2142–2147.

Schindelin, J., Arganda-Carreras, I., Frise, E., Kaynig, V., Longair, M., Pietzsch, T., Preibisch, S., Rueden, C., Saalfeld, S., Schmid, B., Tinevez, J.-Y., White, D. J., Hartenstein, V., Eliceiri, K., Tomancak, P., & Cardona, A. (2012). Fiji: an open-source platform for biological-image analysis. *Nature Methods*, *9*(7), 676–682.

Schlesinger, W. H., Raikes, J. A., Hartley, A. E., & Cross, A. F. (1996). On the Spatial Pattern of Soil Nutrients in Desert Ecosystems. *Ecology*, *77*(2), 364–374.

Schloss, P. D., Westcott, S. L., Ryabin, T., Hall, J. R., Hartmann, M., Hollister, E. B., Lesniewski, R. A., Oakley, B. B., Parks, D. H., Robinson, C. J., Sahl, J. W., Stres, B., Thallinger, G. G., Van Horn, D. J., & Weber, C. F. (2009). Introducing mothur: open-

source, platform-independent, community-supported software for describing and comparing microbial communities. *Applied and Environmental Microbiology*, *75*(23), 7537–7541.

Schmidt, S., Raven, J. A., & Paungfoo-Lonhienne, C. (2013). The mixotrophic nature of photosynthetic plants. *Functional Plant Biology: FPB*, *40*(5), 425–438.

Schoch, C. L., Seifert, K. A., Huhndorf, S., Robert, V., Spouge, J. L., Levesque, C. A., & Chen, W. (2012). Nuclear ribosomal internal transcribed spacer (ITS) region as a universal DNA barcode marker for Fungi. *Proceedings of the National Academy of Sciences of the United States of America*, *109*(16), 6241–6246.

She, W., Bai, Y., Zhang, Y., Qin, S., Feng, W., Sun, Y., Zheng, J., & Wu, B. (2018). Resource Availability Drives Responses of Soil Microbial Communities to Short-term Precipitation and Nitrogen Addition in a Desert Shrubland. *Frontiers in Microbiology*, *9*, 186.

Sinsabaugh, R. L. (2010). Phenol oxidase, peroxidase and organic matter dynamics of soil. *Soil Biology & Biochemistry*, *42*(3), 391–404.

Smith, C. J., & Chalk, P. M. (2020). The role of ^{15}N in tracing N dynamics in agro-ecosystems under alternative systems of tillage management: A review. *Soil and Tillage Research*, *197*, 104496.

Smith, C. J., & Chalk, P. M. (2021). Organic N compounds in plant nutrition: have methodologies based on stable isotopes provided unequivocal evidence of direct N uptake? *Isotopes in Environmental and Health Studies*, *57*(4), 333–349.

Sokol, N. W., Slessarev, E., Marschmann, G. L., Nicolas, A., Blazewicz, S. J., Brodie, E. L., Firestone, M. K., Foley, M. M., Hestrin, R., Hungate, B. A., Koch, B. J., Stone, B. W., Sullivan, M. B., Zablocki, O., & Pett-Ridge, J. (2022). Life and death in the soil

microbiome: how ecological processes influence biogeochemistry. *Nature Reviews. Microbiology*, *20*(7), 415–430.

Stahl, V. M., Beyschlag, W., & Werner, C. (2011). Dynamic niche sharing in dry acidic grasslands -a ^{15}N -labeling experiment. *Plant and Soil*, *344*(1), 389–400.

Stajich, J. E., Berbee, M. L., Blackwell, M., Hibbett, D. S., James, T. Y., Spatafora, J. W., & Taylor, J. W. (2009). The fungi. *Current Biology: CB*, *19*(18), R840-5.

Stark, J.M. & Firestone, M.K. (1995). Mechanisms for soil moisture effects on activity of nitrifying bacteria. *Appl. And Environ. Microb.* 218-221.

Sterflinger, K., Tesei, D., & Zakharova, K. (2012). Fungi in hot and cold deserts with particular reference to microcolonial fungi. *Fungal Ecology*, *5*(4), 453–462.

Steven, B., Gallegos-Graves, L. V., Belnap, J., & Kuske, C. R. (2013). Dryland soil microbial communities display spatial biogeographic patterns associated with soil depth and soil parent material. *FEMS Microbiology Ecology*, *86*(1), 101–113.

Steven, B., Gallegos-Graves, L. V., Yeager, C., Belnap, J., & Kuske, C. R. (2014). Common and distinguishing features of the bacterial and fungal communities in biological soil crusts and shrub root zone soils. *Soil Biology & Biochemistry*, *69*, 302–312.

Steven, B., Kuske, C. R., Gallegos-Graves, L. V., Reed, S. C., & Belnap, J. (2015). Climate change and physical disturbance manipulations result in distinct biological soil crust communities. *Applied and Environmental Microbiology*, *81*(21), 7448–7459.

Stevenson, A., Cray, J. A., Williams, J. P., Santos, R., Sahay, R., Neuenkirchen, N., McClure, C. D., Grant, I. R., Houghton, J. D., Quinn, J. P., Timson, D. J., Patil, S. V., Singhal, R. S., Antón, J., Dijksterhuis, J., Hocking, A. D., Lievens, B., Rangel, D. E. N., Voytek, M. A.,

… Hallsworth, J. E. (2015). Is there a common water-activity limit for the three domains of life? *The ISME Journal*, *9*(6), 1333–1351.

Stursova, M., Crenshaw, C. L., & Sinsabaugh, R. L. (2006). Microbial responses to long-term N deposition in a semiarid grassland. *Microbial Ecology*, *51*(1), 90–98.

Stursova, M., & Sinsabaugh, R. L. (2008). Stabilization of oxidative enzymes in desert soil may limit organic matter accumulation. *Soil Biology & Biochemistry*, *40*(2), 550–553.

Sweeney, C. J., de Vries, F. T., van Dongen, B. E., & Bardgett, R. D. (2021). Root traits explain rhizosphere fungal community composition among temperate grassland plant species. *The New Phytologist*, *229*(3), 1492–1507.

Taylor, D. L., & Sinsabaugh, R. (2015). The Soil Fungi. In *Soil Microbiology, Ecology and Biochemistry* (pp. 77–109). unknown.

Tegeder, M., & Masclaux-Daubresse, C. (2018). Source and sink mechanisms of nitrogen transport and use. *The New Phytologist*, *217*(1), 35–53.

Teste, F. P., Karst, J., Jones, M. D., Simard, S. W., & Durall, D. M. (2006). Methods to control ectomycorrhizal colonization: effectiveness of chemical and physical barriers. *Mycorrhiza*, *17*(1), 51–65.

Thomey, M. L., Collins, S. L., Friggens, M. T., Brown, R. F., & Pockman, W. T. (2014). Effects of monsoon precipitation variability on the physiological response of two dominant C_4 grasses across a semiarid ecotone. *Oecologia*, *176*(3), 751–762.

Thomey, M. L., Collins, S. L., Vargas, R., Johnson, J. E., Brown, R. F., Natvig, D. O., & Friggens, M. T. (2011). Effect of precipitation variability on net primary production and soil respiration in a Chihuahuan Desert grassland. *Global Change Biology*, *17*(4), 1505–1515.

Thornton, B., & Robinson, D. (2005). Uptake and assimilation of nitrogen from solutions containing multiple N sources. *Plant, Cell & Environment*, *28*(6), 813–821.

Throop, H. L., & Archer, S. R. (2009). Resolving the Dryland Decomposition Conundrum: Some New Perspectives on Potential Drivers. In U. Lüttge, W. Beyschlag, B. Büdel, & D. Francis (Eds.), *Progress in Botany* (pp. 171–194). Springer Berlin Heidelberg.

Treseder, K. K. (2008). Nitrogen additions and microbial biomass: a meta-analysis of ecosystem studies. *Ecology Letters*, *11*(10), 1111–1120.

Tu, C., Booker, F. L., Watson, D. M., Chen, X., Rufty, T. W., Shi, W., & Hu, S. (2006). Mycorrhizal mediation of plant N acquisition and residue decomposition: Impact of mineral N inputs. *Global Change Biology*, *12*(5), 793–803.

Turnbull, L., Wainwright, J., Brazier, R. E., & & Bol, R. (2010). Biotic and abiotic changes in ecosystem structure over a shrub-encroachment gradient in the Southwestern USA. *Ecosystems*, *13*(8), 1239–1255.

van der Heijden, M. G. A., Martin, F. M., Selosse, M.-A., & Sanders, I. R. (2015). Mycorrhizal ecology and evolution: the past, the present, and the future. *The New Phytologist*, *205*(4), 1406–1423.

van der Heijden, M. G. A., Streitwolf-Engel, R., Riedl, R., Siegrist, S., Neudecker, A., Ineichen, K., Boller, T., Wiemken, A., & Sanders, I. R. (2006). The mycorrhizal contribution to plant productivity, plant nutrition and soil structure in experimental grassland. *The New Phytologist*, *172*(4), 739–752.

Vidal, E. A., Alvarez, J. M., Araus, V., Riveras, E., Brooks, M. D., Krouk, G., Ruffel, S., Lejay, L., Crawford, N. M., Coruzzi, G. M., & Gutiérrez, R. A. (2020). Nitrate in 2020: Thirty years from transport to signaling networks. *The Plant Cell*, *32*(7), 2094–2119.

Vierheilig, H., Coughlan, A. P., Wyss, U., & Piche, Y. (1998). Ink and vinegar, a simple staining technique for arbuscular-mycorrhizal fungi. *Applied and Environmental Microbiology*, *64*(12), 5004–5007.

Wallander, H., Nilsson, L. O., Hagerberg, D., & Bååth, E. (2001). Estimation of the biomass and seasonal growth of external mycelium of ectomycorrhizal fungi in the field. *The New Phytologist*, *151*(3), 753–760.

Wan, C., Sosebee, R. E., & McMichael, B. L. (1995). Water acquisition and rooting characteristics in northern and southern populations of *Gutierrezia sarothrae*. *Environmental and Experimental Botany*, *35*(1), 1–7.

Wang, L., & Macko, S. A. (2011). Constrained preferences in nitrogen uptake across plant species and environments. *Plant, Cell & Environment*, *34*(3), 525–534.

Wang, Q., Garrity, G. M., Tiedje, J. M., & Cole, J. R. (2007). Naive Bayesian classifier for rapid assignment of rRNA sequences into the new bacterial taxonomy. *Applied and Environmental Microbiology*, *73*(16), 5261–5267.

Warren, C. R. (2006). Potential organic and inorganic N uptake by six Eucalyptus species. *Functional Plant Biology: FPB*, *33*(7), 653–660.

Warren, C. R. (2014). Organic N molecules in the soil solution: what is known, what is unknown and the path forwards. *Plant and Soil*, *375*(1), 1–19.

Warren, D., & Silverman, B. W. (1987). Density estimation for statistics and data analysis. *Journal of the Royal Statistical Society. Series A* , *150*(4), 403.

Warren, S. D., Clair, L. L., Stark, L. R., Lewis, L. A., Pombubpa, N., Kurbessoian, T., Stajich, J. E., & Aanderud, Z. T. (2019). Reproduction and Dispersal of Biological Soil Crust

Organisms. *Frontiers in Ecology and Evolution*, *7*. https://doi.org/10.3389/fevo.2019.00344

Weber, B., Belnap, J., Büdel, B., Antoninka, A. J., Barger, N. N., Chaudhary, V. B., Darrouzet-Nardi, A., Eldridge, D. J., Faist, A. M., Ferrenberg, S., Havrilla, C. A., Huber-Sannwald, E., Malam Issa, O., Maestre, F. T., Reed, S. C., Rodriguez-Caballero, E., Tucker, C., Young, K. E., Zhang, Y., … Bowker, M. A. (2022). What is a biocrust? A refined, contemporary definition for a broadening research community. *Biological Reviews of the Cambridge Philosophical Society*. https://doi.org/10.1111/brv.12862

Wei, L., Chen, C., & Yu, S. (2015). Uptake of organic nitrogen and preference for inorganic nitrogen by two Australian native Araucariaceae species. *Plant Ecology & Diversity*, *8*(2), 259–264.

Weigelt, A., King, R., Bol, R., & Bardgett, R. D. (2003). Inter-specific variability in organic nitrogen uptake of three temperate grassland species. *Journal of Plant Nutrition and Soil Science*, *166*(5), 606–611.

Wen, Z., White, P. J., Shen, J., & Lambers, H. (2022). Linking root exudation to belowground economic traits for resource acquisition. *The New Phytologist*, *233*(4), 1620–1635.

Westcott, S. L., & Schloss, P. D. (2015). De novo clustering methods outperform reference-based methods for assigning 16S rRNA gene sequences to operational taxonomic units. *PeerJ*, *3*, e1487.

White, T. J., Bruns, T., Lee, S. J. W. T., & Taylor, J. (1990). Amplification and direct sequencing of fungal ribosomal RNA genes for phylogenetics. *PCR protocols: a guide to methods and applications*, *18*(1), 315-322.

Whitford, W. G., & Duval, B. D. (2019). *Ecology of Desert Systems*. Academic Press.

Whitney, K. D., Mudge, J., Natvig, D. O., Sundararajan, A., Pockman, W. T., Bell, J., Collins, S. L., & Rudgers, J. A. (2019). Experimental drought reduces genetic diversity in the grassland foundation species Bouteloua eriopoda. *Oecologia*, *189*(4), 1107–1120.

Wilkinson, A., Hill, P. W., Vaieretti, M. V., Farrar, J. F., Jones, D. L., & Bardgett, R. D. (2015). Challenging the paradigm of nitrogen cycling: no evidence of in situ resource partitioning by coexisting plant species in grasslands of contrasting fertility. *Ecology and Evolution*, *5*(2), 275–287.

Williams, J.P. & Hallsworth, J.E. (2009). Limits of life in hostile environments: no barriers to biosphere function? *Environ. Microb.* 11(12), 3292-3308.

Xia, J., & Wan, S. (2008). Global response patterns of terrestrial plant species to nitrogen addition. *The New Phytologist*, *179*(2), 428–439.

Yahdjian, L. et al. (2011). Nitrogen limitation in arid-subhumid ecosystems: A meta-analysis of fertilization studies. *Journal of Arid Environments*, *75*(8), 675–680.

Yan, L., & Yan, M. L. (2023). *Package "ggvenn."* cran.uvigo.es. https://cran.uvigo.es/web/packages/ggvenn/ggvenn.pdf

Yang, S., Xu, Z., Wang, R., Zhang, Y., Yao, F., Zhang, Y., Turco, R. F., Jiang, Y., Zou, H., & Li, H. (2017). Variations in soil microbial community composition and enzymatic activities in response to increased N deposition and precipitation in Inner Mongolian grassland. *Applied Soil Ecology: A Section of Agriculture, Ecosystems & Environment*, *119*, 275–285.

Yang, Z., Li, Y., Wang, Y., Cheng, J., & Li, F. Y. (2022). Preferences for different nitrogen forms in three dominant plants in a semi-arid grassland under different grazing intensities. *Agriculture, Ecosystems & Environment*, *333*, 107959.

Yanoff, S., & Muldavin, E. (2008). Grassland–shrubland transformation and grazing: A century-scale view of a northern Chihuahuan Desert grassland. *Journal of Arid Environments*, *72*(9), 1594–1605.

Yoder, C. K., Vivin, P., Defalco, L. A., Seemann, J. R., & Nowak, R. S. (2000). Root growth and function of three Mojave Desert grasses in response to elevated atmospheric CO_2 concentration. *The New Phytologist*, *145*, 245–256.

Young, K. E., Ferrenberg, S., Reibold, R., Reed, S. C., Swenson, T., Northen, T., & Darrouzet-Nardi, A. (2022). Vertical movement of soluble carbon and nutrients from biocrusts to subsurface mineral soils. *Geoderma*, *405*, 115495.

Zelikova, T. J., Housman, D. C., Grote, E. E., Neher, D. A., & Belnap, J. (2012). Warming and increased precipitation frequency on the Colorado Plateau: implications for biological soil crusts and soil processes. *Plant and Soil*, *355*(1–2), 265–282.

Zelles, L. (1999). Fatty acid patterns of phospholipids and lipopolysaccharides in the characterisation of microbial communities in soil: a review. *Biology and Fertility of Soils*, *29*(2), 111–129.

Zenova, G.M. et al. (2007). Influence of moisture on the vital activity of actinomycetes in a cultivated low-moor peat soil. *Eurasian Soil Science* 40, 560-564.

Zhang, J., Feng, Y., Maestre, F. T., Berdugo, M., Wang, J., Coleine, C., Sáez-Sandino, T., García-Velázquez, L., Singh, B. K., & Delgado-Baquerizo, M. (2023). Water availability creates global thresholds in multidimensional soil biodiversity and functions. *Nature Ecology & Evolution*. https://doi.org/10.1038/s41559-023-02071-3

Zhang, T., Jia, R.-L., & Yu, L.-Y. (2016). Diversity and distribution of soil fungal communities associated with biological soil crusts in the southeastern Tengger Desert (China) as revealed by 454 pyrosequencing. *Fungal Ecology*, *23*, 156–163.

Zhou, Z., Wang, C., Zheng, M., Jiang, L., & Luo, Y. (2017). Patterns and mechanisms of responses by soil microbial communities to nitrogen addition. *Soil Biology & Biochemistry*, *115*, 433–441.

Zhuang, W., Downing, A., & Zhang, Y. (2015). The influence of biological soil crusts on ^{15}N translocation in soil and vascular plant in a temperate desert of northwestern China. *Journal of Plant Ecology*, *8*(4), 420–428.

Zhuang, W., Li, J., Yu, F., Dong, Z., & Guo, H. (2020). Seasonal nitrogen uptake strategies in a temperate desert ecosystem depends on N form and plant species. *Plant Biology* , *22*(3), 386–393.

Supplementary Information

CHAPTER 2

Table S2.1 Mean N uptake ± standard error (μmol ^{15}N per g dw) of ^{15}N-enriched leaf samples from each ^{15}N tracer × species combination at each time point (12, 24, and 48 h) following ^{15}N tracer application (Fig. 2.1), and mean N uptake rate (μmol ^{15}N per g dw per h) of each ^{15}N tracer × species combination averaged across all 3 post-addition time points. Sample size (*n*) values represent the total number of samples for each ^{15}N tracer × species group (*N* = 220).

			Leaf N Uptake			
Plant Species	^{15}N Tracer	*n*	12	24	48	N Uptake Rate
Bouteloua eriopoda	NH_4^+	26	0.18 ± 0.10	0.31 ± 0.14	1.26 ± 0.40	0.019 ± 0.004
	NO_3^-	20	0.54 ± 0.33	1.08 ± 0.63	1.83 ± 0.83	0.043 ± 0.013
	Glu	11	0.03 ± NA	0.07 ± 0.02	0.21 ± 0.10	0.004 ± 0.001
Achnatherum hymenoides	NH_4^+	28	0.16 ± 0.04	0.23 ± 0.07	0.65 ± 0.18	0.012 ± 0.002
	NO_3^-	35	0.31 ± 0.13	0.39 ± 0.15	0.58 ± 0.19	0.018 ± 0.005
	Glu	25	0.06 ± 0.02	0.11 ± 0.04	0.25 ± 0.07	0.005 ± 0.001
Gutierrezia sarothrae	NH_4^+	29	0.31 ± 0.13	0.21 ± 0.08	1.09 ± 0.41	0.019 ± 0.005
	NO_3^-	28	0.46 ± 0.12	0.47 ± 0.09	1.25 ± 0.34	0.028 ± 0.004
	Glu	18	0.15 ± 0.08	0.18 ± 0.07	0.51 ± 0.28	0.011 ± 0.003

Table S2.2 Model variance measures due to random effects of repeated sampling of the same plant individual (Pot ID, *N* = 86). Note that while the marginal r-squared considers only the variance of the fixed effects, the conditional R^2 comprises variance explained by both fixed and random effects (i.e., variance explained by the whole model). Total *N* observations = 220.

Random Effects	Value
σ^2	0.333
τ00 Pot ID	1.561
ICC	0.824
Conditional R^2	0.876
Marginal R^2	0.294

Table S2.3 Mean ± standard error (SE) background values of extractable soil inorganic nitrogen (N) summarized from published data collected from experiments in *Bouteloua*-dominated grasslands at Sevilleta National Wildlife Refuge (SNWR). All values are from control/untreated plots only and extractable soil ammonium (NH_4^+) and nitrate (NO_3^-) are presented as μg N per g dry soil.

	Sampling Data			Soil N Concentration		
Reference	Year	Month	Depth (cm)	NH_4^+	NO_3^-	SNWR Experiment
Stursova et al., 2006[x]	2004	July	5	0.80 (0.03)	5.57 (0.27)	N Fertilization Plots
	2005	March		1.32 (0.44)	4.08 (1.51)	
Zeglin et al., 2007[x]	2004	Aug	5	0.661 (NA)	4.50 (NA)	N Fertilization Plots
Brown et al., 2022[+]	2014	July	15	2.00 (0.33)	1.72 (0.24)	Monsoon Rainfall
		Aug		1.62 (0.37)	4.69 (0.26)	Manipulation Expt.
		Sept		4.34 (0.80)	3.63 (0.48)	(MRME)
Kwiecinski et al., 2019[x]	2016	Aug	10	0.69 (0.07)	1.27 (0.35)	MRME
		Sept		0.86 (0.14)	1.20 (0.15)	
Holguin et al., 2022*	2017	June	10	1.22 (0.09)	0.80 (0.14)	Extreme Drought in
		July		0.80 (0.08)	1.50 (0.16)	Grassland Expt.
		Oct		0.83 (0.05)	2.06 (0.23)	(EDGE)
Stricker et al., 2022*	2018	June	2	3.87 (0.72)	0.66 (0.40)	Soil Disturbance
			10	0.62 (0.06)	0.60 (0.30)	Plots (Grassland)

[+]extracted in 2 M KCl containing 0.5 μg phenylmercuric acetate
*extracted in 0.5 M K_2SO_4
[x]extracted in 2 M KCl

Table S2.4 Study information for dryland N uptake literature review results presented in Table 2.5 and Table S2.5.

Reference (chronological)	Expt[a]	System[b]	Location	N Form(s)	N Addition(s)	Response[c]
Jackson et al., 1989	Field Intact	GS	CA	$(^{15}NH_4)_2SO_4$ $K^{15}NO_3$	115 mL of: $^{15}NH_4$: 5 *M* sol'n (70.5%) $^{15}NO_3$: 4 *M* sol'n (98%) avg. conc. = ~2 μg ^{15}N g^{-1} soil	R; %Nr
BassiriRad & Caldwell, 1992	GH Intact	S	UT	$K^{15}NO_3$	100 mL sol'n pot^{-1} (10%)	R
Bassirirad et al., 1993	LA Roots	S	UT	$K^{15}NO_3$	5.00 ×10^{-4} *M* sol'n (99%)	R
Jackson & Reynolds, 1996	LA Roots	GS	CA	$^{15}NH_4Cl$ $K^{15}NO_3$	1.00 ×10^{-4} *M* sol'n	R
BassiriRad et al., 1997	LA Intact	S	NM	NO_3^-	1.86 ×10^{-4} *M* sol'n	R
Cui & Caldwell, 1997	LA Roots	GS	UT	CH_3NH_3HCl	1000 mL of 5.00 ×10^{-4} *M* ^{14}C-labeled CH_3NH_3HCl sol'n	R
BassiriRad et al., 1999	LA Roots	S	NM	$K^{15}NO_3$	5.00 ×10^{-4} *M* sol'n (99%)	R
BassiriRad et al., 1999	Field Intact	S	NM	$^{15}NH_4{}^{15}NO_3$	160 mL of 0.02 *M* sol'n (99%)	$\delta^{15}N$
Yoder et al., 2000	LA Roots	GS	NV	$^{15}NH_4Cl$ $K^{15}NO_3$	2.50 ×10^{-4} *M* sol'n	R*
Booth et al., 2003	Field Intact	S	UT	$(^{15}NH_4)_2SO_4$	0.2 μg ^{15}N g $soil^{-1}$ (99%)	R*
Ivans et al., 2003	LA	S	UT	$^{15}NH_4Cl$	2.50 ×10^{-4} *M* sol'n (99%)	R

	Roots			$K^{15}NO_3$		
Ivans et al., 2003	Field Intact	MGS	UT	$K^{15}NO_3$	32 mg N L^{-1} sol'n (99%)	$\delta^{15}N$
Jankju-Borzelabad & Griffiths, 2006	GH Intact	MGS	UK	$K^{15}NO_3$	50 mL of 0.3 *M* sol'n (99.97%)	R*
James et al., 2006	Field Intact	S	CA	$K^{15}NO_3$	5 g N m^{-2} (10%) in 20 mm simulated rainfall treatment	R
James & Richards, 2006	Field Intact	S	CA	$^{15}NH_4{}^{15}NO_3$	120 mg (10%) in 10 mm simulated rainfall treatment	%Nr
Green et al., 2008	Field Intact	MGS	NM	$Na^{15}NO_3$ ^{15}N-glutamate	$^{15}NO_3$: 1.25 mL of 0.68 *M* sol'n, ^{15}N-glu: 5 mL of 0.34 *M* sol'n total = 12.5 mg ^{15}N $plot^{-1}$	%Nr
James et al., 2008	Field Intact	S	OR	$^{15}NH_4Cl$ $K^{15}NO_3$	60 mL of 0.0119 *M* sol'n (80%)	R*; %Nr
Aanderud & Bledsoe, 2009	GC Intact	MGS	CA	$^{15}NH_4Cl$ $K^{15}NO_3$ ^{15}N-glycine	40 mL of: $^{15}NH_4$: 2.00 $\times 10^{-3}$ *M* sol'n (99%) $^{15}NO_3$: 2.00 $\times 10^{-3}$ *M* sol'n (99%) ^{15}N-gly: ~2 µg ^{15}N g^{-1} soil	%Nr
James et al., 2009	LA Roots	S	OR	$^{15}NH_4Cl$ $K^{15}NO_3$	5.00 $\times 10^{-4}$ *M* sol'n	R
Jin & Evans, 2010	GC Intact	S	NV	$^{15}NH_4$ $^{15}NO_3$ ^{15}N-glycine	12 mL of each N sol'n (99%) total = 0.7 mg ^{15}N pot^{-1}	R
Leffler et al., 2011	LA Intact	GS	UT	$K^{15}NO_3$	250 mL sol'n (60 at%)	R

Gherardi et al., 2013	LA Intact	MGS	Argen- tina	$(NH_4)_2SO_4$ $Ca(NO_3)_2$	NH_4 only: 2.00 $\times 10^{-3}$ *M* NO_3 only: 2.00 $\times 10^{-3}$ *M* $NH_4 + NO_3$: 1.00 $\times 10^{-3}$ *M* of both	R
Zhuang et al., 2015	Field Intact	GS	China	$^{15}NH_4Cl$ $Na^{15}NO_3$	1.25 mL of 0.68 *M* sol'n	$\delta^{15}N$
Wang et al., 2016	Field Intact	GS	China	$^{15}NH_4$ $^{15}NO_3$ ^{15}N-glycine	45 mL sol'n containing: $^{15}NH_4$: 0.2 g N m^{-2} (99.14%) $^{15}NO_3$: 0.2 g N m^{-2} (99.19%) ^{15}N-gly: 0.2 g N m^{-2} (99.04%) total = 0.6 g ^{15}N m^{-2} $subplot^{-1}$	%Nr
Ouyang et al., 2016	Field Intact	GS	China	$(^{15}NH_4)_2SO_4$ $K^{15}NO_3$ ^{15}N-glycine	4 mL sol'n containing: $^{15}NH_4$: 3.00 $\times 10^{-4}$ *M* (98.4%) $^{15}NO_3$: 4.00$\times 10^{-4}$ *M* (98.2%) ^{15}N-gly: 5.00 $\times 10^{-4}$ *M* (95%) total = 0.06 g ^{15}N m^{-2}	R
Aanderud et al., 2018	Field Intact	GS	UT	$(^{15}NH_4)_2SO_4$ $K^{15}NO_3$	3 mL of: $^{15}NH_4$: 0.72 *M* sol'n (99%) $^{15}NO_3$:1.43 *M* sol'n (99%)	$\delta^{15}N$
Zhuang et al., 2020	Field Intact	GS	China	$^{15}NH_4$ $^{15}NO_3$ ^{15}N-glycine	112.5 mL sol'n containing: $^{15}NH_4$: 0.2 g N m^{-2} (99.14%) $^{15}NO_3$: 0.2 g N m^{-2} (99.19%) ^{15}N-gly: 0.2 g N m^{-2} (99.04%) total = 0.6 g ^{15}N m^{-2} $subplot^{-1}$	R; %Nr
Carvajal Janke & Coe, 2021	Field Intact	S	AZ	$(^{15}NH_4)_2SO_4$	5 mL of 0.75 *M* sol'n (99%)	$\delta^{15}N$
Adelizzi et al., 2022	Field Intact	MGS	NM	$^{15}NH_4{}^{15}NO_3$	2.5 mL of 6.00$\times 10^{-2}$ *M* sol'n	$\delta^{15}N$

Yang et al., 2022	Field Intact	GS	China	$^{15}NH_4Cl$ $K^{15}NO_3$ ^{15}N-glycine	150 mL sol'n containing: $^{15}NH_4$: 0.2 g N m^{-2} $^{15}NO_3$: 0.2 g N m^{-2} ^{15}N-gly: 0.2 g N m^{-2} total = 0.6 g ^{15}N m^{-2}	R*; %Nr
Present Study	GH Intact	MGS	NM	$^{15}NH_4Cl$ $K^{15}NO_3$ ^{15}N-glutamate	0.5 mL of: $^{15}NH_4$: 5.7 $\times 10^{-2}$ *M* sol'n $^{15}NO_3$: 4.8 $\times 10^{-2}$ *M* sol'n ^{15}N-glu: 5.7$\times 10^{-2}$ *M* sol'n total = 0.43 or 0.36 mg ^{15}N $plant^{-1}$	R; %Nr

[a] **Expt Type**: GC = Growth Chamber experiment, GH = Greenhouse experiment, Field = Field-based experiment, Intact = Intact plant (roots and shoots connected), Roots = Excised roots only

[b] **System:** GS – Grassland; S – Shrubland; W – Woodland, MGS – Mixed Grassland

[c] **Response**: R = N uptake rate (µmol ^{15}N per g dw per h); R* = excess N (µmol ^{15}N per g dw) converted to rate (per h); %Nr = percent N recovery in leaves (%); $\delta^{15}N$ = leaf $\delta^{15}N$ (‰)

Table S2.5 Results of dryland studies measuring short-term N uptake from inorganic and organic N sources in intact plant and/or excised roots of different plant species listed by response (N Uptake Rate and Plant $\delta^{15}N$) and then chronologically by study publication year. Values for N uptake rate are expressed as μmol ^{15}N per g plant dw per h and for plant $\delta^{15}N$ are expressed as permille (‰) in plant shoots. Values for each uptake ratio are unitless. If more than one inorganic N form was used in the study, then the Inorganic:Organic uptake ratios were calculated as the average NH_4^+ and NO_3^- uptake divided by the value of amino acid uptake. Data are from control (no treatment) plots unless otherwise noted. An "--" indicates that the variable was not measured in the study. An "NA" indicates that the variable could not be determined or calculated based on the data provided in the study.

				N Uptake Rate			Uptake Ratio	
	Reference	Plant Species	Time	NH_4^+	NO_3^-	AA^d	NH_4^+:NO_3^-	Inorg:Org
Laboratory Assay Experiments	BassiriRad et al., 1993	*Agropyron desertorum*	30 m	--	2.71	--	--	--
	Jackson & Reynolds 1996	*Avena fatua*	30 m	11.53	5.94	--	1.94	--
		Bromus hordeaceus		25.23	8.63	--	2.92	--
		Lolium multiflorum		23.31	6.71	--	3.48	--
		Vulpia microstachys		9.84	--	--	NA	--
		Lasthenia californica		13.18	10.14	--	1.30	--
		Plantago erecta		10.37	9.26	--	1.12	--
	BassiriRad et al., 1997	*Bouteloua eriopoda*	4 h	--	30.98	--	--	--
		Larrea tridentata		--	43.25	--	--	--
		Prosopis glandulosa		--	18.29	--	--	--
	Cui & Caldwell 1997	*Agropyron desertorum*	10 m	6.89	--	--	--	--
	BassiriRad et al., 1999	*Larrea tridentata*	30 m	--	2.07	--	--	--

Laboratory Assay Experiments

Yoder et al., 2000	*Bromus madritensis spp. rubens*	30 m	13.15	3.80	--	3.46	--
	Achnatherum hymenoides		5.56	3.13	--	1.78	--
	Pleuraphis rigida		4.58	2.38	--	1.92	--
Ivans et al., 2003	*Agropyron desertorum*	30 m	7.82	5.17	--	1.51	--
	Artemesia tridentata		8.07	5.18	--	1.56	
James et al., 2009	*Achnatherum thurberianum*	30 m	9.14	*	--	NA	--
	Festuca idahoensis		7.41	*	--	NA	--
	Pseudoroegneria spicata		4.73	*	--	NA	--
	Balsamorhiza sagittata		4.57	*	--	NA	--
	Centaurea diffusa		8.75	*	--	NA	--
	Chondrilla juncea		7.27	*	--	NA	--
	Crepis intermedia		3.18	*	--	NA	--
	Linaria dalmatica		8.37	*	--	NA	--
	Phlox longifolia		1.62	*	--	NA	--
Leffler et al., 2011	*Agropyron cristatum*	2 h	--	17.85	--	--	--
	Bromus tectorum		--	16.42	--	--	--
	Elymus elymoides		--	11.42	--	--	--
	Pseudoroegneria spicata		--	10.71	--	--	--
Gherardi et al., 2013	*Mulinum spinosum, Adesmia volckmanni,Senecio filaginoides*	9 d	7.79×10^{-4}	1.03×10^{-3}	--	0.75	--
	Poa ligularis, Pappostipa speciosa, Pappostipa humilis		6.01×10^{-4}	4.97×10^{-4}	--	1.21	--
Jackson et al., 1989	*Avena barbata, Bromus mollis, Lolium multiflorum*	24 h (Feb)	[x]3.38	[x]1.71	--	1.98	--
		24 h (Apr)	[x]4.58	[x]3.46	--	1.33	--

Soil-Based Experiments

BassiriRad & Caldwell 1992	*Artemesia tridentata*	4 d	--	4.40	--	--	--
		14 d	--	4.59	--	--	--
Booth et al., 2003	*Artemisia tridentata*	14 d	2.28×10^{-3}	--	--	--	--
	Bromus tectorum		0.04	--	--	--	--
	Elymus elymoides		0.02	--	--	--	--
James et al., 2006	*Atriplex confertifolia*	20 d	1.01	--	--	--	--
	Atriplex parryi		0.60	--	--	--	--
	Sarcobatus vermiculatus		0.24	--	--	--	--
Jankju-Borzelabad & Griffiths 2006	*Panicum antidotale*	24 h	--	0.41	--	--	--
James et al. 2008	*Bromus tectorum*	72 h	0.36	*	--	0.36	--
	Taeniatherum caput-medusae		0.27	*	--	0.39	--
	Elymus elymoides		0.07	*	--	0.29	--
	Poa secunda		0.18	*	--	0.61	--
	Pseudoroegneria spicata		0.06	*	--	0.40	--
	Crepis intermedia		0.07	*	--	0.49	--
	Lomatium triternatum		0.04	*	--	0.66	--
Jin & Evans 2010	*Larrea tridentata*	48 h	1.42	14.91	Gly: 1.70	0.09	2.51
		10 d	2.10	5.16	Gly: 1.98	0.41	2.53
		24 d	1.53	2.53	Gly: 1.33	0.61	3.83
		49 d	1.32	1.58	Gly: 1.24	0.83	4.13
Ouyang et al. 2016	*Artemisia capillaris*	2 h	0.20	1.77	Gly: 0.25	0.11	3.89
	Artemisia frigida		0.05	0.19	Gly: 0.02	0.26	4.92
	Cleistogenes squarrosa		0.20	0.78	Gly: 0.18	0.26	2.71

Zhuang et al. 2020	*Erodium oxyrrhynchum*	24 h	0.20	0.24	Gly: 0.16	0.81	1.36
	Hyalea pulchella		0.25	0.26	Gly: 0.18	0.96	1.39
	Nonea caspica		0.48	0.42	Gly: 0.27	1.15	1.66
	Lactuca undulata		0.24	0.39	Gly: 0.20	0.62	1.58
Yang et al. 2022	*Cleistogenes squarrosa*	3 h	0.01	0.13	Gly: 0.01	0.13	4.11
	Leymus chinensis		0.01	0.23	Gly: 0.02	0.08	6.62
	Stipa grandis		0.01	0.05	Gly: 0.01	0.20	4.86
Present Study	*Achnatherum hymenoides*	12 h	0.18	0.36	Glu: 0.06	0.50	4.19
		24 h	0.13	0.22	Glu: 0.06	0.59	2.83
		48 h	0.19	0.17	Glu: 0.07	1.13	2.45
	Bouteloua eriopoda	12 h	0.21	0.62	Glu: 0.03	0.34	14.59
		24 h	0.18	0.63	Glu: 0.04	0.29	10.85
		48 h	0.37	0.53	Glu: 0.06	0.69	7.50
	Gutierrezia sarothrae	12 h	0.36	0.53	Glu: 0.17	0.67	2.56
		24 h	0.12	0.27	Glu: 0.10	0.44	1.93
		48 h	0.32	0.37	Glu: 0.15	0.87	2.30

			Plant $\delta^{15}N$ (‰)			Recovery Ratio	
Reference	Plant Species	Time	NH_4^+	NO_3^-	AA	NH_4^+:NO_3^-	Inorg:Org
BassiriRad et al. 1999	*Larrea tridentata*	12 h	12.52	**	--	--	--
		28 h	48.35	**	--	--	--
		48 h	96.35	**	--	--	--
		72 h	112.70	**	--	--	--
	Prosopis glandulosa	12 h	0.00	**	--	--	--
		28 h	4.78	**	--	--	--
		48 h	6.37	**	--	--	--
		72 h	11.65	**	--	--	--
Ivans et al. 2003	*Agropyron desertorum*	1 h	--	8.33	--	--	--

Soil-Based Experiments			3 h	--	14.10	--	--	--
			6 h	--	18.60	--	--	--
			12 h	--	209.62	--	--	--
			24 h	--	287.82	--	--	--
			48 h	--	395.19	--	--	--
		Artemesia tridentata	1 h	--	6.98	--	--	--
			2 h	--	5.67	--	--	--
			4 h	--	5.91	--	--	--
			10 h	--	8.58	--	--	--
			24 h	--	9.06	--	--	--
			48 h	--	47.67	--	--	--
	Zhuang et al. 2015	*Erodium oxyrrhynchum*	24 h	6.63	5.07	Glu: 6.21	1.31	0.94
	Aanderud et al. 2018	*Achnatherum hymenoides*	24 h	6.70	1.73	--	3.88	--
	Carvajal Janke & Coe 2021	*Larrea tridentata*	24 h	10.45	--	--	--	--
			72 h	8.46	--	--	--	--
			6 d	690.94	--	--	--	--
	Adelizzi et al. 2022	*Bouteloua eriopoda*	24 h	1.82	**	--	--	--
			7 d	9.76	**	--	--	--

*Study combined results from $^{15}NH_4^+$ and $^{15}NO_3^-$ treatments

**Study added ammonium nitrate ($^{15}NH_4{}^{15}NO_3$)

[x] Rate could not be converted because units were reported by plot area in this study (mg N m^{-2} h^{-1})

Table S2.3 References

Brown, R. F., Sala, O. E., Sinsabaugh, R. L. & Collins, S. L. (2022). Temporal effects of monsoon rainfall pulses on plant available nitrogen in a chihuahuan desert grassland. *Journal of Geophysical Research. Biogeosciences*, *127*(6).

Holguin, J., Collins, S. L. & McLaren, J. R. (2022). Belowground responses to altered precipitation regimes in two semi-arid grasslands. *Soil Biology & Biochemistry*, *171*, 108725.

Kwiecinski, J. V., Stricker, E., Sinsabaugh, R. L. & Collins, S. L. (2020). Rainfall pulses increased short-term biocrust chlorophyll but not fungal abundance or N availability in a long-term dryland rainfall manipulation experiment. *Soil Biology & Biochemistry*, *142*, 107693.

Stricker, E., Adelizzi, R.Z., O'Brien, E.A., & Hoelrich, M. (2022). Effect of foot disturbance to cyanobacteria-dominated biocrusts on microbes and nitrogen in Chihuhuahan grassland and shrubland. *Environmental Data Initiative*. doi:10.6073/pasta/040dcef4073b1b63691b4392acc50f93

Stursova, M., Crenshaw, C. L. & Sinsabaugh, R. L. (2006). Microbial responses to long-term N deposition in a semiarid grassland. *Microbial Ecology*, *51*(1), 90–98.

Zeglin, L. H., Stursova, M., Sinsabaugh, R. L. & Collins, S. L. (2007). Microbial responses to nitrogen addition in three contrasting grassland ecosystems. *Oecologia*, *154*(2), 349–359.

Table S2.4 References

Aanderud, Z. T., & Bledsoe, C. S. (2009). Preferences for ^{15}N-ammonium, ^{15}N -nitrate, and ^{15}N -glycine differ among dominant exotic and subordinate native grasses from a California oak woodland. *Environmental and Experimental Botany*, *65*(2), 205–209.

Aanderud, Z. T., Smart, T. B., Wu, N., Taylor, A. S., Zhang, Y., & Belnap, J. (2018). Fungal loop transfer of nitrogen depends on biocrust constituents and nitrogen form. *Biogeosciences*, *15*(12), 3831–3840.

Adelizzi, R., O'Brien, E. A., Hoellrich, M., Rudgers, J. A., Mann, M., Fernandes, V. M. C., Darrouzet-Nardi, A., & Stricker, E. (2022). Disturbance to biocrusts decreased cyanobacteria, N-fixer abundance, and grass leaf N but increased fungal abundance. *Ecology*, *103*(4), e3656.

BassiriRad, H., & Caldwell, M. M. (1992). Root growth, osmotic adjustment and NO_3^- uptake during and after a period of drought in *Artemisia tridentata*. *Functional Plant Biology*: *FPB*, *19*(5), 493–500.

Bassirirad, H., Caldwell, M. M., & Bilbrough, C. (1993). Effects of soil temperature and nitrogen status on kinetics of $^{15}NO_3^-$ uptake by roots of field-grown *Agropyron desertorum* (Fisch. ex Link) Schult. *The New Phytologist*, *123*(3), 485–489.

BassiriRad, H., Reynolds, J. F., Virginia, R. A., & Brunelle, M. H. (1997). Growth and root NO_3^- and PO_4^{3-} uptake capacity of three desert species in response to atmospheric CO_2 enrichment. *Australian Journal of Plant Physiology*, *24*, 354–358.

BassiriRad, H., Tremmel, D. C., Virginia, R. A., Reynolds, J. F., de Soyza, A. G., & Brunell, M. H. (1999). Short-term patterns in water and nitrogen acquisition by two desert shrubs following a simulated summer rain. *Plant Ecology*, *145*, 27–36.

Booth, M. S., Caldwell, M. M., & Stark, J. M. (2003). Overlapping resource use in three Great Basin species: implications for community invasibility and vegetation dynamics. *Journal of Ecology*, *91*(1), 36-48.

Carvajal Janke, N., & Coe, K. K. (2021). Evidence for a fungal loop in shrublands. *Journal of Ecology*, *109*(4), 1842–1857.

Cui, M., & Caldwell, M. M. (1997). A large ephemeral release of nitrogen upon wetting of dry soil and corresponding root responses in the field. *Plant and Soil*, *191*, 291–299.

Gherardi, L. A., Sala, O. E., & Yahdjian, L. (2013). Preference for different inorganic nitrogen forms among plant functional types and species of the Patagonian steppe. *Oecologia*, *173*(3), 1075–1081.

Green, L. E., Porras-Alfaro, A., & Sinsabaugh, R. L. (2008). Translocation of nitrogen and carbon integrates biotic crust and grass production in desert grassland. *Journal of Ecology*, *96*(5), 1076–1085.

Ivans, C. Y., Leffler, A. J., Spaulding, U., Stark, J. M., Ryel, R. J., & Caldwell, M. M. (2003). Root responses and nitrogen acquisition by *Artemisia tridentata* and *Agropyron desertorum* following small summer rainfall events. *Oecologia*, *134*(3), 317–324.

Jackson, R. B., & Reynolds, H. L. (1996). Nitrate and ammonium uptake for single- and mixed-species communities grown at elevated CO_2. *Oecologia*, *105*, 74–80.

James, J. J., Aanderud, Z. T., & Richards, J. H. (2006). Seasonal timing of N pulses influences N capture in a saltbush scrub community. *Journal of Arid Environments*, *67*(4), 688–700.

James, J. J., Davies, K. W., Sheley, R. L., & Aanderud, Z. T. (2008). Linking nitrogen partitioning and species abundance to invasion resistance in the Great Basin. *Oecologia*, *156*(3), 637–648.

James, J. J., Mangold, J. M., Sheley, R. L., & Svejcar, T. (2009). Root plasticity of native and invasive Great Basin species in response to soil nitrogen heterogeneity. *Plant Ecology*, *202*(2), 211–220.

James, J. J., & Richards, J. H. (2006). Plant nitrogen capture in pulse-driven systems: interactions between root responses and soil processes. *Journal of Ecology*, *94*(4), 765–777.

Jankju-Borzelabad, M., & Griffiths, H. (2006). Competition for pulsed resources: an experimental study of establishment and coexistence for an arid-land grass. *Oecologia*, *148*(4), 555–563.

Jin, V. L., & Evans, R. D. (2010). Elevated CO_2 increases plant uptake of organic and inorganic N in the desert shrub *Larrea tridentata*. *Oecologia*, *163*(1), 257–266.

Leffler, A. J., Monaco, T. A., & James, J. J. (2011). Morphological and physiological traits account for similar nitrate uptake by crested wheatgrass and cheatgrass uptake. *Natural Resources and Environmental Issues*, *17*(10), 63–70.

Ouyang, S., Tian, Y., Liu, Q., Zhang, L., Wang, R., & Xu, X. (2016). Nitrogen competition between three dominant plant species and microbes in a temperate grassland. *Plant and Soil*, *408*(1), 121–132.

Wang, R., Tian, Y., Ouyang, S., Xu, X., Xu, F., & Zhang, Y. (2016). Nitrogen acquisition strategies used by *Leymus chinensis* and *Stipa grandis* in temperate steppes. *Biology and Fertility of Soils*, *52*(7), 951–961.

Yang, Z., Li, Y., Wang, Y., Cheng, J., & Li, F. Y. (2022). Preferences for different nitrogen forms in three dominant plants in a semi-arid grassland under different grazing intensities. *Agriculture, Ecosystems & Environment*, *333*, 107959.

Yoder, C. K., Vivin, P., Defalco, L. A., Seemann, J. R., & Nowak, R. S. (2000). Root growth and function of three Mojave Desert grasses in response to elevated atmospheric CO_2 concentration. *The New Phytologist*, *145*, 245–256.

Zhuang, W., Downing, A., & Zhang, Y. (2015). The influence of biological soil crusts on ^{15}N translocation in soil and vascular plant in a temperate desert of northwestern China. *Journal of Plant Ecology*, *8*(4), 420–428.

Zhuang, W., Li, J., Yu, F., Dong, Z., & Guo, H. (2020). Seasonal nitrogen uptake strategies in a temperate desert ecosystem depends on N form and plant species. *Plant Biology*, *22*(3), 386–393.

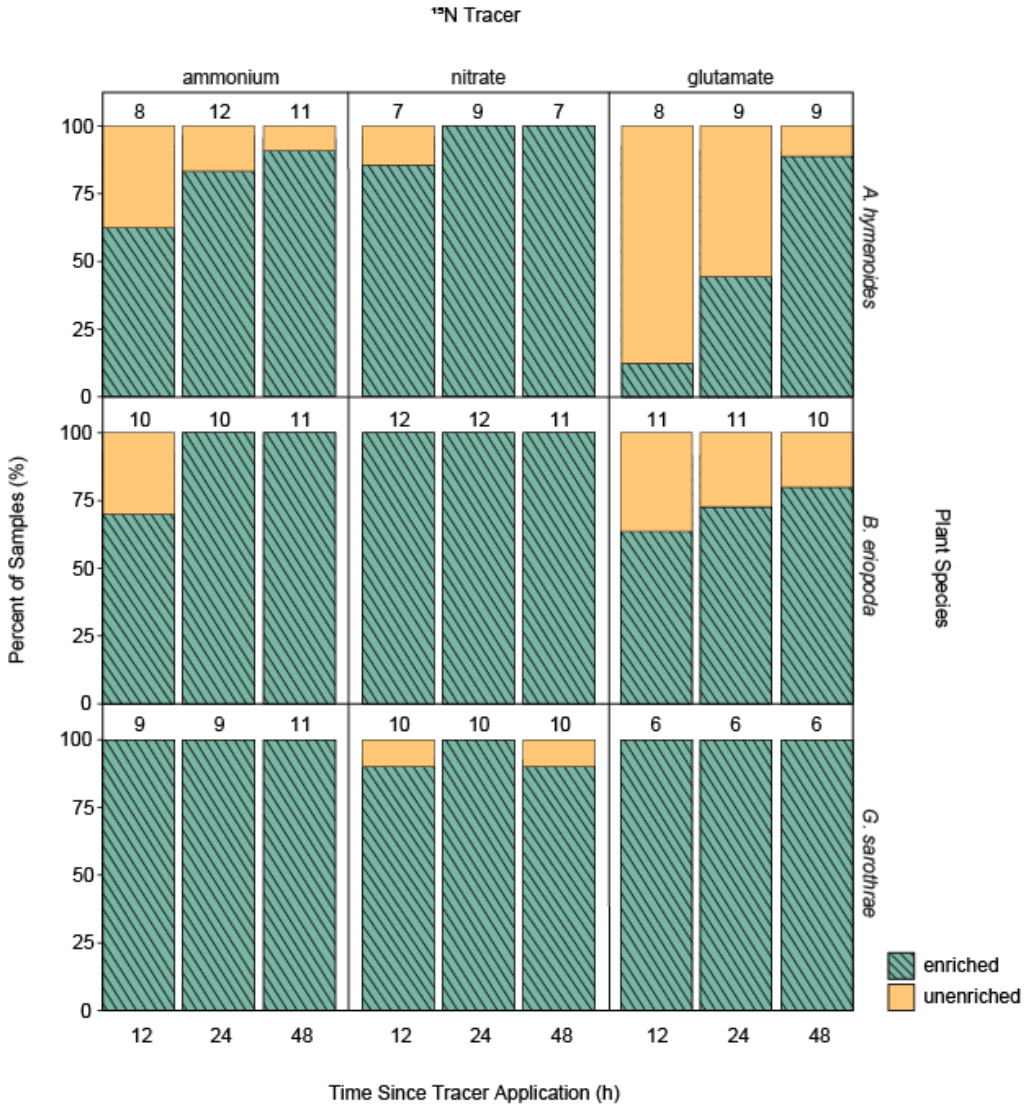

Fig S2.1 Percentage (%) of total leaf samples considered enriched (sample $\delta^{15}N$ > cutoff value) and unenriched (sample $\delta^{15}N$ < cutoff value) at each timepoint (12, 24, 48 hours post application) for each ^{15}N tracer × species group. Sample size (*n*) is provided above each bar. Natural abundance and enrichment cutoff $\delta^{15}N$ values for each species are provided in Table 2.1. Note that zero percent indicates that no samples were enriched, and 100 percent indicates that all samples were enriched.

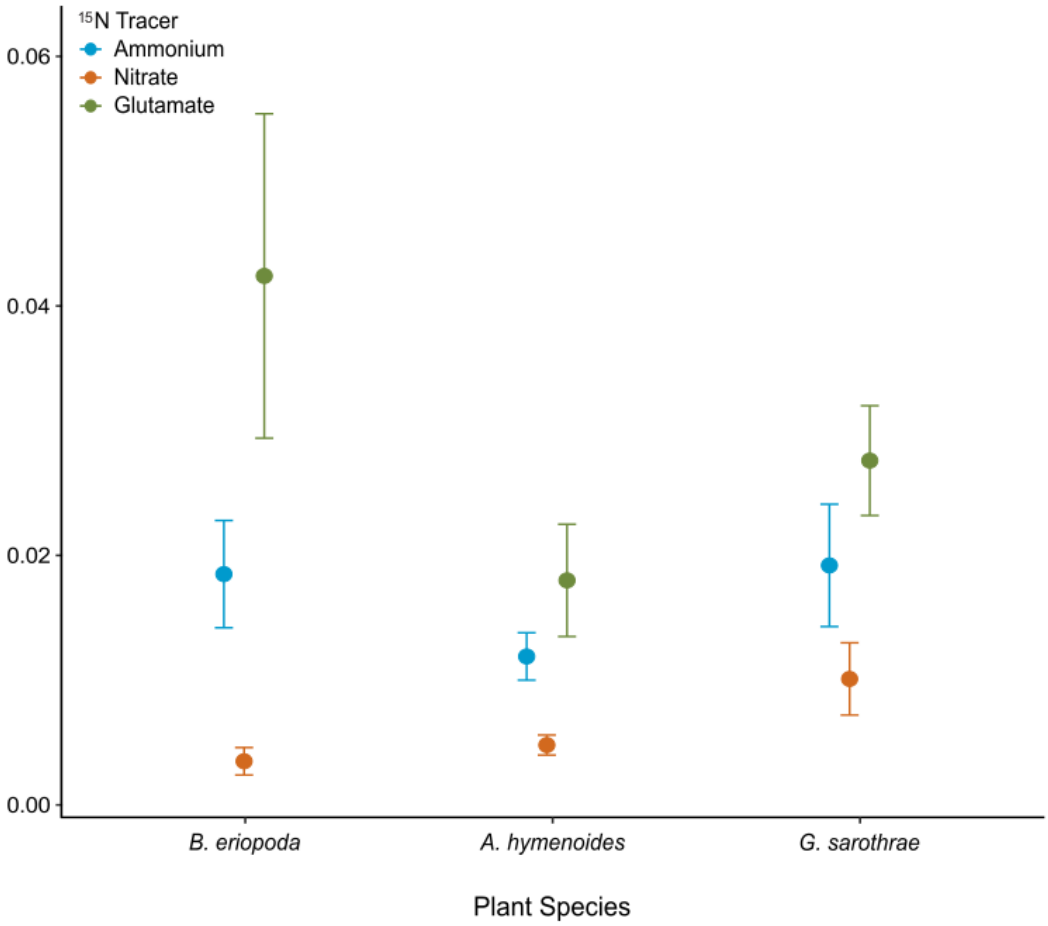

Fig S2.2 Mean N uptake rates ± standard error (µmol ^{15}N per g dw per h) of each ^{15}N tracer × species group averaged across all 3 post-addition time points ($N = 220$). Sample size and values can be found in Table S2.1.

Table S3.1 Results from linear mixed effects ANOVA models testing for main and interacting effects of sample type (biocrust or root), experimental treatment (N addition only, water only, and water + N additions) on fungal richness, diversity, and evenness metrics for each of 3 experiments (MRME, NutNet, WENNDEx). Significant values ($P < 0.05$, Type II Wald Chi-square tests) are bolded.

		MRME			NutNet			WENNDEx		
Response	**Predictors**	df	X^2	P	df	X^2	P	df	X^2	P
OTU Richness (S_{obs})	Sample Type	1	0.01	0.920	1	33.86	**< 0.001**	1	519.05	**< 0.001**
	Treatment	5	15.34	**0.009**	1	2.63	0.105	3	1.01	0.799
	Sample Type:Treatment	5	28.58	**< 0.001**	1	2.05	0.152	3	11.42	**0.010**
Chao Richness	Sample Type	1	0.21	0.650	1	22.50	**< 0.001**	1	222.86	**< 0.001**
	Treatment	5	6.78	0.238	1	1.92	0.166	3	1.35	0.717
	Sample Type:Treatment	5	24.07	**< 0.001**	1	2.41	0.121	3	5.40	0.145
Shannon Diversity	Sample Type	1	0.59	0.444	1	57.21	**< 0.001**	1	476.89	**< 0.001**
	Treatment	5	53.98	**< 0.001**	1	2.29	0.130	3	1.49	0.684
	Sample Type:Treatment	5	16.90	**0.005**	1	4.39	**0.036**	3	3.863	0.277
Pielou's Evenness	Sample Type	1	0.59	0.443	1	35.21	**< 0.001**	1	188.53	**< 0.001**
	Treatment	5	47.81	**< 0.001**	1	1.35	0.246	3	1.65	0.649
	Sample Type:Treatment	5	12.85	**0.025**	1	2.94	0.087	3	1.68	0.642

Table S3.2 Results from linear models testing for main effects of experimental N addition on soil fungal biomass including: (a) soil ergosterol content; (b) ratio of bacterial:fungal fatty acid methyl ester (FAME) biomarkers; and (c) proportion of fungal biomarkers (% of total FAME) detected in biocrust soils from 3 experiments (MRME, NutNet, WENNDEx). Note that a linear mixed-effects model was fit for responses from MRME only to account for the random effect of N addition subplots nested within each control plot.

		MRME			**NutNet**			**WENNDEx**		
Response	**Predictors**	df	X^2	*P*	df	*F*	*P*	df	*F*	*P*
Soil ergosterol concentration	N Treatment	1	0.97	0.324	1	0.27	0.619	1	< 0.01	0.977
Bacterial:Fungal FAME ratio	N Treatment	1	1.33	0.249	1	0.87	0.377	1	0.08	0.788
Proportion of FAME from Fungi	N Treatment	1	1.70	0.193	1	0.95	0.358	1	0.01	0.920

Table S3.3 Results from linear mixed effects ANOVA models testing for main and interacting effects of hyphal morphotype (aseptate or septate), experimental treatment (N addition only, water only, and water + N additions) on fungal root colonization (% root length colonized) of *B. eriopoda* roots from each of 3 experiments (MRME, NutNet, WENNDEx). Significant values ($P < 0.05$) are bolded.

	MRME			**NutNet**			**WENNDEx**		
Predictors	df	X^2	*P*	df	X^2	*P*	df	X^2	*P*
Hyphal Type	1	57.53	**< 0.001**	1	0.22	0.643	1	19.23	**< 0.001**
Treatment	5	1.55	0.907	1	0.01	0.906	3	12.37	**0.006**
Hyphal Type:Treatment	5	3.50	0.623	1	1.82	0.178	3	5.85	0.119

Table S3.4. Diversity Index Calculations

Diversity Metric	Symbol	Formula	Description
Good's Coverage	G	$G = 1 - (\frac{n_1}{N})$	n_1 = the number of OTUs that only appear once in a sample ("singletons") N = the total number of OTUs in the sample
Total Richness	S_{obs}	NA	S_{obs} = count of OTUs observed per sample
Estimated Richness (Chao1 Index)	S_{Chao1}	$S = S_{obs} + \frac{n_1(n_1 - 1)}{(2n_2 + 1)}$	n_1 = the number of OTUs that only appear once in a sample ("singletons") n_2 = the number of OTUs that only appear twice in a sample ("doubletons")
Shannon Diversity	H^1	$H^1 = \sum p_i \times \ln(p_i)$	p_i = proportional abundance of species i
Pielou's Evenness	J	$J = \frac{H^1}{\log(S_{obs})}$	H^1 = Shannon Diversity Index S_{obs} = number of OTUs observed per sample

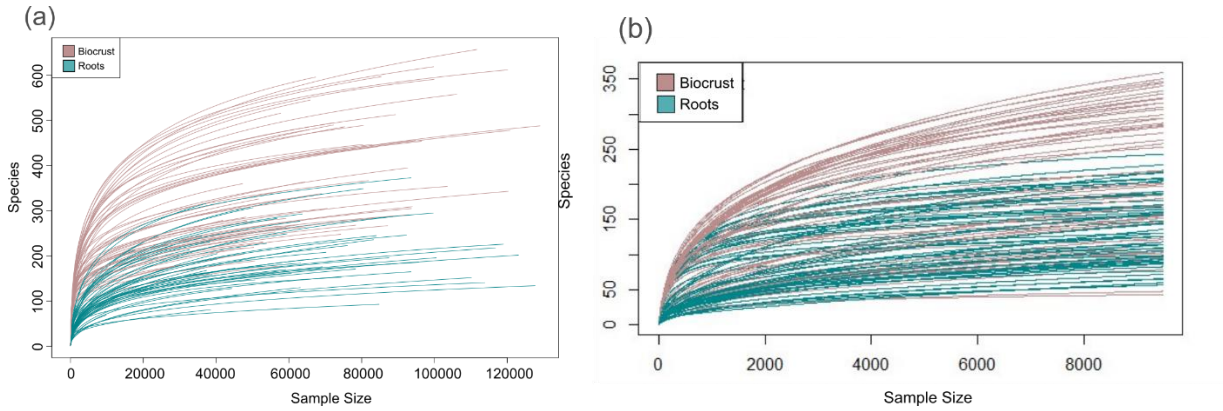

Fig. S3.1 Rarefaction curves generated for biocrust (brown) and root (teal) samples based on (a) raw sequence data and (b) sequences rarefied to an even sampling depth of 9484 sequences per sample. Samples were rarefied to the same number of sequences as the second lowest sample overall (N38R) in order to prevent artificial overestimation of OTUs due to uneven sampling depth. Values for Good's Coverage Index were > 0.98 for all samples, suggesting adequate sampling of target fungal communities in both sample types.

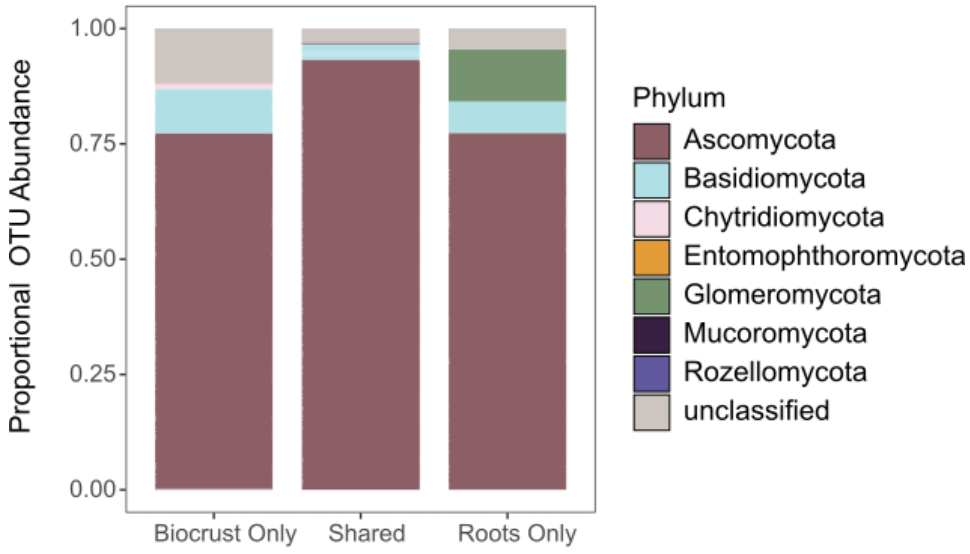

Fig. S3.2 Proportional/relative abundance of unique and shared fungal Phyla in biocrust and root communities from control (no treatment) plots from three experiments, MRME, NutNet, and WENNDEx combined (*N* = 30 samples)

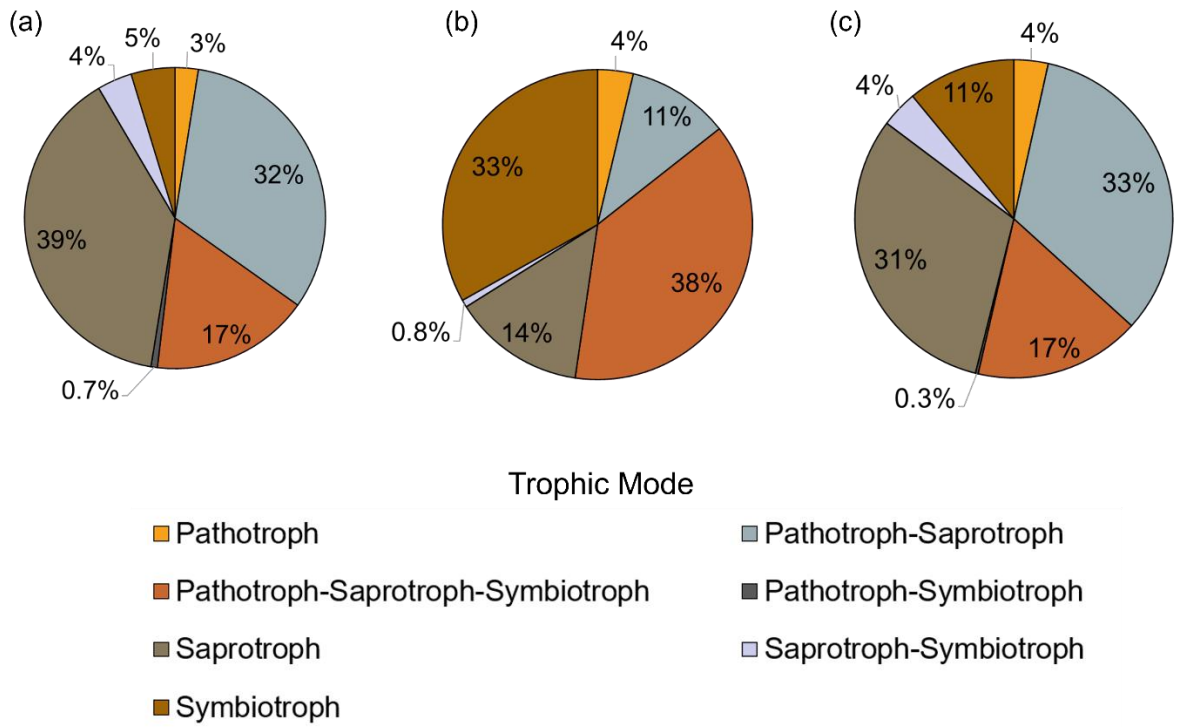

Fig. S3.3 Proportional distribution of fungal OTUs assigned to 7 trophic modes found in (a) biocrust only, (b) root only, (c) shared by both sample types. Only OTUs classified to >80% confidence at the genus level (N = 1740 OTUs) were used for FUNGuild assignment.

Table S4.1 Mean ± standard error leaf excess N values (µg ^{15}N per g dry biomass) and sample sizes (*n*) of enriched samples from each experiment year: (a) 2017, (b) 2018, and (c) 2019. Note that *B. eriopoda* was the only species tested in the 2017 and 2019 mesh experiments; and data from both sites are combined for 2018. An "NA" indicates that value could not be determined.

		JOR		SEV	
(a) 2017	Treatment	*n*	Mean	*n*	Mean
	Coarse mesh	3	85.1 ± 82. 8	6	5.9 ± 2.5
	Fine mesh	5	54.1 ± 13.7	7	12.5 ± 7.7
	None	8	123.8 ± 42.1	7	51.5 ± 46.1

		B. eriopoda		*G. sarothrae*	
(b) 2018	Treatment	*n*	Mean	*n*	Mean
	2 cm	4	1.2 ± 0.1	8	6.9 ± 3.0
	None	1	0.9 ± NA	6	8.2 ± 1.6

		SEV	
(c) 2019	Treatment	*n*	Mean
	Coarse mesh	8	89.1 ± 16.9
	Fine mesh	16	70.6 ± 9.1
	None	18	45.4 ± 3.6

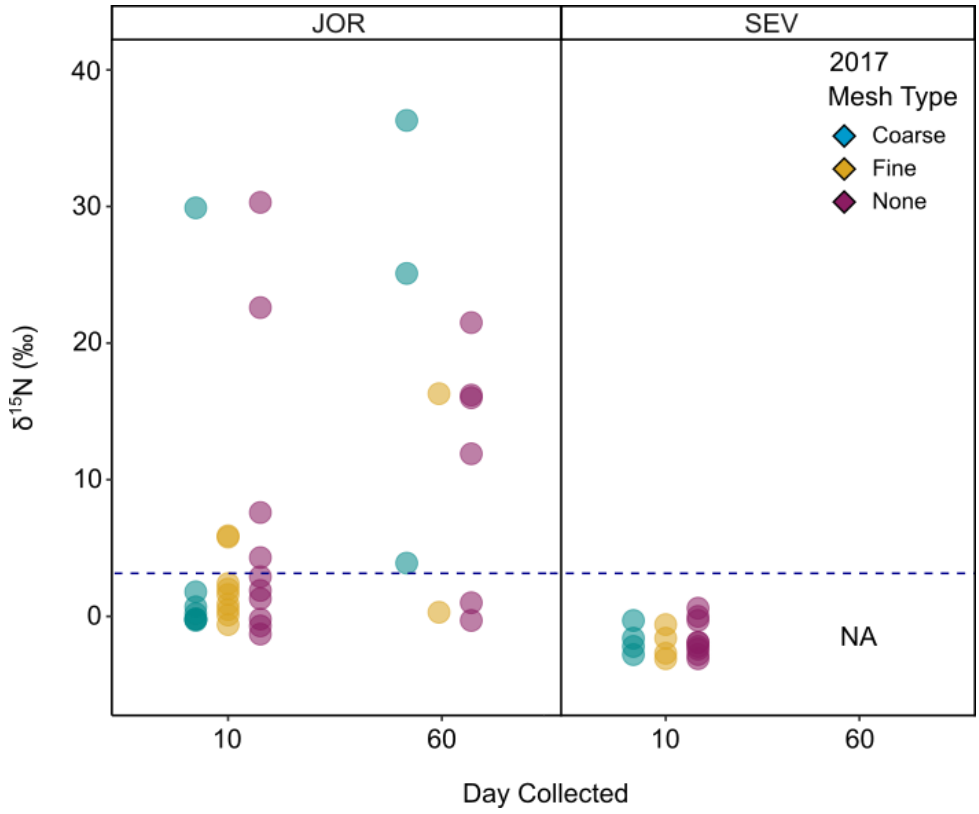

Fig. S4.1 $\delta^{15}N$ (‰) values of all root samples collected from *B. eriopoda* plants 10 and 60 days following ^{15}N tracer addition to biocrusts in the 2017 monsoon season mesh experiment plots (treatments: vertical coarse mesh, fine mesh, no mesh) at two sites (JOR and SEV). An "NA" indicates no samples collected for that site/collection day.

Vita

Catherine Cort earned a B.S. in Conservation Biology from the State University of New York-College of Environmental Science and Forestry (SUNY-ESF) in 2012, where she completed an undergraduate thesis project based on the phylogenetic analysis of a rare fungal taxon. Before coming to the University of Texas at El Paso (UTEP), Cat worked at Red Butte Garden & Arboretum at the University of Utah where her research focused on conservation, seed banking and restoration of rare and endangered plant communities. In 2017, she was accepted into the UTEP Ecology & Evolutionary Biology (EEB) Doctoral Program where she began research into dryland biogeochemistry, biological soil crusts, and fungal connections in the Chihuahuan Desert. Cat received the 2019 Sevilleta LTER Graduate Student Summer Fellowship and the 2020 UTEP Les and Harriet Dodson Research Grant to support her project on fungal community responses to global change. Cat served as a teaching assistant for seven undergraduate courses at UTEP and was a guest lecturer for several others, and in 2022 she developed a new lab unit for the undergraduate Organismal Biology course centered around the diversity and adaptations of biocrust microbes. Outside of UTEP, she founded the El Paso Pod of 500 Women Scientists in 2017 to facilitate more opportunities for local scientists to connect and share their research through free public events within the community. She also volunteers as an educational tour guide with the Frontera Land Alliance and at Hueco Tanks State Park where she specializes in lichen hikes. Cat hopes to pursue a teaching career focused on community-based science and environmental education after graduation.